JAERI-Review 2002-032

Annual Report of Naka Fusion Research Establishment From April 1, 2001 to March 31, 2002

Naka Fusion Research Establishment

Japan Atomic Energy Research Institute
Naka-machi, Naka-gun, Ibaraki-ken

(Received September 25, 2002)

This report provides an overview of research and development activities at Naka Fusion Research Establishment, JAERI, including those performed in collaboration with other research establishments of JAERI, during the period from April 1, 2001 to March 31, 2002. The activities in the Naka Fusion Research Establishment are highlighted by high performance plasma researches in JT-60 and JFT-2M, and completion of ITER Engineering Design Activities (EDA) in July 2001, including technology R&D.

Objectives of the JT-60 project are to contribute the physics R&D for ITER and to establish the physics basis for a steady state tokamak fusion reactor like SSTR. In this fiscal year, most of JT-60 experiments have been devoted to the improvement, sustainment and integration of the high plasma performance.

Highlights of JT-60 experiments are summarized as follows;

1) Using high-power negative-ion-based neutral beam (N-NB) injection (5.7 MW, 402 keV), the highest record for the fusion product ($n_i(0)\,\tau_E\,T_i(0) = 3 \times 10^{20}$ m^{-3} s keV) under the full non-inductive current drive condition was obtained in a high-β_p ELMy H-mode discharge.
2) In a reversed shear discharge, the DT-equivalent fusion power gain Q_{DT}^{eq} above 0.8 was sustained for 0.55s.
3) By the extension of the operational region for the high-triangularity configuration, the quasi-steady beta values maintained for longer than $5\tau_E$ were improved to $\beta_N = 3.05$ at a low 95% flux surface ($q_{95} \sim 3.7$). Long sustainment (7.4 s, 60 τ_E) of a high β_N (~ 2.7) was also demonstrated.
4) High confinement ($H_{89P} \sim 2.7$, where H_{89P} is the energy confinement improvement factor

---

Editors: Ando, T., Matsumoto, H., Moriyama, S., Tanaka, F., Tuda, T., Tsuji, H.

compared with the ITER89-P (L-mode) scaling) was achieved at an electron density of ~ 0.7 times Greenwald density in a reversed shear discharge with q_{95} ~ 5 using lower hybrid range of frequency (LHRF). By Ar injection, high confinement (HH_{y2} > 0.9, where HH_{y2} is the energy confinement improvement factor compared with the IPB98(y, 2) scaling), high density (~ 0.8 times Greenwald density) and high radiation loss power (~ 0.8 times heating power) were simultaneously obtained in discharges with the outer separatrix strike point located on the divertor dome top.

5) Physics on fusion plasmas, i.e. mechanisms of the current hole, formation of internal transport barriers (ITBs) and transport within it, dynamics of density collapse due to ELMs, the mechanism of in-out asymmetry of divertor particle flux, etc., have been studied under reactor-relevant conditions.

The highlights of technological progress in JT-60 are as follows;

1) Feedback control of a steerable injection mirror to control electron cyclotron range of frequency (ECRF) power deposition was successfully tested using JT-60 discharges. A digital integrating system which has “intelligence” to automatically select unsaturated signals during disruptions has been developed.
2) A digital phase controller of thyristor converters, which is applicable to JT-60 superconducting tokamak (JT-60SC), has been developed to replace the aged analog controller for the poloidal magnetic field power supplies of JT-60.
3) Surface analyses of the first wall exposed to DD plasmas were initiated with various methods. Tritium deposition profiles on the W-shaped divertor tiles were examined by using tritium imaging plate technique, and compared with the triton deposition calculated with orbit following Monte Carlo code (OFMC) code.
4) The injection power of the negative-ion based neutral beam system reached 5.8 MW at 400 keV, and the operation with a pulse length of 10 s at 2.6 MW with one ion source was successfully achieved by improving the beam.
5) The electron cyclotron (EC) system for JT-60 achieved the world highest injected power of 2.8 MW for 3.6 s at 110 GHz by improving performances of the gyrotron with built-in RF absorber and realigning the transmission line so as to have high efficiencies of 70-80%.

Objectives of the JT-60SC program are to realize the high-beta steady-state operation of reactor-relevant plasmas and to demonstrate the compatibility of the reduced-activation ferritic steel with the plasma. Physics and engineering design of the JT-60SC made progress on the basis of the objectives.

On JFT-2M, advanced and basic research for the development of high performance

tokamak plasma has been promoted, making use of the flexibility of a medium-sized device. In this fiscal year, inside wall of the vacuum vessel was fully covered with ferritic steel plates. A fine structure of the magnetic field inside the vacuum vessel was measured using a three-dimensional magnetic field measurement apparatus. In parallel with this program, advanced and basic study on H-mode plasmas and a compact toroid (CT) injection, etc. has been pursued on JFT-2M.

The principal objective of theoretical and analytical studies is to understand physics of tokamak plasmas. The dynamics of internal transport barrier formation and the relation between the core confinement and the L-mode base were investigated. Progress was also made on the study of MHD instabilities. Surveys on the universality of vertical displacement event (VDE), the effect of polarization current on neoclassical tearing mode (NTM), the feasibility of suppressing NTM by electron cyclotron current drive (ECCD) and divertor characteristics in JT-60SC were carried out. The NEXT (Numerical EXperiment of Tokamak) project has been progressed in order to research complex physical processes both in core and in divertor plasmas by using massively parallel computers. Substantial progresses were made in the studies of turbulence and MHD reconnection and codes were developed to analyze divertor transport in a realistic geometry.

Research and development of fusion reactor technologies have been carried out both to assure the technologies required for the construction of ITER and to accumulate technological data base to assure the design of DEMO, which include the development of the blanket for electric power generation and of reduced activation structural materials and their neutron irradiation facility. Major achievements in the area of fusion reactor technologies in this fiscal year are as follows;

1) Superconducting Magnet: A Nb_3Sn test coil, wound with a diameter of 1.5 m by the Efremov Institute, Russia, successfully generated the target magnetic field of 13 T stably at an operating current of 46 kA at JAERI facility.
2) Neutral Beam Injection: A hydrogen negative ion beam with an intense current density of 31 mA/cm^2 was successfully achieved at a low pressure of 0.1 Pa. The ion beam with a current of 37 mA was accelerated up to a high energy of 0.97 MeV.
3) Radio Frequency Heating: An advanced wave launching system called “Remote Steering Launcher” successfully demonstrated a steering capability of +/-10º at 500 kW RF beam power.
4) Blanket: By a blanket designed with a pebble-bed of Li_2TiO_3, the local tritium breeding ratio of 1.4 was expected, assuring the overall TBR of more than 1 in a fusion device
5) Structural Materials: Radiation hardening of F82H low activation steel was reduced with

tempering temperatures above 700°C (<835°C).

6) In the R&D of International Fusion Material Irradiation Facility (IFMIF), an intense ion source was developed and the performance of a liquid Li target was investigated in detail.
7) Tritium Technology: An irradiation of ultraviolet laser of 1 J/cm^2 successfully removed a carbon co-deposited layer with tritium on the plasma-facing components.
8) Fusion Neutronics: A micro fission chamber was developed successfully for a neutron monitor with a good response which was required for the design of the ITER.

In July 2001, nine-year ITER EDA was successfully completed. The first comprehensive design of a fusion experimental reactor based on well-established physics and technology was produced through the activities. The results of the design activities have been completely documented by the hierarchically organized ITER Final Design Report (FDR). The EDA R&D activities with extensive industrial involvement had demonstrated that the main ITER components can function properly.

Following the completion of the EDA, “Co-ordinated Technical Activities (CTA)” were started. CTA means technical activities which are deemed necessary to maintain the integrity of the international project, so as to prepare for ITER Joint Implementation. The central missions of CTA are design adaptation to the specific site(s) conditions, preparation of procurement documents, and assurance of the coherence of the ITER project including design control.

In fusion reactor design activities, a conceptual design of a power reactor with tight aspect ratio was newly proposed for cost reduction. Fuel supply by pellet injection and the erosion rate of the first wall by charge exchange neutrals and alpha particles were studied quantitatively in a fusion power reactor. High heat flux first walls, use of fusion power for fuel production and a reduction of radioactive wastes from the DEMO plant were mainly investigated from importance in socio-economic aspects.

Keywords; JAERI, Fusion Research, JT-60, JFT-2M, NEXT, Fusion Engineering, ITER, EDA
CTA, Fusion Reactor

Contents

I. JT-60 PROGRAM

Objectives of the JT-60 project are to make a contribution to International Thermonuclear Experimental Reactor (ITER) through physics R&D and to establish the physics basis for a steady state tokamak fusion reactor like SSTR. In the fiscal year of 2001, most of JT-60 experiments have been devoted to the improvement, sustainment and integration of the high plasma performance. In addition, physics on fusion plasmas has been studied under reactor-relevant conditions.

Using high-power negative ion-based neutral beam injection (N-NB, 5.7 MW, 402 keV), the record value for the fusion product ($n_i(0)\tau_E T_i(0) = 3 \times 10^{20}$ m^{-3} s keV) under full non-inductive current drive was obtained in a high-β_p ELMy H-mode discharge. In a reversed shear discharge, the DT-equivalent fusion power gain Q_{DT}^{eq} above 0.8 was sustained for 0.55s. By extension of the operational region for the high-triangularity configuration (δ=0.6 at I_p=1MA, for example), the quasi-steady state beta value, β_N = 3.05 was maintained for longer than 5 τ_E at a low safety factor q_{95} ~ 3.7. In addition, a high β_N value ~ 2.7 was sustained for 7.4s (60 τ_E), which was limited by hardware capability. With regard to extension of the high-confinement regime toward high density (high Greenwald factor), high confinement (H_{89P} ~ 2.7, where H_{89P} is the energy confinement improvement factor over the ITER89-P (L-mode) scaling) was achieved at an electron density of ~ 0.7 times Greenwald density (n_{GW}) in a reversed shear discharge at q_{95} ~ 5 using LHRF. By Ar injection, high confinement (HH_{y2} > 0.9, where HH_{y2} is the energy confinement improvement factor compared with the ITER98(y, 2) (ELMy H-mode) scaling), high density (~ 0.8n_{GW}), and high radiation loss power (~ 0.8 heating power) were simultaneously obtained in discharges with the outer separatrix strike point located on the divertor dome top.

Mechanisms of the current hole were investigated in detail by accurate current profile measurement and electron cyclotron (EC) current drive. Formation of internal transport barriers (ITBs) and transport at ITBs were extensively studied in normal- and reversed-shear plasmas. In H-mode plasmas, dynamics (the time scale, penetration depth, and poloidal asymmetric structure) of density collapse due to the type I edge localized modes (ELMs) was measured with a reflectometer. Using three reciprocating Mach probes, plasma flow reversal was observed and the mechanism of in-out asymmetry of divertor particle flux was studied. With regard to impurity behavior, chemical sputtering yields were measured at the carbon divertor tiles and accumulation of heavy impurity (Ar) inside ITBs was found in reversed shear discharges. Study on MHD instabilities, Alfvén-eigen modes, disruption and current drive progressed steadily.

The above-mentioned results were obtained using improved machine capability. For the N-NB system, high-power injection of 6.2 MW (381 keV, 1.7 s) and long-pulse injection of 10 s (355 keV, 2.6 MW) were achieved. The injection power of the four-gyrotron ECRF system reached 3 MW.

1. Experimental Results and Analyses

1.1 Sustainment of High Performance and Non-inductive Current Drive

1.1.1 Achievement of a high fusion triple product

We have performed optimization of high β_p ELMy H-mode discharges, in which important issues are (a) simultaneous achievement of high-β and high-confinement with a high fraction of non-inductive driven current and (b) steady-state sustainment of the high performance plasma [1.1-1-3]. After improvement of the power supply for poloidal coils in 2001, even at high plasma current of I_P~1.8MA, a high triangularity plasma (δ_x~0.3) can be produced for 5 s, which is much longer than the typical energy confinement time τ_E (~several hundred milliseconds). In addition, improvement of the negative ion-based NB (N-NB) injector increased the beam energy and injection power. Typical waveforms of a high β_p ELMy H-mode discharge are shown in Fig.I.1.1-1, where a high-β and high-confinement plasma was obtained after injection of N-NB (E_{NNB}=402keV, P_{NNB}=5.7MW). At t=6.5s, a high performance plasma with W_{dia}=7.5MJ, H_{89P}=2.5, HH_{y2} =1.2, β_P=1.7, β_N=2.4, $n\tau T$=3.0x10^{20} m^{-3}skeV, Q_{DT}^{eq}=0.185 was obtained under full non-inductive current drive condition (Figs. I.1.1-1 (c), (d)). Note that in evaluating the internal inductance l_i, equilibria have been reconstructed by using motional Stark effect (MSE) diagnostics. A loop voltage profile obtained by MSE diagnostics also shows V_{loop}~0V at l_i >0.7 (V_{loop} in the core region is ambiguous due to large error bars.). The fusion triple product obtained in shot E39713 exceeds the previous record (2.0x10^{20} m^{-3}skeV under full non-inductive current drive condition) by as large as 50%. Fractions of driven current by neutral beams (f_{NB}), bootstrap current (f_{BS}), and electron cyclotron wave are 48%, 50%, and 2% respectively, which are close to those required in the steady-state operation in ITER (f_{BS}~f_{NB}~0.5)[1.1-4].

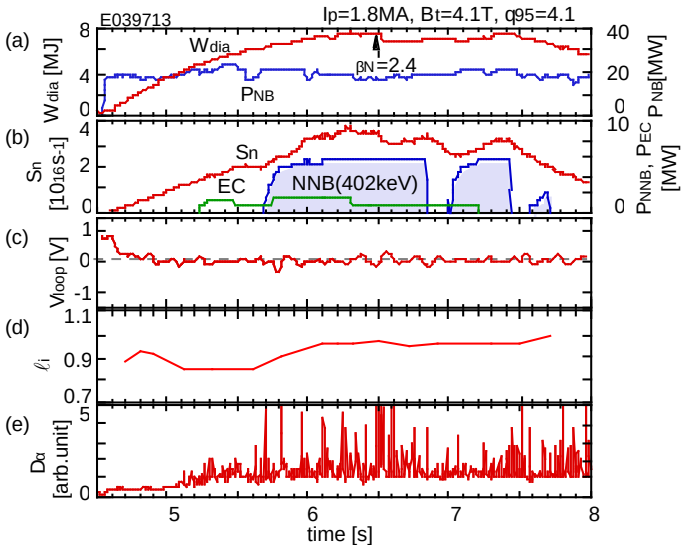

Fig. I. 1.1-1 Typical waveforms of a high β_p H-mode discharge.

1.1.2 High Fusion Performance Experiments with Reversed Shear Plasmas

High current (I_p>~2.5MA) reversed shear experiments with a high elongation configuration was performed aiming at a new record of DT-equivalent fusion power gain (Q_{DT}^{eq}) and extension of the duration of Q_{DT}^{eq} >1. In parallel with high performance experiments, physics studies on reversed shear plasmas including internal transport barriers (ITBs), MHD stability and plasma disruption, were also planned and various data were obtained. The previous record of

Q_{DT}^{eq} was 1.25, which was achieved in 1998 [1.1-5] and the longest duration of Q_{DT}^{eq} >1 was ~140 ms in the same discharge. To improve the fusion performance, impurity reduction, confinement improvement with pellet injection, H-mode transition, enlargement of ITB radius and/or N-NB injection were attempted. The results of each trial are described below.

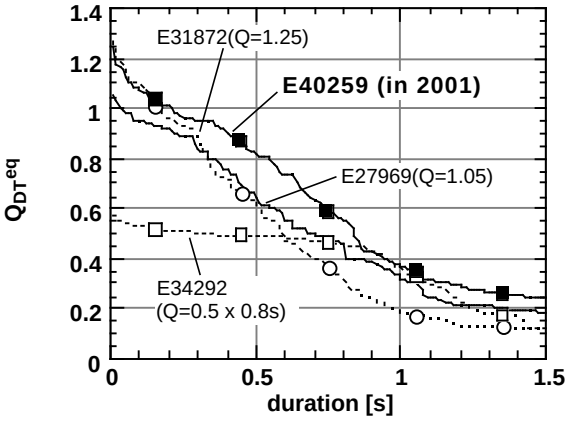

Fig.I.1.1-2 Q_{DT}^{eq} as a function of sustained duration.

1) Impurity reduction: Impurity reduction was attempted by lowering the wall temperature (T_{wall}), wall conditioning with boronization, pellet injection and gas puffing. In a preliminary experiment, reversed shear plasmas were produced and compared with T_{wall} of ~280 °C, which is a standard case, and ~150 °C. High performance plasmas with Q_{DT}^{eq}~1 were also obtained with T_{wall} of 150 °C and no serious problems were encountered during the wall conditioning after the disruption. The value of Z_{eff} was reduced from 3.5 to 3.0 due to decrease of oxygen impurity content by lowering T_{wall}. According to this encouraging result, in the campaign in autumn, T_{wall} was fixed to 150 °C and boronization was carried out typically once per two weeks. As a result, the oxygen content was kept at a low level (~1%), but the carbon content stayed at ~4% and the neutron production rate S_n did not increase. Pellet injection and gas puffing were also attempted to improve the fuel purity, but no significant increase in S_n was observed.

2) Confinement improvement with pellet injection: It was observed that density fluctuation at the ITB layer was reduced and confinement was improved when pellets were injected into reversed shear plasmas at the current flat-top with 2.2 MA. However, no clear confinement improvement was observed, though reduction of magnetic and density fluctuations were obtained when pellets were injected during current ramp-up phase with I_p >2.2 MA.

3) H-mode: In a discharge with a strong gas puff of 10 Pam^3/s, clear L to H transition, appearance of ELMs and formation of pedestal were observed, but the ITB radius became small and S_n was low. On the other hand, in discharges with B_t = 3.73 T, which was lower than the standard value (4.05T), L to H transition was sometimes observed without strong gas puffing, but the growth of pedestal was small and no improvement of performance was obtained.

4) Enlargement of ITB radius: Optimization of pressure and current profiles through adjustment of waveforms of plasma current and heating power was attempted to enlarge the radii of q_{min} and ITB and improve the confinement. A new discharge scenario was employed, in which EC was injected during an early phase with a limiter configuration. With injecting ECRF, the time with q_{min} ~3 was successfully passed through with higher beta (β_N~0.9) than in a standard scenario without ECRF (β_N~0.7) and larger radius of q_{min} was obtained. However, collapses at I_p

~ 2.2 MA (q_{min} ~ 2.4, q_{95} ~ 3.7) were frequently observed. These collapses were suppressed by reducing the ITB strength by reducing the central heating power and applying gas puffing. In a shot E40259, the plasma was maintained for 0.3 s during 2.6 MA flat-top and high performance was achieved. The peak value of Q_{DT}^{eq} in this discharge was 1.24 and the duration of $Q_{DT}^{eq}>1$ was ~140 ms, both of which were close to or equal to the previous records. Other parameters are I_p = 2.60 MA, q_{95} = 3.3, W_{dia} = 8.3 MJ, S_n = 4.6x10^{16} n/s, β_N = 1.6, τ_E = 0.89 s, H_{89P} = 3.0. The time-derivative of plasma stored energy, dW_{dia}/dt, was small and hence P_{DT}^{eq}/P_{NB}^{abs} reached 0.8. The duration of $Q_{DT}^{eq}>0.8$ reached 0.55 s and was extended from the previous value (0.35 s) as shown in Fig.I.1.1-2.

5) N-NB injection: N-NB was injected into reversed shear plasmas aiming at control of magnetic shear in the central region, reduction of ripple-induced fast ion loss by replacing perpendicular NBs, improvement of stability by changing the pressure profile. Though the effects of the first two were unclear, improvement of stability was obtained. In a shot with N-NB injection, $Q_{DD} = P_{DD}/P_{net}$ reached 6.0x10^{-3} and the record value of Q_{DD} (5.7x10^{-3}) was renewed. However, the fraction of fast ion component was large and Q_{DT}^{eq} was 0.7.

References

[1.1-1] Kamada, Y., *et al.*, *Fusion Energy 1996*, Proc. Int. Conf., Montreal (IAEA, Vienna, 1997) **1**, 247(1997).
[1.1-2] Kamada, Y., *et al.*, Nucl. Fusion **39,** 1845 (1999).
[1.1-3] Isayama, A., *et al.*, Nucl. Fusion **41,** 761 (2001).
[1.1-4] Shimomura, Y., *et al.*, Nucl. Fusion **41,** 309 (2001).
[1.1-5] Fujita, T., et al., Nucl. Fusion **39**, 1627 (1999).

1.2 Study of Improved Confinement

1.2.1 Internal Transport Barrier (ITB)

ITB is one of the attractive phenomena in magnetically confinement plasmas from a viewpoint of its reduced transport and accompanying substantial bootstrap current. Motivated by this property, goals of ITB study in JT-60 was set on (i) understanding the physics of ITB formation and transport characteristics, and on (ii) development of control methods of ITB, e.g. degree of reduced transport and radial position of ITB; both of the two should be addressed in connection with its application to future devices.

This year, we first carried out systematic parameter scan to examine heating power required for ITB formation (P_{th}) in relation to the objective (i) mentioned above. Formation properties of ITB have been studied in weak positive magnetic shear (PS) plasmas and reversed magnetic shear (RS) plasmas by changing the heating power. Two features of the ITB formation were experimentally confirmed [1.2-1]: (1) A weak ITB is formed in spite of the absence of an apparent transition in an ion temperature profile ($T_i(r)$); (2) On the other hand, a strong ITB appears with an apparent transition from weak one (Fig I.1.2-1). In case of weak positive magnetic shear plasmas, ion thermal diffusivity (χ_i) in the core region shows L-mode state, weak ITB or strong ITB depending upon the heating power. In case of reversed magnetic shear

plasmas, however, no power degradation of χ_i is observed. This suggests that there is no P_{th} for the formation of the weak ITB in reversed shear case. In addition, it was found that the χ_i for the weak ITB is gradually reduced with increasing heating power.

Dependence of P_{th} on global parameters such as plasma current (I_p), toroidal magnetic field (B_T) and safety factor (q_a) in the reversed shear plasmas was examined. Here, we tested a criterion of ITB formation as $\chi_i / \chi_i^{NC} < 1/2$, where χ_i is experimentally derived ion thermal diffusivity and χ_i^{NC} is based on neo-classical theory [1.2-2]. This kind of definition is useful when we quantify the magnitude of reduction in χ_i, i.e. ITB quality, even for different global parameters. Quantitatively speaking, this criterion roughly corresponds to the regime of transition from weak ITB to strong ITB in reversed shear case shown in Fig I.1.2-1. Transport analysis was carried out in the quasi-steady state, where plasma stored energy was almost constant. Line averaged electron density (n_e) in the target plasmas was fixed at a constant value ($n_e = 1 \times 10^{19}$ m^{-3}). Also the profile shape of the safety factor was fixed among plasmas with different I_p and/or B_T. The threshold absorption power was 6-8MW for I_p/B_T=1.3MA/3.73T, ~3MW for I_p/B_T=0.73MA/3.73T and ~3MW for I_p/B_T=0.73MA/2.10T. Although there was slight coupling between I_p and n_e, positive dependence of P_{th} on I_p was confirmed. No significant dependence of P_{th} on B_T was observed.

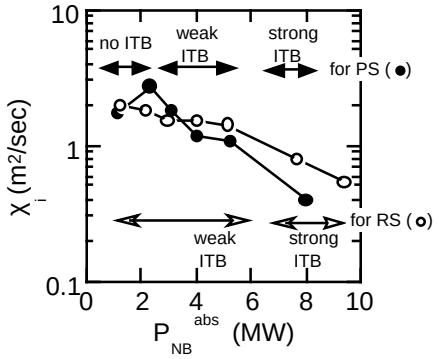

Fig.I.1.2-1. Relation between P_{NB}^{abs} and χ_i at r/a~0.46 for the cases of PS (closed circles) and RS (open circles) in a series of P_{NB} scan. In the case of weak ITB, χ_i decreases gradually with increasing P_{NB}^{abs} for both PS and RS plasmas.

Secondly, particle and heat transport of ITB plasmas was studied where impurity transport, a relationship between helium diffusivity (D_{He}) and χ_i, and a role of density fluctuation were addressed for the objective (i) mentioned above. In the RS plasma with highly improved energy confinement (H_{89P}=2.8), helium and carbon density profiles are flatter than or similar to the electron density profile. In the high-β_p ELMy H-mode plasma (H_{89P}=2.0), both helium and carbon density profiles are flat. These results indicate that light impurities such as helium and carbon are not accumulated inside the ITB. On the other hand, in the Ar injected RS plasma with the box-type ITB, the measured soft X-ray profile is much more peaked than that calculated by assuming the argon density profile same as the electron density profile, suggesting accumulation of heavy impurity ions such as argon inside the ITB. The value of D_{He} seems to be linked with χ_i. However, the ratio of D_{He}/χ_i varies in the range of 0.2-1.0 in both RS and high-β_p ELMy H-mode plasmas. As the ion temperature profile changes from parabolic- to box-type, D_{He} decreases by a factor of about 2 as well as χ_i in the RS plasma. Clear reduction of density fluctuation has been observed, when a pellet is injected into RS plasma with a strong ITB. The stored energy starts to increase from the onset of the reduction in density fluctuation. The

central ion temperature is not changed, while the central density increases inside the ITB, which suggests different dependence of particle and heat transport on the reduction of density fluctuation.

Thirdly, the ITB foot location (ρ_{foot}) was found to be as large as nearly 90% of the minor radius in a RS plasma. The ITBs in T_i, T_e and n_e are located almost at the same position. These wide ITBs are desirable from a viewpoint of confinement, since confinement is expected to increase with ρ_{foot} in RS plasmas. The ITBs locate in the vicinity of the minimum q as usual RS plasmas. Therefore, the q profile is reversed to a large extent in the plasma cross-section. In other words, the inside of nearly 90% of the minor radius is negative shear region. This is very different from usual tokamak plasmas in which all or most of the plasma is in positive shear region. Furthermore, such an ITB with large ρ_{foot} was observed with an H-mode edge in some cases. Although ELMs were not so frequently observed so far, no clear interaction has been observed. However, these plasmas with wide ITB are presently unstable: the plasma disrupts shortly after ITB expands up to 90 % of the minor radius. In some sense it is not surprising, since RS ITB plasmas are unstable by nature against both ideal and resistive MHD modes. Extension of the life time of these wide ITBs would largely deepen studies of ITB physics, including an interaction between ITB and edge transport barriers (ETBs).

1.2.2 Study of Electron Heating on ITB Plasmas

Sustainment of ITB is one of the most effective schemes in achieving high confinement and high bootstrap fraction in a plasma. Therefore, ITB is a very important issue in the research of steady state operation of a fusion reactor. Although very impressive and important results in high performance ITB plasmas have been achieved, most of them have been obtained in NBI heated plasmas in the dominant ion heating regime. In a fusion plasma, electron heating by α particles is predominant. Ions are heated via collision with electrons. Therefore T_e is expected to be higher than T_i. For stability of ITG mode, which can be a dominant source of anomalous transport, it is expected that the mode can be unstable as T_e/T_i increases near unity. Therefore it is important to investigate formation and sustainment of ITB under dominant electron heating. On JT-60U, electron heating in ITBs, both negative and positive magnetic shear plasmas, using RF and N-NB injection has been investigated [1.2-3, 1.2-4].

Electron heating in RS plasmas: In RS plasmas it has been confirmed that even with strong electron heating or $T_e >> T_i$, no harmful effect has been observed. For example, in an RS plasma of I_p = 1.35 MA high confinement of H_{89P}=2.9 and HH_{y2}=1.5 was maintained by directly feeding more power to electrons than to ions with $T_e > T_i$. In other cases, ITBs in n_e, T_i and T_e were maintained with T_e/T_i ~2.

Electron heating in PS plasmas: On the contrary, it has been observed that in PS plasmas, T_i ITB is degraded or even lost with ECRF heating. In PS plasma of 1 MA, T_i ITB was formed

with about 10 MW of NBI heating. After the T_i ITB was formed, about 1.5 MW of ECRF power was injected near on axis. As T_e increased, T_i started decreasing to the contrary. The profile of T_i which had indicated an ITB structure before the ECRF injection became smoother as T_i decreased. That suggests degradation of the T_i ITB. The V_t profile had a notch structure at the ITB location before the ECRF injection. The notch structure is closely related to the existence of T_i ITB. With the injection of ECRF, it was found that the notch structure was lost and the V_t profile became flatter as the T_i profile became smoother. This is also an indication of the degradation or loss of the T_i ITB. Detailed conditions for such ITB degradation should be investigated systematically in future experiments.

1.2.3 Relation between Core and Edge in ELMy H-mode Plasma [1.2-5]

The energy transport properties in case of the temperature profile stiffness were investigated for high triangularity and Ar gas injected ELMy H-mode plasmas. The temperature profiles of the plasma core ($0.2 < r/a < 0.8$) are self-similar for all triangularities. At low triangularity, χ_{eff} is raised with a similar temperature profile including the plasma edge as the heat flux increases. However, in high triangularity discharges, the boundary temperature is raised with an increase in β_p due to high NB heating power while the core $(\ln T_i)$ remains nearly unchanged. In Ar seeded plasmas, the temperature becomes higher than that of the case without Ar injection at a fixed density throughout the entire range of the minor radius. The conductive heat flux is reduced with increasing the radiation loss flux due to Ar gas injection and thus χ_{eff} decreases. Higher boundary temperature is obtained at lower pedestal density due to the peaked density profile in Ar seeded discharges. When the temperature profiles are nearly compatible at different densities between D_2 and D_2 + Ar injected plasmas, a small reduction in χ_{eff} is observed due to the increase in the radiation loss flow in Ar gas injected plasmas.

References

[1.2-1] Sakamoto, Y., et al., submitted to 2002 IAEA Conf., "Property of Internal Transport Barrier Formation in JT-60U".
[1.2-2] JT-60 Team., Review of JT-60U Experimental Results in 1997, JAERI research **98-039** (1998).
[1.2-3] Ide, S., et al., J. Plasma Fusion Res., SERIES, **4**, 99 (2001).
[1.2-4] Ide, S., et al., J. Plasma Phys. Control. Fusion, **44**, A137 (2002).
[1.2-5] Urano, H., et al., Plasma Phys. Control. Fusion, **44**, A437 (2002).

1.3 MHD Instabilities, ELM, Disruption and High Energy Particles

1.3.1 Resistive Instabilities in Reversed Shear Discharges and Wall Stabilization

Two of the resistive MHD activities observed in reversed shear discharges are identified as the resistive interchange modes (RIMs) and the resistive wall modes (RWMs) [1.3-1, 1.3-2]. The RIM is characterized by a localized burst-like MHD activity with $n > 3$ observed in the negative shear region with large pressure gradient near the internal transport barrier (n is the toroidal mode number). While the RIM itself has no significant effect on the internal transport

barrier and stored energy, it can cause a major collapse through non-linear coupling with a tearing mode in the positive shear region. The RWMs are observed associated with ideal magneto hydrodynamic current-driven ($\beta_N < 0.2$) and pressure-driven ($\beta_N > 2.4$) kink modes with low toroidal mode number n ($n = 1$). The pressure-driven RWM occurs at the plasma toroidal rotation of about $0.01v_A$ without clear continuous slowing down of the plasma toroidal rotation (v_A is the Alfvén velocity). Occurrence of the $n = 1$ RWMs results in a thermal quench accompanied by higher-n modes ($n \geq 2$). In the case of the current-driven RWMs, the thermal quench occurs only at the peripheral region just after the RWM. In case of the pressure-driven RWMs, on the other hand, the thermal quench occurs in the whole plasma region with drastic growth of the RWM, whose growth rate ranges from an order of τ_w^{-1} to larger than $10^2\ \tau_w^{-1}$ (τ_w^{-1} is the resistive diffusion time of the wall).

1.3.2 Development of a Real-time Tearing Mode Stabilization System

In high β_p H-mode discharges, neoclassical tearing modes (NTMs) such as m/n=3/2 and 2/1 appear and limit the achievable beta (m is the poloidal mode number). It was demonstrated that the structure of a magnetic island can be measured by using the heterodyne radiometer and that a 3/2 NTM can be completely stabilized by using the 110 GHz ECRF system [1.3-3] encouraging to develop a real-time NTM stabilization system. In the real-time system, the standard deviation of electron temperature perturbations is considered as a measure of the amplitude of the NTM. The method is advantageous in that the mode amplitude can be evaluated without calculating the mode frequency. In 2000, the amplitude of electron temperature perturbations was evaluated every 10 ms, and EC wave was injected about 200 ms after the mode onset, which is much shorter than the typical time scale for the mode growth [1.3-4]. In 2001, the system has been upgraded, where the mode location is identified in real-time and EC injection angle is changed so that the EC wave is deposited at the center of the magnetic island. Initial result shows that the EC mirror is successfully steered in accordance with the target value of the EC injection angle. Real time execution of equilibrium reconstruction, identification of the mode location, and EC mirror steering is planned in 2002.

1.3.3 Dynamic Behaviors of Type I ELM

Detailed dynamic behaviors of the collapse due to type I ELM were measured using O-mode reflectometer. The collapse reached 10 cm inside the separatrix, which corresponds to twice the pedestal width of 5 cm. When we assume that the density collapse is poloidally uniform, the number of lost particles by an ELM is estimated to be 2.3×10^{20}, which is much larger than the particle source of $<10^{19}$ during an ELM including enhancement of the divertor recycling. This result suggests asymmetry in collapse of the density pedestal. In order to confirm the asymmetric ELM structure, simultaneous measurements of edge density on the high-

field side (HFS) and low-field side (LFS) plasma was performed using the FIR interferometer (FIR-U1) and the reflectometer, respectively. If the collapse was a poloidally symmetric event, the line-integrated density on FIR-U1 would be reduced by 0.57×10^{19} m^{-2} as shown in Fig. I.1.3-1. There was, however, no response on FIR-U1 before the increase of D_α^{div} signal. When FIR-U1 measured only the HFS SOL plasma by horizontal plasma shift, we also confirmed that there was no clear density increase before the increase of D_α^{div} signal. These results indicate that collapse of the density pedestal occurs only around the LFS midplane. [1.3-5]

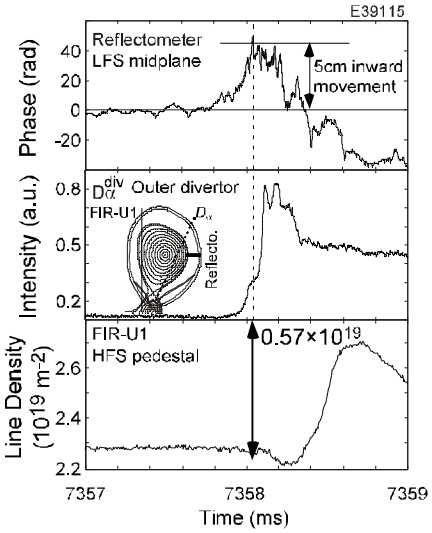

Fig. I.1.3-1. Time evolution of phase change of reflectometer signal, D_α intensity and line-integrated electron density during an ELM.

1.3.4 ELM Activity with Injecting Ar and Changing Plasma Configuration [1.3-6]

Heat flux due to ELMs can be changed by injecting Ar and changing the plasma configuration. In Ar injected ELMy H-mode plasmas with I_p = 1.2 MA, B_T =2.5 T and δ ~0.35, the outer strike point position was moved from the dome-top to the dome-side with the same shape of main plasma. Although electron density, radiation loss power, Ar XV line emission, NB heating power, stored energy were almost constant during this phase, the ELM activity changed rapidly after changing the strike point position. Then, key pedestal parameters for ELM activities such as triangularity, safety factor at 95% of the minor radius, ion collisionality, ion temperature gradient at the shoulder of the pedestal and pedestal stored energy were almost the same. It suggests that this rapid change of ELM activity cannot be explained simply by the above measured parameters.

1.3.5 Giant and Grassy ELMing Regime

The operational regimes of giant and grassy ELMing discharges are characterized by the plasma parameters such as q_{95}, δ_X and β_p. MHD Stability analysis for these discharges supports the explanation of ELM phenomena by peeling-ballooning instability. Both current density and pressure gradient in the edge drive peeling-ballooning instability. In order to clarify the roles of infinite-n ballooning modes and lower-n peeling-ballooning modes in ELM phenomena, edge current profile modification by plasma current (I_p) ramp was attempted. Theoretically, it is expected that infinite-*n* ballooning modes are stabilized in I_p ramp-up and destabilized in I_p ramp-down due to change of the edge magnetic shear and peeling-ballooning modes are destabilized in I_p ramp-up and stabilized in I_p ramp-down. Plasma current ramp-up during grassy ELM state increased the ELM amplitude and changed the ELM character to type I as shown in

Fig.I.1.3-2 (a). Decreasing edge current by I_P ramp-down during giant ELM state, pure grassy ELM state was obtained at q_{95}=3.7, δ_X=0.5 and β_p=1.6, where normally giant ELMs are expected (Fig.I.1.3-2 (b)). These results indicate that the amount of edge current affects ELM size and support the peeling-ballooning ELM model.

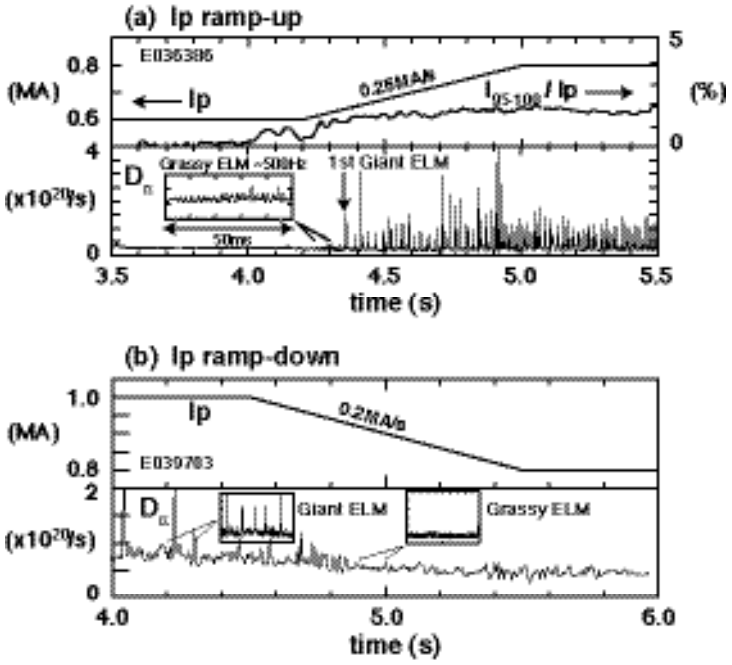

Fig. I.1.3-2. ELMs with (a) I_p ramp-up or (b) I_p ramp-down.

1.3.6 Alfvén Eigenmodes

Two topics of Alfvén Eigen-modes (AEs) have been mainly studied. One is the property of AEs in RS and weak shear (WS) plasmas. The other is the transport of energetic ions induced by AEs. The observation of rapid frequency chirping modes in low-β_h (β_h is the beta value of energetic particles) RS discharges with N-NB injection or ICRH can be explained by considering the properties of reversed-shear-induced AE (RSAE) near q_{min} and their coupling to toroidal AEs (TAEs). We verify the existence of RSAEs and their coupling to TAEs for the first time from magnetic fluctuations and measured q-profile in JT-60U plasmas. The resonance condition for the RSAEs is the same as for global Alfvén eigenmodes (GAEs), however, RSAE is predicted to be much more localized near q_{min}. The frequency of respective AEs is as follows:

1. HRSAE, $f_{HRSAE} \sim V_A/(2\pi R)(n\text{-}m/q_{min})$: $\{(m+1/2)/n + c < q_{min} [< (m+1)/n]\}$
2. LRSAE, $f_{LRSAE} \sim -V_A/(2\pi R)(n\text{-}(m+1)/q_{min})$: $\{(m+1/2)/n + c < q_{min} [< (m+1)/n]\}$
3. TAE, $f_{TAE} \sim V_A/(4\pi R q_{TAE})$, $q_{TAE} = (m+1/2)/n$: $\{[m/n<] q_{min} < ((m+1)/2)/n + c\}$

Where c is constant $c \sim r_{min}/(nR)$ and R is the major radius of plasma. Because AEs are very sensitive to q profile, especially q_{min}, it is important for AE experiment to measure accurate q-profile. Recent progress of the q-profile measurement with MSE including reconstruction of magnetic surface is outstanding. Magnetic field of the NNB-AE experiment in the JT-60U RS plasma is relatively high (B_T=3.7T) for more accurate q-profile measurement. In this condition, the beta value of energetic particles is relatively low ($<\beta_h>\sim$0.1-0.2) and is approximately equal to that of ITER. Above equations can explain the observed frequency sweep of the n=1 NNB-AE. The amplitude of the magnetic fluctuation is largest corresponding to the transition from the RSAE to the TAE as predicted by numerical calculation [1.3-7]. The n~2-11 AEs with

upward sweeping frequency destabilized by ICRF in the JT-60U RS plasma can be also reproduced with calculation of above equations.

Drop of the neutron emission rate and increase in fast neutral fluxes have been observed as a result of enhanced radial transport of fast ions during the bursting modes. The increased fast neutral flux is consistent with the wave-particle resonance and loss mechanism [1.3-8] depending on its energy. Recently we have measured the neutron emission profile for investigating fast ion transport further. On occurrence of ALE bursting modes [1.3-9] in the plasma of V_b/V_A~1 and $<\beta_h>$~0.6 %, peripheral signals ($r/a \geq 0.48$) increase and center signals ($r/a \leq 0.34$) decrease, which shows the redistribution of energetic ions. It is estimated by OFMC code that the fast ion profile around r/a~0.2-0.4 is steep. This suggests that fast ions in such region mainly interact with AE modes and such steeper gradient is relaxed in terms of redistribution of the fast ions to the outer plasma region of r/a>~0.4.

1.3.7 Disruption Study

Several experiments were carried out on topics in disruption avoidance and mitigation studies such as: i) sensitivity of neutral point, ii) fast plasma shutdown by gas injection.

i) Sensitivity of neutral point: Recent international collaboration with Alcator C-Mod and ASDEX-Upgrade clarifies that “neutral point” does exist widely in any tokamak, and “neutral point” appears to have its individual character [1.3-10]. As a next step, further understanding of robustness or sensitivity of “neutral point” to plasma shape parameters is required to establish VDE avoidance in a fusion reactor like ITER. For this purpose, the experiment was carried out to study the VDE behaviors by scanning the height of plasma current center Z_j of 8 to 20 cm for different plasma triangularity δ of 0.1 and 0.4, and for different plasma current profile made by current ramp-up and ramp-down. Consequently, the neutral point was confirmed to exist around Z_j ~14 cm in consistent with the previous understanding in JT-60U. It was found that the speed of displacement was slower in high δ case than that in the low δ case. Additionally, the VDE behavior in high δ case is less sensitive to the current profile in comparison with the low δ case. This behavior was theoretically investigated by means of computer simulation.

ii) Fast plasma shutdown by gas injection: Simultaneous injection of impurity and deuterium (or hydrogen) into a plasma is an attractive plasma shutdown method, where impurity contributes to plasma cooling and stored energy dissipation via enhancement of radiation power, and deuterium (or hydrogen) contributes to enhancement of radiation power and increase in the threshold of electric filed for runaway electron generation. In 2000, its feasibility was confirmed by utilizing the gas injection of argon impurity and hydrogen for fast shutdown with few runaway electrons [1.3-11]. Considering the cooling rate of impurities, krypton is expected to be preferable than argon for reducing the heat flux to the divertor plate and avoiding runaway electron generation. In 2001, the experiment to compare characteristics of plasma shutdown

with krypton, argon, and xenon was performed. As a result, the heat flux to the divertor plate was reduced for with gas injection of krypton and hydrogen in comparison with other impurities. This shows krypton is the suitable impurity to use for fast plasma shutdown.

References

[1.3-1] Takeji, S., Tokuda, S., Fujita, T., *et al.*, Nucl. Fusion, **42**, 5 (2002).
[1.3-2] Takeji, S., Tokuda, S., Kurita, G., *et al.*, J. Plasma Fusion Res., **78**, 447 (2002).
[1.3-3] Isayama, A., Kamada, Y., Ide, S., *et al.*, Plasma Phys. Control. Fusion, **42**, L37 (2000).
[1.3-4] Isayama, A., Ikeda, Y., Ide, S., *et al*., '*Radio Frequency Power in Plasmas*' (Proc. 14th Topical Conference on Radio Frequency Power in Plasmas (Oxnard, California, USA), American Institute of Physics, New York, Nov. 2001, ISBN 0-7354-0038-5) pp.267-274.
[1.3-5] Oyama, N., et al., "Asymmetry of Collapse of Density Pedestal by Type I ELM on JT-60U", submitted to Nuclear Fusion.
[1.3-6] Higashijima, S. and JT-60 team, "Control of Divertor Heat Load by Ar Injection with Keeping High Performance in ELMy H-mode Plasmas on JT-60U" submitted to J. Nucl. Mater..
[1.3-7] Fukuyama, A., et al., Proceeding of 6th IAEA Technical Committee Meeting on Energetic Particles in Magnetic Confinement Systems (12~14 October 1999, Naka).
[1.3-8] Kusama, K., et al., Nucl. Fusion 38, 1215 (1998).
[1.3-9] Shinohara, K., et al., to be published in Nuclear Fusion (2002).
[1.3-10] Nakamura, Y., Pautasso, G., Gruber, O., et al., "Axisymmetric Disruption Dynamics Including Current Profile Changes in the ASDEX-Upgrade Tokamak", Plasma Phys. Control. Fusion (in press).
[1.3-11] Bakhtiari, M., Kawano, Y., Tamai, H., et al., "Fast Plasma Shutdown Scenarios in the JT-60U Tokamak Using Intense Mixed Gas Puffing", accepted for publication in Nuclear Fusion.

1.4 Heating, Current Drive and Plasma Control

1.4.1 Study on Current Hole

A stable tokamak plasma with nearly zero toroidal current in the central region (a "current hole") has been sustained for several seconds in the JT-60U tokamak for the first time [1.4-1]. Figure I.1.4-1 shows radial profiles of current density (j) and ion and electron temperatures (T_i and T_e) in a typical discharge with q_{95}~5. The radius of the current hole extended up to ~40% of the plasma minor radius and the absolute value of q(0) was estimated to be greater than 70. Though the profiles of T_i, T_e and electron density (n_e) were extremely flat in the current hole, ITBs were formed outside the current hole, and high temperature plasmas were confined in the current hole by ITBs. In this discharge, the current hole with a normalized radius of ρ>0.25 was maintained for 4-5 s (~$10\tau_E$) without any global MHD instabilities. These observations imply the possibility of stable operation of tokamaks with no toroidal current at the axis.

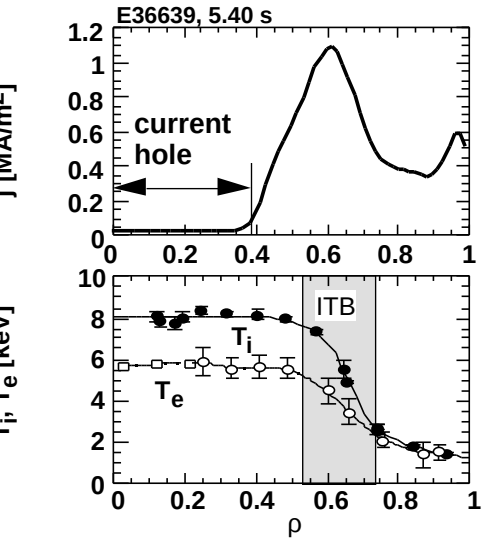

Fig.I.1.4-1. Radial profiles j, T_i and T_e in a plasma with a current hole. From [1.4-1].

It was observed, by starting the injection of MSE beam at the plasma breakdown, that j(0) was not zero but positive just after the breakdown and started to decrease during the increase of off-axis bootstrap current and that the current hole was fully formed. This indicates that decrease in the toroidal electric field $E_\varphi(0)$, caused by the increase of the off-axis non-inductive current, is a cause of the formation of the current hole. This process was also

involved in the formation of the current hole in JET where the lower hybrid current drive supplied the off-axis non-inductive current [1.4-2].

The above process can lead to negative j(0) in principle, but no significant negative j(0) has been observed so far but j(0) was kept nearly zero for several seconds. This suggests that the current hole is not a result of a transient zero $E_\varphi(0)$ near the axis, but some mechanism works to clamp j(0) at zero level. One possibility is that j(0) cannot be negative even with negative $E_\varphi(0)$ for some reason and is therefore kept zero. Resistive kink instability was proposed to explain the absence of negative j(0) [1.4-3], but this is unlikely to be the case in JT-60U where no MHD instabilities are observed. To address this issue, response to current drive by electron cyclotron waves (ECCD) was investigated. An EC wave of 0.8 MW was injected at r/a ~0.15 or into the current hole with n_e~1.4x10^{19}m^{-3} and T_e~5.9 keV. The expected EC-driven current was 53 kA, but no change (no generation) of current density was observed in the current hole in 0.5 s. On the other hand, a peak of current density was generated at r/a~0.15 within the same time scale when EC was injected into a plasma without the current hole and with similar n_e and T_e. This suggests that the EC wave cannot drive the current in the current hole or $E_\varphi(0)$ was highly negative and eliminated the EC-driven current (however j(0) was not negative but zero), either of which strongly supports existence of mechanism to clamp j(0) at zero level.

1.4.2 Current Drive by Electron Cyclotron Waves

Particles trapped in the toroidicity induced magnetic well are considered to reduce non-inductively driven current. The so-called trapped particle effect affects also the efficiency of ECCD. ECCD is important for the current profile control of a tokamak plasma to suppress instabilities, such as sawtooth instability or neoclassical tearing mode (NTM). Experimental validation of the ECCD theory is underway, and hence the trapped particle effect on ECCD was studied, since it affects the required EC power for the current profile control.

Trapped particle effect was investigated on normalized CD efficiency $\zeta=e^3\eta_{CD}/\varepsilon_0{}^2kT_e$, where T_e is electron temperature at CD location and current drive efficiency η_{CD} is defined as $\eta_{CD}=I_{EC}n_eR_p/P_{abs}$, where I_{EC}, n_e, R_p, P_{abs} represent EC driven current, averaged electron density, plasma major radius, and absorbed EC power, respectively. Increase in η_{CD} along with T_e is included in ζ. It is expected that the normalized

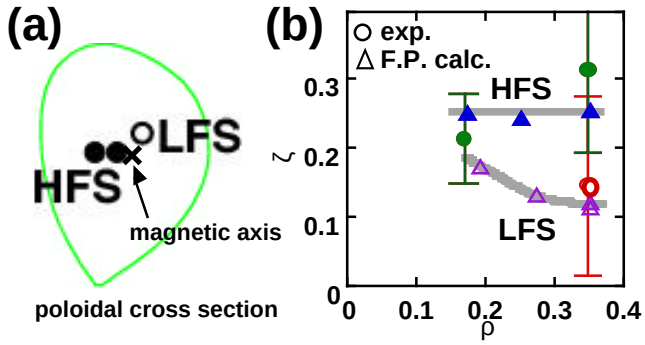

Fig. I.1.4-2. (a): Schematic view of the CD location in the experiment. (b): Normalized current drive efficiency ζ against the CD location in normalized minor radius ρ. Circles and Triangles represent experimental and calculated results, respectively. Open and closed symbols indicate deposition locations for LFS and for HFS, respectively in (a) and (b).

CD efficiency is different between higher field side (HFS) deposition (smaller trapped particle effect) and lower field side (LFS) deposition (larger effect). Since the fraction of the trapped particle is considered to be a function of inverse aspect ratio, dependence of ζ on minor radius is also expected. Two curves in Fig. I.1.4-2 show the expected ζ by the linearized Fokker-Planck calculations including the trapped particle effect. The lower curve represents the LFS deposition, showing reduction in ζ with minor radius. The upper curve is for the HFS deposition, where no significant decrease in ζ. Thus we can experimentally validate the ECCD theory on the trapped particle effect, when the deposition location is changed by toroidal field and by steerable antenna of EC waves. Experimental measurement of EC driven current is based on the loop voltage profile analysis which evaluates transient inductive electric field in the plasma [1.4-4]. Circles (closed/open) denote measured ζ in HFS/LFS deposition respectively. They seem to agree with the calculated values. Significant decrease (by a half) in ζ is seen in the case of LFS deposition at ρ=0.35.

1.4.3 Plasma Current Start-up without Center Solenoid

In usual tokamaks, plasma current is initiated and increased inductively with a use of center solenoid coils. However, center solenoids require certain space around a torus axis. It is desirable to remove the center solenoid for designing a compact tokamak reactor. There is a significant merit of cost saving. Especially, for spherical tokamaks (STs) it is difficult to design a ST reactor with center solenoids, therefore operation without center solenoid is crucial for the future. Plasma current initiation and start-up have been demonstrated in several small and medium size tokamaks by means of RF current drive such as ECCD and LHCD. On JT-60U, plasma current initiation and ramp-up were tried by means of RF and NBI current drive and heating for the first time. Although plasma current initiation has not been successful only by RF, I_p = 0.12 MA was achieved by combination of inductive flux injection by vertical field coils and ECRF injection. Furthermore I_p ramp-up by LHCD and NBI was successful from 0.35 MA, initial tokamak plasma was created by lower inductive field with assistance of ECRF, to 0.4 MA in 4.5 s in a hydrogen plasma. This research has been carried out under collaboration with University of Tokyo, Kyoto University, Kyushu University and Kyushu Tokai University.

References

[1.4-1] Fujita, T., et al., Phys. Rev. Lett., **87**, 245001 (2001).
[1.4-2] Hawkes, N. C., et al., Phys. Rev. Lett., **87**, 115001 (2001).
[1.4-3] Huysmans, G. T. A., et al., Phys. Rev. Lett., **87**, 245002 (2001).
[1.4-4] Suzuki, T., et al., Plasma Physics and Controlled Fusion, **44**, 1 (2002).

1.5 Divertor and Scrape-off-Layer (SOL) Plasma Physics and Impurity Study

1.5.1 SOL Flow and Plasma Drift Effect

SOL plasma flow plays an important role in the plasma transport along the field lines, and influences helium exhaust and impurity retention in the divertor. In 2001, plasma flow at the

high-field-side (HFS) SOL was, for the first time, measured by new reciprocating Mach probe installed at the inner baffle of the W-shaped divertor. Measurements of the SOL flow profile as well as electron density, temperature and potential profiles both at the HFS and low-field-side (LFS) determined the SOL flow pattern, which is produced by parallel and drift motions of the SOL plasma [1.5-1]. Fast sampling of ELM particle flux showed the SOL flow profile at the HFS, which was different from that at the LFS (indicating convective transport of the heat flux).

Drift flow was dominant in narrow region near separatrix (corresponding to 3-5 mm at LFS midplane), where large E_r and plasma pressure gradient were observed. At the outer flux surfaces, the drift flow became smaller than the parallel SOL flow. "Flow reversal" in the parallel plasma transport was found both at HFS and LFS near separatrix of the main plasma. The reversal of the SOL flow is presumably driven to reduce poloidal asymmetry in the drift flow, which is produced by the change in B_T [1.5-2], E_r, grad-p_i and pitch angle of the field line.

From the profiles of the parallel SOL flow ($n_iV_{//} = n_iMC_s$) and the drift flow ($n_iV_s = n_iE_r/B_T$), particle fluxes towards the HFS and LFS divertors were evaluated for the ion grad-B drift towards the divertor. Influence of the plasma drift on in-out asymmetry in divertor particle flux was investigated. At low density, particle fluxes towards the HFS and LFS divertors (including components of the parallel SOL flow and drift flow) were comparable. An E_rxB drift flow at the private flux region, evaluated by the X-point Mach probe, was found out to be a dominant contributor to produce HFS-enhanced asymmetry in the divertor particle flux under the attached divertor condition. On the other hand, when the LFS divertor was detached at high density, the E_rxB drift flow at the private flux region disappeared, and parallel SOL flow towards the LFS divertor became dominant compared to that towards the HFS divertor. Thus, LFS-enhanced in-out asymmetry was observed. This result explained reversal of the in-out asymmetries in the divertor particle flux, recycling flux and neutral pressure at the onset of detachment. It was found that, at the low density SOL, the drift flow has a large contribution to produce the plasma flux towards the divertor.

Effects of gas puff location on the SOL plasma and parallel flow were investigated for the ion grad-B drift towards the divertor. Gas puff from top of the main plasma (puff and pump) produced large enhancement (1.2-1.6 times larger) of the electron density at the HFS SOL (n_e^{HFS}) and reduction (0.7-0.8 times lower) in electron temperature, T_e^{HFS}, compared with those for gas puff from the divertor. Enhancement of the SOL flow velocity was rather small (15-20%). On the other hand, those values at the LFS SOL (n_e^{LFS} and T_e^{LFS}) were comparable for the two gas puff cases. This result suggests that the parallel SOL flow from LFS SOL to HFS divertor is produced through the plasma top. As a result, HFS-enhanced in-out asymmetry in the particle flux was increased by the increment of the parallel SOL flow towards the HFS divertor. At the same time, collisionality at the HFS SOL increased during the main gas puff, which would explain improvement of impurity shielding during the puff and pump. Application of the drift

and parallel flows on impurity transport in SOL and divertor would help understanding the in-out asymmetry in helium distribution, carbon re-deposition and tritium co-deposition at the divertor.

1.5.2 ELM Heat and Particle Transport in SOL

The SOL flow pattern after ELM event is an important issue to determine particle and impurity transport in ELMy H-mode plasma. It is also important to determine a transport model of ELM heat flow, i.e. conduction and convection. Measurements of particle flux and Mach number, simultaneously, at the HFS and LFS SOLs were performed [1.5-3]. Deposition time of heat flux, τ_{IR} = 250-350μs, was comparable to the duration of ELM-enhanced ion flux and the SOL flow velocity (i.e. Mach number increased to ion sonic level) measured with X-point Mach probe at the LFS SOL. The convective heat flux was evaluated from the ELM-enhanced particle flux with pedestal T_e and T_i, and it reaches up to 60-80% of the total heat flux measured by IRTV. This is in agreement with a good correlation found between τ_{IR} and $\tau_{//,ped}$ providing a good physics basis on which to extrapolate present experimental results to ITER. On the other hand, at the HFS SOL, the fast convective SOL flow to the HFS divertor was not observed, and the flow reversal occurred gradually (in 400-600μs) after ELM events. The heat and particle flows at the HFS SOL could not be understood by convective transport similar to the LFS SOL.

1.5.3 Impurity Study

Carbon materials have been widely used as plasma facing components in many tokamaks. Carbon, however, has the property of strong chemical reactions with hydrogen isotopes. In recent cold and dense divertor plasmas, it was found that not only CH_4 (or CD_4) but also C_2H_x (or C_2D_x) is produced by a chemical sputtering process. The chemical sputtering yields of CH_4 (or CD_4) and C_2H_x (or C_2D_x) have been measured at the carbon divertor plates of JT-60U [1.5-4]. At the surface temperature of 380, 440 and 560 K, the CH_4 yield is ~ 0.8%, 1-2% and 2-3%, the C_2H_x yield 1-2%, 3-4% and 4-5 %, and the total sputtering yield by hydrogen ions 3-4%, ~8% and ~10%, respectively. With increasing ion flux to the divertor plates (Γ_{ion}), the sputtering yields (Y) decreases, i.e. $Y \propto \Gamma_{ion}^{(-0.05 \text{ to } -0.40)}$. With increasing electron temperature (T_e), the sputtering yield increases, i.e. $Y \propto T_e^{0.5}$. It is concluded from the result of regression analysis of $Y \propto T_e^{0.5}$ [1.5-5] that the negative dependence of the yields on the ion flux ($\Gamma_{ion}^{(-0.05 \text{ to } -0.40)}$) is attributed to the sheath accelerated incident ion energies to the carbon plates. The ratio of the sputtering yield by deuterium ions to that by hydrogen ions is estimated to be $\geq$ 1.5 based on the ion flux measurement by H_α(or D_α) intensity. The C_2H_x (or C_2D_x) sputtering yield accounts for ~80% of the total number of sputtered carbon atoms. The effect of the reduction of the chemical sputtering yield on the core carbon content was investigated by lowering the wall temperature from 560 to 440 K. The carbon content was reduced by ~ 15% with ~ 40% reduction of chemical

sputtering flux in the deuterium L-mode plasma with a neutral beam heating power of ~ 4 MW.

Wall conditioning is one of the key elements to obtain high performance plasmas in nuclear fusion experimental devices. Boronization is one of the most effective methods in suppression of oxygen release from the walls. In JT-60U, boronization using deuterated-decaborane ($B_{10}D_{14}$) by a glow discharge under a helium support gas is performed every 200-500 tokamak discharges to reduce oxygen impurity [1.5-6]. In order to investigate the reduction of the core impurity content and the durability of the boronization effects systematically, about 100 discharges with identical conditions were repeated [1.5-7]. In ~ 50 shots after boronization using 70 g of $B_{10}D_{14}$, the boron content increased while the carbon content decreased due to suppression of the chemical sputtering at the carbon tiles. Since then, the boron and the carbon contents were almost constant (~0% and ~ 2.5%, respectively). In contrast to the boron and the carbon contents, the oxygen content gradually increased from ~0.8% to ~ 1.3% in ~ 500 shots. Continual boronization using 10-20 g of $B_{10}D_{14}$ every ~ 200 shots successfully kept the oxygen content $\leq$ ~ 1.0%. However, durability of boronization using 20 g of $B_{10}D_{14}$ is much shorter than that of boronization using 70 g after vacuum vessel ventilation.

References

[1.5-1] Asakura, N., et al., "Plasma Flow Measurements in High and Low Field Side SOL and Influence on the Divertor Plasma in JT-60U", submitted to J. Nucl. Mater.(2002).
[1.5-2] Asakura, N., Sakurai, S., Shimada, M., et al., Phys. Rev. Lett., **84**, 3093 (2000).
[1.5-3] Asakura, N., Sakurai, S., Naito, O., et al., Plasma Phys. Control. Fusion, **44**, A313 (2002).
[1.5-4] Nakano, T., Kubo, H., Higashijima, S., et al., Nucl. Fusion, **42**, 689 (2002).
[1.5-5] White, D.G., Tynan, G. R., Doerner, R. P., et al., Nucl. Fusion, **41,** 47 (2001).
[1.5-6] Yagyu, J., Arai, T., Kaminaga, A., et al., Proc. of 19th IEEE/NPSS Symposium on Fusion Engineering (SOFE), 152 (2002).
[1.5-7] Nakano, T., Higashijima, S., Kubo, H., et al., "Boronization Effects Using Deuterated-decaborane ($B_{10}D_{14}$) in JT-60U", accepted to J. Nucl. Mater..

1.6 High Density and High Radiation Plasmas

1.6.1 Ar Injected ELMy H-mode Plasmas [1.6-1, 1.6-2]

ITER requires high confinement ELMy H-mode plasmas with HH_{y2} = 1, radiation-loss-power fraction (P_{rad}/P_{heat}) of ~0.5, and high plasmas purity of ~80% at the density of ~0.8 n_{GW}. Confinement degradation at high density in large tokamaks [1.6-3] is still significant concern for ITER. Control of divertor heat load in high performance plasmas is also one of crucial issues for fusion devices, and large ELMs may limit the lifetime of divertor tiles. Therefore, a method to reduce ELM heat load with simultaneous achievement of high density, high radiation loss power and high confinement is necessary.

Impurity injection is one candidate to reduce divertor heat load by radiation enhancement with high confinement at high density. In JT-60U, Ar injected ELMy H-mode plasmas have been investigated. The high performance plasmas of HH_{y2}~1 could be obtained in the range of P_{rad}/P_{heat} ~0.8 at the density ~0.66 n_{GW}, and large ELMs were also observed in this discharge [1.6-4]. However, the electron density was lower than ITER requirement, and large ELMs harmful to the divertor plates could not be avoided disappeared. In order to further increase the density in high

confinement plasmas and to mitigate the ELM heat load, the plasma configuration was changed with Ar injection. Here, three plasma configurations were explored in ELMy H-mode plasmas with Ar injection. Those are (a) standard configuration with the triangularity, δ, of ~0.35 and both strike points located on the divertor, (b) dome-top configuration with δ ~0.35 and the outer strike point located on the dome top, and (c) high triangularity configuration with δ of ~0.5 and both strike points located on the divertor plate. In the dome-top configuration, an efficient fueling of deuterium and argon is expected due to particle recycling near the x-point. In the high triangularity configuration, we expected that the confinement would be improved due to a high critical edge pressure gradient and large ELMs, which are considered harmful to the divertor plates in ITER, would disappear.

Fig.I 1.6-1 (a) shows the change of HH_{y2} against the n_e/n_{GW}. In the standard configuration without Ar injection, HH_{y2} decreased from 0.9 to 0.6 as the n_e/n_{GW} increased from 0.45 to 0.66. On the other hand, the HH_{y2} was kept high in the case of Ar injection. In the standard configuration, the HH_{y2} remained ~1 up to n_e ~0.66 n_{GW}, but it rapidly decreased around 0.7 n_{GW}. The HH_{y2} in the dome-top case remained ~1 up to the density range of 0.8 n_{GW}. The HH_{y2} factor was higher in the high triangularity case than in the standard case. However, the n_e range could not extend over 0.66 n_{GW} so far. For the confinement, the improvement by ~50% could be achieved at 0.66 n_{GW} compared with the case of no Ar injection. The fuel purity, the ratio of deuterium ion density to the n_e, n_D/n_e, was decreased from ~80% to ~60% at 0.66 n_{GW}. As a result, the value of $n_D \times \tau_E^{th}$, where τ_E^{th} is the confinement time of thermal energy, was increased by ~20% by Ar injection, and furthermore the fusion product, $n_i(0)\tau_E T_i(0)$, where $n_i(0)$ and $T_i(0)$ are the deuterium ion density and temperature at the center, was increased from 1.5 to 4.4 x 10^{19} $m^{-3} \cdot s \cdot keV$ because of a significant confinement improvement.

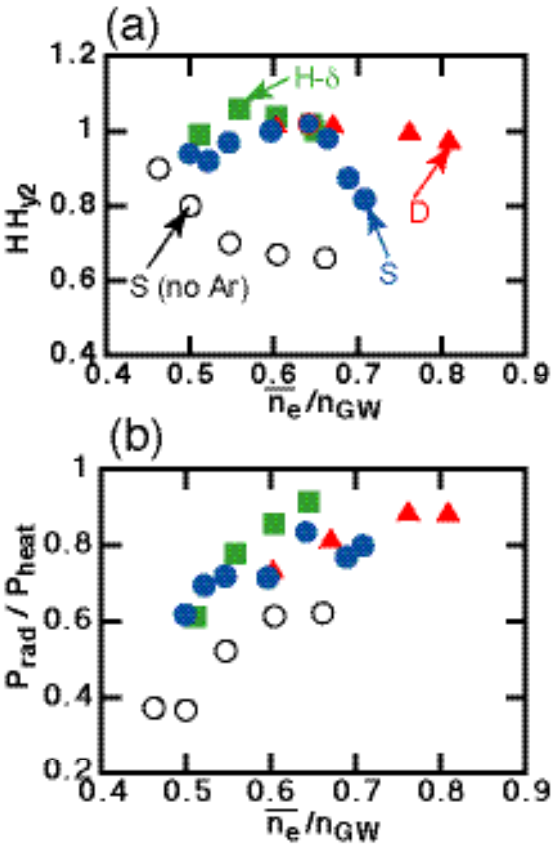

Fig.I 1.6-1. (a) HH_{y2} and (b) radiation-loss-power fraction as a function of electron density normalized by n_{GW}. Open circles; standard without Ar injection, Closed circles, triangles and squares; standard, dome-top, high-δ with Ar injection, respectively.

Fig.I 1.6-1 (b) shows radiation loss power fraction as a function of the n_e/n_{GW}. The radiation-loss-power fraction increased with the

density. With Ar injection, the radiation-loss-power fraction could achieve ~80% in the n_e range above 0.66 n_{GW} in all cases. In the standard case with Ar injection, although the ELM frequency decreased by a factor of 2, the maximum heat flux did not decrease. The decrease in the ELM frequency could not be explained by an increase in reheating time due to a decrease in the edge heating power by the edge radiation loss power enhancement. In the high-triangularity and dome-top cases with Ar injection, the maximum heat flux decreased by a factor of 3 - 5 with keeping high confinement. Ar injection with high-triangularity and dome-top configurations was effective to reduce the transient heat flux due to ELMs.

1.6.2 High Density and High Confinement in ELMy H-mode Plasmas

In order to understand physical mechanisms responsible for confinement degradation at high density and to achieve high confinement at high density in ELMy H-mode plasmas, the effects of the NB heating and gas-puffing scenarios on the confinement degradation were first investigated. High confinement at high density was obtained with I_P=1.0 MA, B_T=2.1 T, δ=0.31 and q_{95}=3.7 in the discharge where high power heating of 11-18 MW and gas-puffing of 20 Pam^3/s were simultaneously started. In this discharge, relatively fast density ramp-up (~1 s) was observed, and HH_{y2}=0.96 (H_{89P}=1.85) was achieved with $\bar{n}_e/n_{GW}$=0.61 at 0.5 s after the gas-puffing was switched off. The value of HH_{y2} in this discharge is higher than HH_{y2} of 0.7 at the similar density range in the low power heating (~9 MW) discharge and slow density ramp-up (~4 s) discharge. In the high confinement discharge, the higher pedestal temperature was observed compared with that in the low confinement discharge, and both core and pedestal confinements was improved. A good correlation between the pedestal ion temperature and HH_{y2} was observed including high and low confinement discharges. High core confinement (or high β_p) improves the edge stability by modification of edge magnetic shear due to Shafranov shift. The high pedestal pressure produced by the improved edge stability makes the high core confinement as a boundary condition through the stiffness of the core plasma profiles. This could play as a positive feedback loop for confinement improvement. A combination of high power heating and fast density ramp-up could be a method to enter the positive feedback loop. Further increase in the density to $\bar{n}_e/n_{GW}$=0.8 led to a decrease in the pedestal temperature, resulting in the confinement degradation to HH_{y2}=0.8.

Secondly, the effects of configuration on the confinement degradation were investigated in the outward shifted and large volume configurations. These configurations were expected to enhance a plasma-surface-interaction around the main plasma region. In addition, Greenwald density is small in the large volume configuration. In the outward shifted plasma, the density could be increased by a long pulse gas-puffing with a small rate of 6 Pam^3/s, however, the confinement was not high. In the large volume configuration, dependence of the confinement on $\bar{n}_e/n_{GW}$ showed similar tendency to that in the small volume configuration.

Furthermore, the effects of toroidal rotation and wall temperature were investigated. Toroidal rotation changed from counter- to co-direction in the whole plasma region by changing the combination of NB from counter-tangential (4.2 MW) and perpendicular (11 MW) injections to co-tangential (4.2 MW for PNB and 5 MW for N-NB) and perpendicular (2.2 MW) injections. However, confinement was not changed drastically in both cases. Confinement at the low wall temperature (~150^{O}C) was smaller than that at the high wall temperature (~300^{O}C). Recycling was enhanced and ELM frequency was high, although Z_{eff} is lower, at the low wall temperature compared with at the high wall temperature. The enhanced recycling and higher ELM frequency could affect confinement.

References

[1.6-1] Kubo, H. and JT-60 team, Phys. Plasmas, **9**, 2127 (2002).
[1.6-2] Higashijima, S. and JT-60 team, "Control of Divertor Heat Load by Ar Injection with Keeping High Performance in ELMy H-mode Plasmas on JT-60U" submitted to J. Nucl. Mater..
[1.6-3] Asakura, N., et al., Plasma Phys. Control. Fusion, **39,** 1295 (1997).
[1.6-4] Kubo, H. and JT-60 team, Nucl. Fusion, **41**, 227 (2001).

2. Operation and Machine Improvements

2.1 Tokamak Machine

2.1.1 Operation Status

The operation and maintenance of JT-60 was carried out on schedule in this fiscal year.

In order to extend the operational region towards a higher plasma density, a centrifugal pellet injector and pellet guide tubes had been developed and installed into JT-60 by FY2000. The multiple pellet injection experiments by a new guide tube from mid-plane high-field side (HFS-mid), installed inside the vacuum vessel, began in April. The new tube was designed based on the injection results of the upper port guide tube in high-field side (HFS-top), in which the pellet speed exceeding 220 m/s often caused pellet destructions. A simple impact model was applied to the design of guide tubes and this model indicated a limited perpendicular pellet velocity to the wall of the tubes to be about 20 m/s from the HFS-top experimental results. This required that the pellet should be injected at the lowest possible velocity into the HFS-mid tube which has the minimum curvature of R=200 mm. On the other hand, the pellet with a velocity less than 100 m/s does not penetrate into the core of the plasma. Finally in the HFS-mid experiments form April 2001, pellets with a velocity of 100 m/s were successfully injected to plasma and the electron density of the plasma was increased much higher than the HFS-top cases [2.1-1].

For the in-situ boronization with deuterated decaboran ($B_{10}D_{14}$) [2.1-2], boron coating discharges have been conducted three times and 50 g of $B_{10}D_{14}$ was used in total. Deuterated decaboran was used instead of the previously used hydride decaboran ($B_{10}H_{14}$) so as to shorten the boronization time and improve an efficiency of the first wall conditioning after the vacuum vessel vent. These advantages of using $B_{10}D_{14}$ were demonstrated in the experiments of FY2001.

2.1.2 Development of High Performance Divertor Components

A mock-up of a flat carbon fiber composite (CFC) tile with screw type coolant tubes was manufactured and tested. To confirm heat removal performance and integrity of the mock-up, high heat load tests were carried out at the JAERI Electron Beam Irradiation Stand (JEBIS) facility. Testing results showed that the heat transfer coefficient of the screw tube at the non-boiling region was roughly three times higher than that of the smooth tube, i.e., 1.5 times of the swirl tube and the mock-up could successfully endure 1400 heat cycles at 10 MW/m^2 [2.1-3].

2.1.3 Development of Diagnostic Sensors

A new type of optical current transformer (optical CT), using the Faraday rotation was developed [2.1-4] for diagnostics of direct currents such as a plasma current and a magnetic field coil current. In a steady state operation, an electromagnetic sensor which needs an integrator in the signal conditioner has a technical problem of zero point drift. On the other hand the new

sensor directly measures the magnetic field generated by the current without using integrators. The direct current passing through the loop of the optical fiber is measured by the rotation angle which is proportional to the magnetic field strength. Plasma currents up to 1.5 MA were measured successfully and continuously without any zero point drift for three hours.

As for the conventional magnetic sensor, tangential probes for plasma equilibrium control used in JT-60, a new sensor which can withstand plasma disruptions was developed. In JT-60 experiments some probes had been damaged by plasma disruptions. So as to tolerate the force applied externally, the structure at contact points between a Mineral insulated (M.I.) cable and a magnetic coil body was improved. Its shock-resisting qualities, electric circuit continuity, air leakage in a vacuum and X-ray fluoroscopic etc., were examined through acceleration tests up to 50 G. Results of these tests confirmed that the performance of the new probe is applicable for the environment inside the vacuum vessel in which the maximum acceleration is evaluated as 40 G in JT-60.

2.1.4 Study of the Plasma-surface Interaction

Retention property of hydrogen isotopes in graphite tiles is one of the most important issues of the plasma-surface interaction. After some preparations for tritium use, surface analysis began for the graphite first wall tiles removed from the vacuum vessel after the DD experiments.

Technical preparations were carried out at the analysis room in the radioactive waste storage building from FY2000. Arrangement of analytical instruments such as a secondary ion mass spectrometry system (SIMS), an X-ray photo-electron spectroscopy (XPS), a liquid scintillation system and a scanning electron microscope (SEM) etc., has been made. In May 2001, the inspection test after licensing of the tritium use in the room has been done by Ministry of Education, Culture, Sports, Science and Technology (MEXT) based on the law of radiation protection regulations. After the permission, the cooperative research program between JAERI and universities using the JT-60 first wall was initiated. The first analysis was performed by various methods on the tiles of the divertor region exposed DD plasma in the experimental campaign from 1997 to 1998. Detailed tritium deposition profiles on the W-shaped divertor and the first wall tiles were examined by tritium imaging plate technique (TIPT) [2.1-5]. The highest tritium concentration was observed at the dome top tile of the divertor. The result was compared with that of the triton deposition simulation code with orbit following Monte-Carlo (OFMC) method. Both results showed that the tritium distribution can be explained by the energetic triton loss due to the toroidal field coil ripple loss. According to the OFMC, 31% of the tritons produced by DD reaction were implanted to the first wall without fully losing the initial energy of 1 MeV [2.1-6].

By the SEM analysis, erosion / re-deposition profile in the W-shaped divertor region was investigated. In-out asymmetry was found: erosion for the outer divertor target, and re-deposition for the inner divertor target. The maximum re-deposition layer with thickness of 60 μm was found at the lower zone of the inner divertor targets. Lamellar/columnar-layered structures were observed there (Fig.I.2.1-1). Elemental composition of the re-deposition layer measured by XPS were C:94-95, B:3-4, and O, Fe, Ni, Cr:0.3-0.6 at %. Boron atoms in the re-deposition layer were considered to be mainly in B-C bonding [2.1-7].

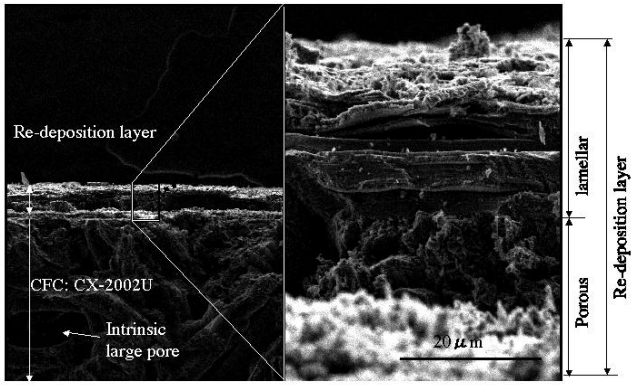

Fig. I.2.1-1 SEM images at poloidal section of surface layers on the lower tile of the inner divertor target of JT-60.

To evaluate the effect of boronization ($B_{10}D_{14}$ + He carrier gas) on the fuel recycling and wall conditioning, hydrogen isotope release properties in the boronized graphite tile were investigated through SIMS observation. Hydrogen isotopes in the boron layer and graphite layer were released at above 573 K and 1023 K, respectively. The result means that the hydrogen isotopes in the boron layer are easily released by 573 K baking on JT-60. The $B_{10}D_{14}$+ He boronization method is clearly effective to attain the high purity deuterium plasma and the low recycling in JT-60 [2.1-8].

References

[2.1-1] Kizu, K., Sasajima, T., et al., "Development of the Guide Tube for Magnetic High Field Side Pellet Injection", Proc. 12h International Toki Conference, (Dec. 2001).
[2.1-2] Yagyu, J., Arai, T., et al., "Boronization using Deuterated-decaborane in JT-60U", Proc. IEEE 19th Symp. on Fusion Engineering (2002).
[2.1-3] Masaki, K., Taniguchi, M., "High Heat Load Test of CFC Divertor Target Plate with Screw Tube for JT-60 Superconducting Modification" Proc. 6th International Symposium on Fusion Nuclear Technology (ISFNT-6), SD, USA (2002).
[2.1-4] Arai, T., Nishiyama, T., et al., "JT-60U Plasma Current Measurement by a Optical Current Transformer", submitted to ANS 15th Topical Meeting on the Technology of Fusion Energy, (Nov.2002).
[2.1-5] Tanabe, T., Miyasaka, K., et al., Fusion Science and Technology, **41**, 877(2002).
[2.1-6] Masaki, K., Sugiyama, K., et al., "Tritium Distribution and its Deposition Process in JT-60U W-shaped Divertor", Proc. PSI-15, Gifu, Japan (2002).
[2.1-7] Gotoh, Y., Masaki, K., et al., "Analyses of Erosion and Re-deposition Layers on Graphite Tiles Used in the W-shaped Divertor Region of JT-60U", Proc. PSI-15, Gifu, Japan (2002).
[2.1-8] Kizu, K., Yagyu, J., et al., Fusion Science and Technology, **41**, 907(2002).

2.2 Control System

2.2.1 Feedback Control of a Steerable Injection Mirror of the ECRF System

A feedback control algorism for determining the direction of a steerable mirror was developed to inject the ECRF power exactly to the region where MHD instabilities grew and to

suppress them. The schematic diagram of the real-time feedback control system is shown in Fig. I.2.2-1. The heating and particle supply control computer (IbR) finds a channel number X_m at the minimum position of an electron temperature fluctuation profile measured by the 12-channel heterodyne radiometer, which corresponds to the center of a magnetic island caused by MHD instabilities. Using an empirical formula of the mirror angle Y as a function of the channel number X_m, $Y=a_0+a_1X_m+a_2X_m^2+a_3X_m^3$, the computer IbR calculates the mirror angle at which the injected ECRF beam is tangent to the magnetic surface where MHD instabilities grow, and sends it as a command to the ECRF system through a high-speed real-time communication network with reflective memories (RM). The feedback control of the mirror angle is executed at a cycle of 10 ms together with the preprogrammed control of ECRF power. The control system was tested using JT-60 discharges in September 2001, and the expected performance was confirmed.

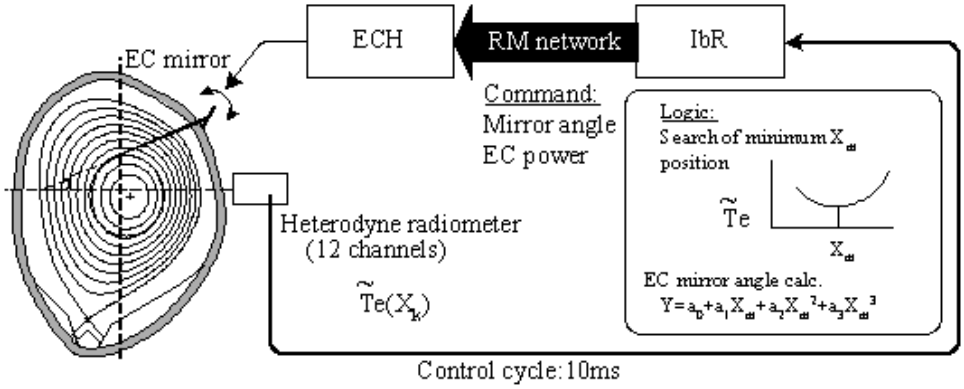

Fig. I.2.2-1. Schematic diagram of the real-time feedback control system.

2.2.2 Long Time Low Drift Intelligent Digital Integrator for Long Pulse Operation

The digital integrator with a voltage-to-frequency converter (VFC), used in JT-60U, is excellent in drift characteristics, but generally suffers from saturation of signal when high voltage is input, causing a large integration error during and after a disruption. To improve this defect, a new digital integrating system has been developed, which consists of three digital integrators with an amplifier with a gain of 10, 1 or 0.1, respectively and an intelligent signal processor with a DSP and a PC commonly used for three integrators. The integrator with a high gain outputs an accurate integrated signal but sometimes suffers from saturation. On the other hand, the integrator with a low gain never gets saturated though the integrated signal is less accurate. The intelligent signal processor selects a most accurate integrated signal from unsaturated signals and sums it up to make a chain of accurately integrated signals without saturation. The function of this integrator has been tested under various disruption conditions in JT-60U.

Reference
[2.2-1] Kawamata, Y., et al., "Development of an Intelligent Integrator for Long-pulse Operation in a Tokamak", IEEE/NPSS 19th Symp. Fusion Engineering, Atlantic City, Jan. 21-25 (2002).

2.3 Power Supply System

A digital phase controller of thyristor converters has been developed using a digital signal processor (DSP) development tool, *PE-View for PE-Expert*, to replace the present phase controllers for power supplies of poloidal magnetic field coils, which consist of analog and digital circuits produced about 20 years ago. This phase controller will be also applicable to a power supply of JT-60SC (superconducting JT-60 under planning) composed of bi-directional thyristor converters with five operational modes as shown in Fig.I.2.3-1. A chart of control algorism for this phase controller is shown in Fig.I.2.3-2. The phase controller detects a variable phase of AC voltage supplied by a motor generator through a phase locked loop (PLL) routine with continuous vector operations. The phase control routine generates fire pulses by comparing the detected phase with the phase of a fire angle command. The protective operation routine consists of three modes, gate shift (GS) mode, by-pass pair (BPP) mode and gate block (GB) mode. In the GS mode, the fire angle is shifted to 120 degrees to generate negative voltage so as to decrease the coil current. In the BPP mode, thyristor converters are switched on to make a closed circuit and the coil current decreases with a time constant determined by the inductance and resistance of the coil circuit. In the GB mode, fire pulses are stopped and thyristor converters stop. Using these modes, the protective interlock routine stops thyristor converters safely. These control functions are beyond general-purpose phase controllers.

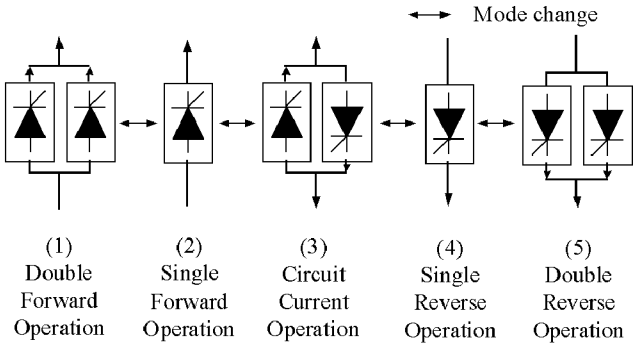

Fig.I.2.3-1. Modes for bi-directional thyristor converters.

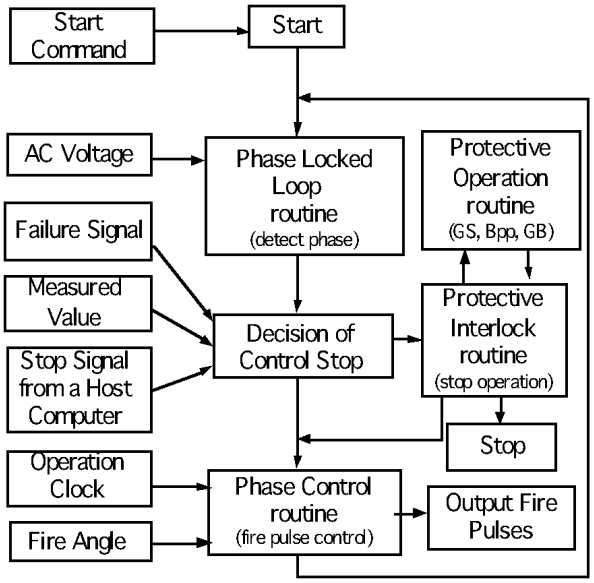

Fig.I.2.3-2. Algorism chart for Digital Phase Controller.

A prototype digital phase controller was made using eight operational boards of *PE-Expert* and the control performance was evaluated. The calculation time for one control loop was

about 200 μs, and thyristor converters could be controlled by 5 kHz clock pulses. The time of phase tracking and detection in the PLL routine was about 10 ms when the phase of the power supply was rapidly changed by 90 degrees. The obtained performance is satisfactory as a phase controller for JT-60U and JT-60SC.

2.4 Neutral Beam Injection System

2.4.1 Development of Negative-ion Based Neutral Beam Injection System

Injection performance of the negative-ion based neutral beam injection (NBI) system for JT-60U has greatly progressed by optimizing ion source parameters, correcting beamlet deflection and improving source plasma non-uniformity. Table I.2.4-1 shows the maximum injection performance achieved with deuterium and hydrogen in this fiscal year. A high injection power of 5.8 MW was realized with deuterium by adjusting the arc discharge to produce the source plasma. Furthermore, the long pulse beam injection for 10 seconds was achieved at 2.6 MW using one ion source by improving the beam convergence.

Item	Species	Max. parameter	Associated parameters (Number of ion sources used)
Injection power	Deuterium	5.8 MW	Eb=400keV, Tb=0.8s (2)
	Hydrogen	6.2 MW	Eb=381keV, Tb=1.65s (2)
Pulse duration	Deuterium	5.4 s	Pinj=1.9MW, Eb=400 keV (1)
	Hydrogen	10.0 s	Pinj=2.6MW, Eb=355keV (1)
Negative ion current	Deuterium	17.4 A	Eb=403keV, PCM=3.8 MW, Tb=0.7 s (1)
	Hydrogen	20.4 A	Eb=406keV, PCM=3.9 MW, Tb=0.5 s (1)

Eb: Beam energy, Tb: Pulse duration, Pinj: Injection power, PCM: Neutral beam power measured by calorimeter

Table I.2.4-1 Performance achieved of N-NBI for JT-60U.

A. High Power Injection

A power flow of the ion source and the beamline for the maximum injection power is illustrated in Fig.I.2.4-1. The power loading on components in the ion source accelerator and the beamline was measured with water calorimeter. The numerals in the figure are the ratio of the power load to the acceleration beam power, which is provided by an acceleration power supply. The losses on the first, second, and grounded grids in the accelerator reached ~20% in total which is twice of the design value.

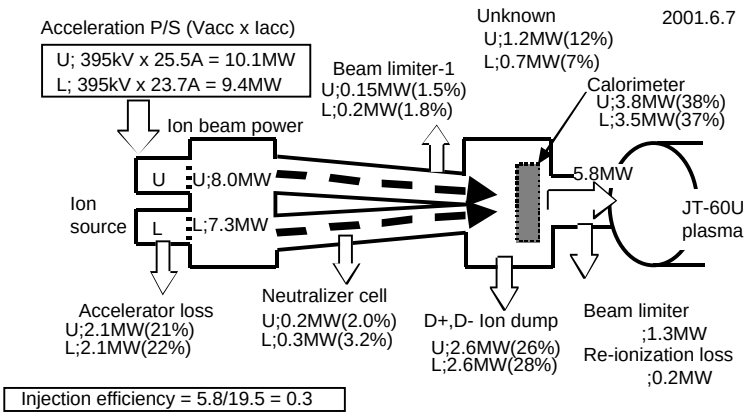

Fig. I.2.4-1 Power flow diagram in the ion source and the beam-line for an injection power of 5.8 MW and a beam energy of 400 keV.

The power load on the grounded grid was dominated by the accelerator. The power loads onto each ion dump of D^- and D^+ are 26 to 28% in total. A neutral beam power of 37 to 38% reached to the calorimeter. These power flows are consistent with theoretical neutralization efficiency of energetic negative-ion beam. The loss in the beam scraper just down-stream of the colorimeter was ~7% of the total acceleration power, and then the loss in the drift duct through re-ionization loss and geometrical loss was ~2%. Consequently, the neutral beam power injected into the JT-60U plasma was 30% of the total acceleration power.

B. Long Pulse Operation

It was found in the measurement of the beam profile at the near field that the outermost beamlets in the grid segments were deflected by the unwanted electric field, which was generated by small grooves at downstream side of the extraction grid segment boundaries. These deflected beamlets resulted in excessive heat load on the beam limiter at the injection port, whose temperature rise limited the injection power and duration. The distorted electric field was corrected by installing copper pieces along the grooves, and then the beamlet deflection was adjusted and the beam convergence was improved. Consequently, the temperature rise of the limiter was reduced by more than 50%, and made the long pulse beam injection possible under high injection power [2.4-2]. Figure I.2.4-2 shows the performance of the injection duration and neutral beam power per ion source. The 10-second duration is the maximum duration that was specified by the system design. It has also been confirmed that the major components of the system (negative ion source, ion damps, etc,) maintain thermally steady states for more than 8 s, thus indicating the possibility of a longer periods operation of the system.

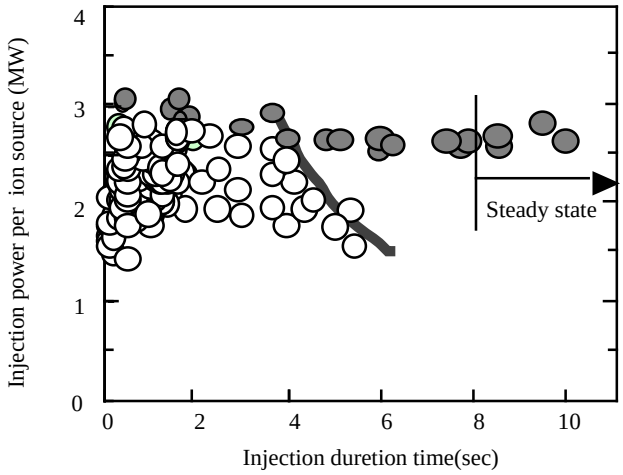

Fig. I.2.4-2 Performance of injection duration time and neutral beam power. The solid circles indicate the results of improved beam convergence and the open circles previous results. The solid line shows the previous limit of the injection power and duration.

References

[2.4-1] Ohga, T., Umeda, N., Akino, N., et al., Rev. Sci. Instrum., 73, 1058 (2002).
[2.4-2] Yamamoto, T., Kuriyama, M., Umeda, N., et al., “Improving Performance of Negative-ion Based Neutral Beam Injector for JT-60U”, Proc. 12th Int. Toki Conf. on Plasma Physics and Controlled Nuclear Fusion, Toki, (2001), to be published.

2.5 Radio-Frequency Heating System

2.5.1 Operational Progress of the EC System

It is one of key issues for attaining higher plasma performance in a large tokamak to control MHD instabilities and a current profile by local heating or current drive. For such a purpose, high power electron cyclotron (EC) system has been developed for JT-60U, whose objective is the injected power of 3 MW at 110 GHz corresponding to the toroidal magnetic field of 3.8 T. The EC system for this purpose has been constructed and improved since 1998. [2.5-1,2].

The power injection performance is progressed. We have now attained the injected power of 3 MW with four radio-frequency (rf) lines by improving two main points of the system. The first point is to improve the gyroton performance at a high power level of 1MW. We had a difficulty in extending pulse length to more than 1 s because the beam current in gyrotron increased with anomalous heating of the cathode by unnecessary rf wave modes [2.5-3,4]. We have improved the gyrotron by setting rf absorber in the beam tunnel since these waves were generated near the cavity and went down to the cathode through the beam tunnel. The absorber suppressed the unnecessary waves and made the beam current steady or gradually decreasing. Then, the pulse length was successfully increased at the high power greater than 1 MW [2.5-4]. The second point was the improvement of the transmission lines. The transmission line is composed of a matching optics unit (MOU), corrugated waveguides, several miter bends, a pair of polarizers and so on. Its designed transmission efficiency was 81%, which was the highest level at these high frequencies because the MOU was designed to have a high transmission efficiency of 95%. The measured transmission efficiency was from 60% to 75% at first, however it was improved to be from 70% to 80% by realignment of the waveguides and adjustment of the MOU.

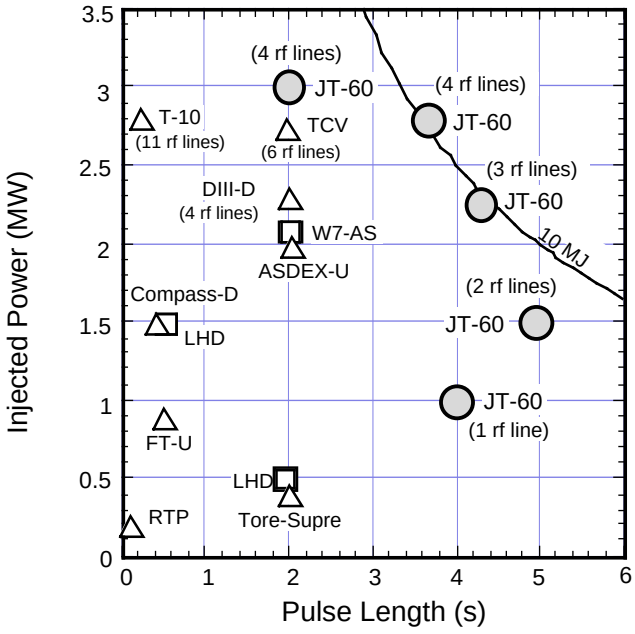

Fig. I.2.5-1 Injected power as a function of pulse length.

As a result of these improvements, the injection power and the pulse width were extended to 1.5 MW for 5 s, 2.8 MW for 3.6 s and 3 MW for 2 s at 110 GHz, as shown in Fig.I.2.5-1, in December 2001 [2.5-3], which are the world record (at least in June, 2002). In a long pulse operation up to 5 s, the temperature rise of the components in the transmission line in general

was not so large without water cooling and are saturated with water cooling. It was an encouraging result towards the steady state operation.

Another progress of the system was with regard to the performance of the rf beam control by two antennas called A and B here. Both antennas can inject the rf beams with an oblique toroidal injection angle for the current drive so as to couple the fundamental O-mode from the low field side, which was the same scheme for EC current drive (ECCD) in ITER. Antenna A can control the poloidal angle of three rf beams from the plasma core to the plasma edge by the steering mirror. Antenna B can control the rf beam injection with the poloidal angle from the plasma core to the middle of the plasma radius and with the toroidal angle from 20 to -20 degrees [2.5-2]. The beam angles could be controlled independently with two antennas. A variety of local heating and current drive was realized. Figure I.2.5-2 shows a typical heating result in changing the poloidal beam angles with both antennas. The electron temperature profile was well controlled. Up to now, extremely high central electron temperatures T_{e0} > 20 keV were generated by on-axis heating or combined on-axis and off-axis heating with four rf beams at a power level 3 MW. Moreover, the poloidal beam angle control was upgraded to be able to make feed-back control, which enables current drive at the location of magnetic island and stabilization of the neo-classical tearing mode.

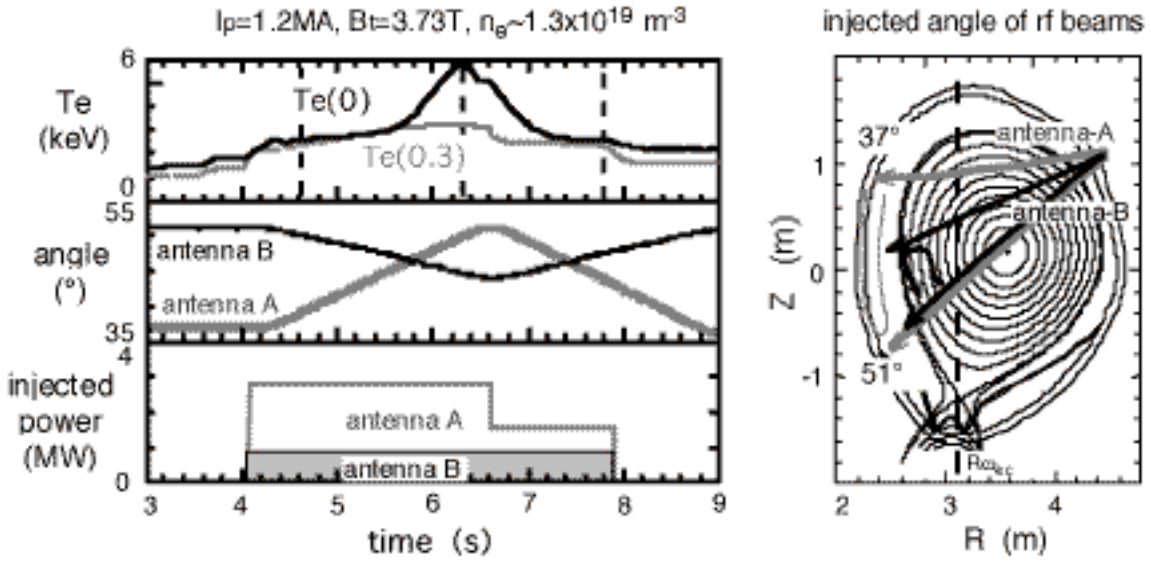

Fig. I.2.5-2 Time evolution of the electron temperatures at r= 0 m and 0.3 m in changing the poloidal angles of the rf beams. Power injected from antenna A is 2.1 MW, 0.9 MW after time 6.6s, and from antenna B is 0.8 MW.

2.5.2 Operation of the IC and LH Systems

The ion cyclotron (IC) system in JT-60 was operated at the power level up to 3.4 MW at 112 MHz for the trial of fast wave electron heating (FWEH). There were two possibilities for

direct electron heating by fast waves in the EC heated plasma. One was to operate the plasma at ~1.9T for second harmonic EC heating, and the other was at ~3.8T for fundamental EC heating. In the theoretical prediction, low magnetic field is favorable for the FWEH. However at 1.9 T, clear electron heating was not observed probably because the number of high-energy electrons in the target plasma was not enough for efficient FWEH. Clear electron heating was not also observed at 3.8 T probably because the single pass power absorption is low.

The lower hybrid (LH) system in JT-60 was operated at ~ 3.7 MW at 2 GHz mainly for two experiments. One is a plasma current ramp-up experiment without operation of the central solenoid coil, which explores a possibility of the tokamak device which is much simplified without the central solenoid coil. The other is an experiment of reversed magnetic shear plasmas with larger radius of internal transport barrier by LH current drive. These experiments require stable operation of the LH system without a breakdown at LH antennas. For this purpose, by chopping the LH pulse at a duty of 90% to suppress the breakdown, stable operation was performed up to 3.8 s.

The improved rf control system enabled simultaneous operation of EC, LH and IC systems by 4 - 5 operators in the control room, compared to 8 – 10 operators before the improvements in FY2001. The total power and the operating duration of these three RF heating system ($P_{EC}+P_{LH}+P_{IC}$) achieved ~7 MW for 1 sec, simultaneously.

References

[2.5-1] Ikeda, Y., et al., Fusion Eng. and Design, **53,** 351 (2001).
[2.5-2] Moriyama, S., et al., "Upgrade of ECH System in JT-60U Featuring an Antenna for Toroidal/Poloidal Beam Scan", Proc. 14th Topical Conf. on Radio Frequency Power in Plasmas, Oxnard, USA, May, 2001.
[2.5-3] Ikeda, Y., et al., "The 110GHz Electron Cyclotron Range of Frequency System on JT-60U: Design and Operation", to be published in Fusion Science and Technology.
[2.5-4] Kajiwara, K., et al., "High Power Operation of 110GHz Gyrotron at 1.2 MW on the JT-60 ECRF System", to be published in Fusion Eng. and Design.

3. Design Progress of the JT-60 Superconducting Tokamak (JT-60SC)

Physics and engineering design of the JT-60 superconducting tokamak (JT-60SC) made progress through the design study activity. The mission of JT-60SC program is to establish scientific and technological bases for low circulating power operations compatible with a high pressure plasma in a steady state (i.e., high performance steady state operation) in an economically attractive DEMO reactor and ITER. In addition, establishment of utilization technology of reduced-activation materials to significantly reduce the influence of radioactive waste to the environment is also a key issue for a DEMO reactor. It is necessary to promote practical use of the reduced-activation ferritic steel as a most promising candidate for the blanket material in a DEMO reactor. In the JT-60SC, it is planned to demonstrate the high-beta steady-state operation of the reactor-relevant plasma and the applicability of the reduced-activation ferritic steel characterized by a ferromagnetic property with the plasma. Typical machine parameters of JT-60SC are shown in Table I.3-1. The aspect ratio of 3.3, the plasma current of 4 MA, the elongation up to 2, the triangularity up to 0.5, the toroidal field of 3.8 T and the major radius of 2.8 m are selected.

The present design of JT-60SC is based on discussions at the joint technical meeting for the modification program on JT-60, which was held from March to September in 2001 in collaboration with universities, institutes and industries.

Table I.3-1. Typical machine parameters of present JT-60 and JT-60SC.

Parameter	JT-60U	JT-60SC
Pulse length	15 s	100 s (flat top)
Max. input power	40 MW (10 s)	44 MW (10s) 15 MW (100s)
Plasma current I_p	3 MA	4 MA
Toroidal field B_t	4 T	3.8 T (R_p=2.8m)
Major radius R_p	3.4 m	2.8-3 m (2.8m*)
Minor radius a_p	0.9 m	0.7-0.9 m (0.85m*)
Elongation κ_{95}	1.8 (δ_{95}=0.06)	≤ 2 (1.8*)
Triangularity δ_{95}	0.4 (κ_{95}=1.33)	≤ 0.5 (0.35*)

*Nominal

3.1 Physics Design

For realization of a compact tokamak reactor to meet the requirement of commercial competitiveness, it is necessary to make the high performance steady state operation feasible, which is characterized by plasma control with sufficiently high normalized beta β_N and bootstrap current fraction f_{bs}, efficient heat and particle control and almost disruption-free operation. Figure I.3.1-1 shows the extended performance capability of the JT-60SC to demonstrate the sustainment of high-β_N plasmas in comparison with the present data from other tokamaks. In comparison with these present achievements,

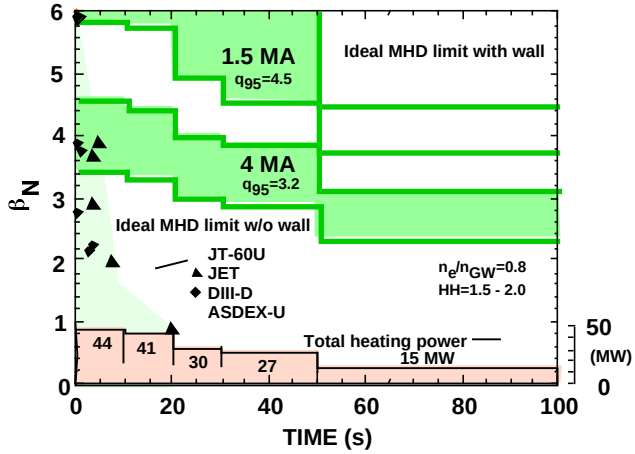

Fig. I.3.1-1. Normalized beta β_N estimated by TOPICS code as a function of time with HH_{y2}=1.5-2.0 and n_e/n_{GW}=0.8 for 1.5 MA and 4 MA corresponding to heating power scenarios in JT-60SC.

CREST and SSTR are designed with β_N =5.5 and 3.5, respectively, and steady-state operation in ITER aims at β_N=2.6-3.5. The concept of the JT-60SC is to create high performance plasmas in an equivalent break-even class (Q_{DT}^{eq}~1) and to sustain the high-β_N plasmas during a long duration of ~100 s sufficiently exceeding a current diffusion time scale (τ_{diff}~30 s) and a particle saturation time at the divertor. Based on conceptual reactor designs of SSTR and CREST emphasizing the reactor economics, the targets are placed on the parameter range of β_N=3.5-5.5, f_{bs}=50-90%, f_{rad}~95% and τ_{He}^*/τ_E~5.

Since the target β_N region is substantially above the ideal MHD limit with a free boundary, the stabilizing plate (passive stabilizer) made of ferritic steel is placed on the location similar to the blanket surface of the DEMO reactor. While the wall acts as a resistive wall for stabilization, the ferromagnetic property of the wall may deteriorate the stability. So, both ferromagnetic and resistive wall effects on MHD stability is being investigated using a linear MHD code based on resistive MHD equations. To stabilize the resistive wall modes (RWM) with multiple toroidal mode numbers of n=1 and 2, eighteen sector coils are installed inside the vacuum vessel and behind the stabilizing plate capable of active feedback control.

Analyses based on the JT-60U data on high-β_P and reversed shear discharges using TOPICS and ACCOME codes show the potential feasibility of high performance steady-state operation required for the JT-60SC. During 100 s, full non-inductive current drive at 2 MA can be sustained with 15 MW and the toroidal electric field profile for a 10 keV plasma is found to become flat zero. A parameter dependence for current drive and heating with 30 MW for 30 s suggests full current drive potentials with HH_{y2}~1.5 β_N~3 and f_{bs}~50%, or HH_{y2}~2, β_N~5 and f_{bs}~80% at 3 MA.

Efficient heat and particle control, which leads to simultaneous achievement of full current drive and partially detached divertor at high beta and reduction of impurity concentration, is necessary for realization of high performance steady-state operation. The achievement can be accomplished with strong SOL flow produced by intense divertor pumping in combination with gas puff or inside-pellet injection. To ensure heat and particle control, the vertical target divertor structure is designed to be compatible with the high beta plasmas as shown in Fig. I.3.1-2. Independent pumping system at inner and outer divertor using separated cryopumps is adopted for partial detachment control where the cryopanel brings out about 50 m^3/s at each pumping slot. This requirement is evaluated from numerical divertor simulation using the SOLDOR/NEUT2D code. Since the divertor heat load could reach about

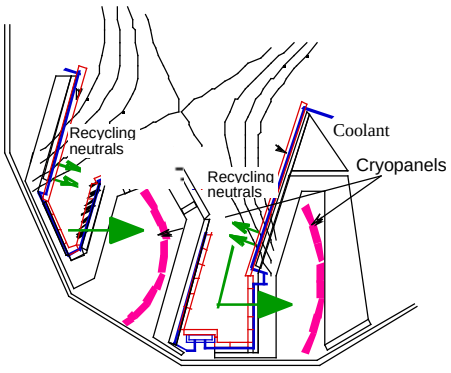

Fig. I.3.1-2. Basic structure of the vertical target divertor equipped with cryopanels for independent inner and outer pumping.

20 MW/m^2 without any radiation loss, effective forced cooling of the target plates is required as well as the radiative divertor. For the plasma facing component in the divertor, low-Z materials such as carbon fiber composite (CFC) is initially used with a local test of high-Z materials such as W-alloy for future.

3.2 Engineering Design

As a result of the toroidal field (TF) coil stress analysis, the maximum mechanical stress of 360 MPa appeared near the fixing key. It is sufficiently lower than its criterion of 660 MPa of the SS316LN at 4.2K. The maximum displacement of the TF coil is evaluated to be about 7 mm in case of nominal plasma current of 4 MA. Detailed structural analysis of the conduit, coil casing, and supporting structures are still in progress now.

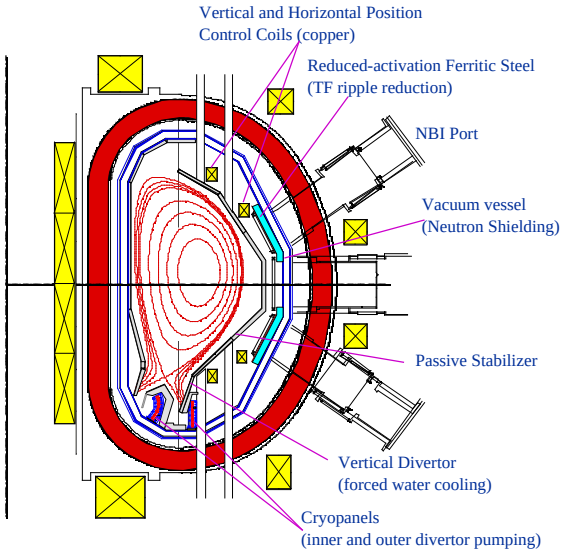

Fig. I.3.2-1. Schematic cross-sectional view of superconducting coils, the vacuum vessel and in-vessel components in the JT-60SC.

The vacuum vessel is a double-walled structure with a polygonal shape having a low toroidal resistance of ~40 μΩ. The double walls made of SS316L with low Co contamination are filled with pure water for neutron shielding. Additionally, SS316L plates are installed outside the vacuum vessel for γ-ray shielding, so that the nuclear heating in the superconducting TF coils is suppressed below 2.5 mW/cm^3 at winding for the maximum neutron emission of 4×10^{17} n/s for 10 s in deuterium plasma. Vertical and kink stabilities for high beta plasmas can be achieved with passive structure of stabilizing plates located inboard and outboard of the plasma as shown in Fig. I.3.2-1. The ferritic steel (F82H) is planned as material for plasma facing armor and the pedestal on the inner wall. The TF ripple is reduced to less than 0.5% corresponding to the fast ion loss (ripple-trapped and banana drift losses) within 2% of the NB injection power by placing the ferritic steel plates (F82H) inside the vacuum vessel behind the TFC.

References

[3.1-1] Ishida, S., et al., Proc. IEEE/NPSS 19th Symp. on Fusion Engineering, Atlantic City (2002).
[3.1-2] Sakurai, S., et al., "Particle Control Design for Modification of JT-60 with Superconducting Coils", Proc. IAEA TCM on Divertor Concepts, 2001, Aix-en Provance, to be published in Fusion Eng. Des..
[3.2-1] Sakasai, A., et al., Proc. IEEE/NPSS 19th Symp. on Fusion Engineering, Atlantic City (2002).
[3.2-2] Ando, T., et al., "Design of Superconducting Coil System for Remodeling JT-60", Proc. 17th Int. Conf. on Magnet Technology, Jeneve, 2001, to be published in IEEE Tran. Appl. Supercond..
[3.2-3] Kizu, K., et al., "Development of High Cu Ratio Nb_3Al and Nb_3Sn CIC Conductors for Superconducting Toroidal Field Coils of JT-60", Proc. 17th Int. Conf. on Magnet Technology, Jeneve, 2001, to be published in IEEE Tran. Appl. Supercond..
[3.2-4] Miura, M. Y., et al., "Development of Nb_3Sn and NbTi CIC Conductors for Superconducting Poloidal Field Coils of JT-60", Proc. 17th Int. Conf. on Magnet Technology, Jeneve, 2001, to be published in IEEE Tran. Appl. Supercond..

II. JFT-2M PROGRAM

On JFT-2M, advanced and basic research for the development of high performance tokamak plasma is being promoted, making use of the flexibility of a medium-sized device and the research cooperation with universities and other institutions. Recently, the Advanced Material Tokamak Experiment (AMTEX) program has been carried out in JFT-2M. The low activation ferritic steel has been tested for the development of the structural material for a fusion reactor. In this fiscal year, the inside wall of the vacuum vessel was fully covered with ferritic steel plates in order to test compatibility of them with high performance plasmas as the third stage test of AMTEX. The ferritic steel plates have a three-dimensional shape and have been installed with a high accuracy (±2 mm). A fine structure of the magnetic field inside the vacuum vessel with ferritic steel plates was measured using a three-dimensional magnetic field measurement apparatus. In parallel with the AMTEX program, JFT-2M is performing the advanced and basic study on H-mode plasmas and a compact toroid (CT) injection, etc. The heavy ion beam probe (HIBP) clarified a decrease in particle flux just inside the separatrix at the L-H transition. Large magnetic fluctuations with frequency chirping were observed just after the CT injection.

1. Advanced Material Tokamak Experiment (AMTEX) Program

1.1 Full Coverage of Vacuum Vessel Wall with Ferritic Steel Plate

The AMTEX program is in progress for the demonstration of compatibility of ferritic steel with high performance plasmas [1.1-1]. The AMTEX program consists of three stages. In the first stage, the toroidal field ripple reduction has been investigated with ferritic steel plates installed outside the vacuum vessel in order to examine the pure effects of ferritic steel, eliminating the effect due to the plasma wall interaction (PSI). For the investigation of both magnetic effects and PSI with ferritic steel, inside wall of the vacuum vessel was covered with the ferritic steel plates partially (~20% of the inside wall) in the second stage. In the fiscal year 2000, the inside wall was fully covered with ferritic steel plates to start the third stage of AMTEX. In order to produce high performance plasmas, the plasma volume should be maintained as same as that in the second stage. Therefore, the distance from the surface of a ferritic plate on the plasma side to the vacuum vessel was set to be small enough (3 cm) to install graphite armor tiles within the same height from the vacuum vessel as before. The ferritic wall consists of ferritic steel plates; 32 pieces on the outboard side, 16 pieces on inboard sides in the toroidal direction and 7 pieces in the poloidal direction. The thickness of ferritic steel plates was optimized in a range of 6-10.5 mm depending on the location in the poloidal and toroidal direction in order to reduce both the fundamental mode ripple and the second harmonic ripple. The layout of ferritic steel plates was determined carefully considering these requirements. It was expected that both the fundamental mode ripple and the second harmonic ripple are less than

0.2% at B_t = 1.3 T over a wide range in the poloidal direction on the outboard side. The toroidal periodicity of the ripple amplitude was considerably improved compared with the first stage, where it was not sufficiently kept because of interference of existing equipments outside the vacuum vessel with the ferritic steel plates. Since the deformation of the vacuum vessel was observed by using a three-dimensional magnetic field measurement apparatus developed newly (next section 2.1), ferritic steel plates were set to the vacuum vessel taking account of the deformation. Magnetic sensors, such as magnetic probes and saddle coils etc., were mainly installed on the ferritic steel plates on the plasma side to minimize shielding effects of the ferritic steel plates on the plasma control. Graphite tiles were installed on the ferritic steel plates continuously on the inboard side, partially on the outboard side and near the divertor legs for the protection of the ferritic steel plates and magnetic sensors from the high heat flux.

Reference

[1.1-1] Kimura, H., et al., "Progress of Advanced Material Tokamak EXperiment (AMTEX) Program on JFT-2", Fusion Engineering Design, **56-57**, 837 (2001).

1.2 Three Dimensional Measurement of Magnetic Field inside Vacuum Vessel

We performed detailed measurements of the magnetic field inside the vacuum vessel to confirm ripple magnitudes and error fields using a three-dimensional magnetic field measurement apparatus before and after the installation of the ferritic steel plates. The measurement apparatus using Hall elements can be moved in the toroidal, vertical, and major radius directions. The view of the apparatus in the vacuum vessel before the installation of the ferritic steel plates is shown in Fig. II.1.2-1.

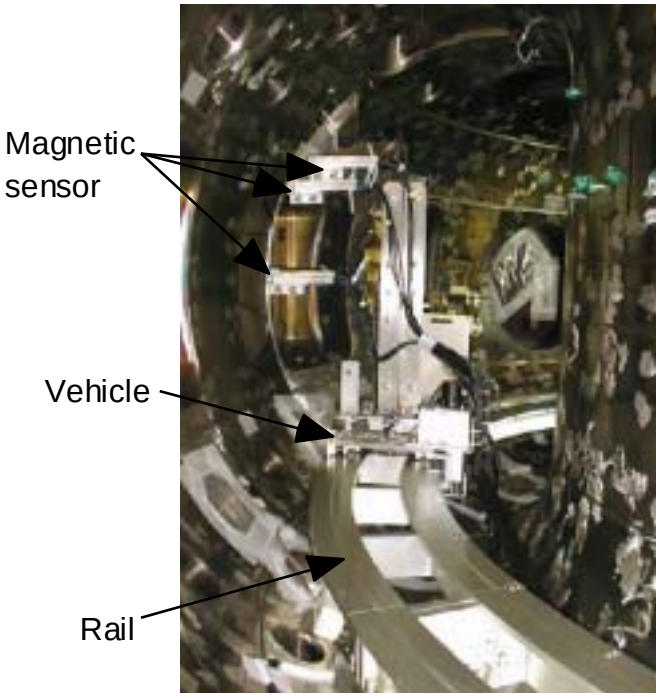

Fig.II.1.2-1 A Photograph of three-dimensional magnetic measurement apparatus in vacuum vessel before installation of ferritic steel plates.

Before the installation of the ferritic steel plates, we measured the ripple amplitude of the toroidal magnetic field as reference data without the ferritic steel plates and the relative shift of the vacuum vessel to the center of each toroidal field coil. Using the measured shift of 3.5mm, the error fields ($B_\rho^{n=1,m=2}$) can be estimated to be 5 x 10^{-6} T. The error field is low compared to the critical error field of the locked mode (~ 3 x 10^{-4} T). Because deformation of the vacuum vessel was observed in the measurement, the ferritic steel plates installed in the vacuum vessel

taking into account of the deformation. After the installation of the ferritic steel plates, the ripple amplitude was measured again. The ripple amplitude on the outboard (R=1.55m, Z=0.2m) was reduced from 1.7% to 0.15%. We have demonstrated that the ripple amplitude of magnetic fields can be reduced as expected in the full coverage of the vacuum vessel wall with the ferritic steel plates.

2. High Performance Experiments

2.1 Formation Mechanism of Edge Transport Barrier and Flow Velocity

Suppression of the plasma turbulence is possible to occur by the plasma flow velocity shear. Then the local suppression of the turbulence at the plasma edge might be the mechanism of the formation of the edge transport barrier during the H-mode. Therefore, it is very important to measure the flow velocity structure in the edge transport barrier to find the mechanism of the formation of the transport barrier. In JFT-2M, we have been studying this problem. The study of the edge flow velocity from the charge exchange recombination (CXR) measurement [2.1-1] needs a hydrogen beam. By this method we obtained the flow velocity at the transport barrier during the neutral beam heating (NBH). However, we could not obtain the flow velocity structure at the transport barrier during the pure electron cyclotron heating (ECH) [2.1-2] by this method, because the neutral beam power for the CXR measurement would be comparable to the ECH power. If the suppression of the turbulence by the shear in flow velocity is the true mechanism of the transport barrier formation, we should also observe the similar flow structure in the ECH H-mode. Previously, we observed the negative radial electric field at the transport barrier by ECH with suppression of turbulent density/potential fluctuation using the heavy ion beam probe (HIBP) [2.1-3] under the cooperation program with National Institute of Fusion Science (NIFS).

In this fiscal year, we studied the **E**x**B** flow velocity structure and its shear structure in the edge transport barrier during the ECH H-mode (Fig.II.2.1-1) with the HIBP measurement [2.1-4]. The poloidal flow of ~-10 km/s in the direction of the electron diamagnetic rotation was observed at the edge transport barrier where the negative radial electric field of E_r ~ -150 V/cm developed. In the scrape-off region, we observed the poloidal flow of opposite direction ~+10 km/s in the direction of ion diamagnetic rotation. Therefore, we found a large

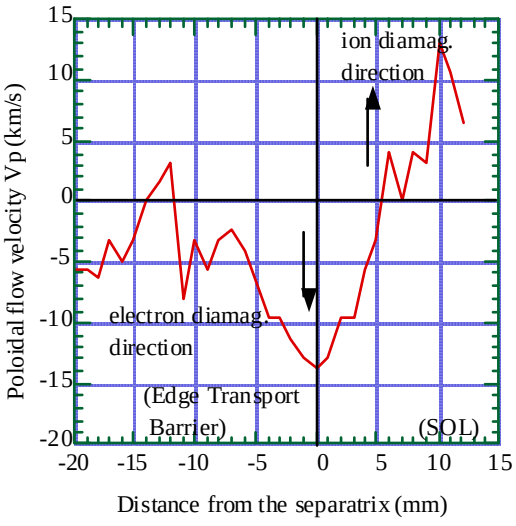

Fig.II.2.1-1 ExB poloidal plasma flow velocity at the edge transport barrier during the H-mode by ECH.

velocity shear of ~-20 km/s/cm inside the separatrix and +20km/s/cm outside the separatrix. This characteristic potential/flow pattern during ECH is very similar to that during NBH. Therefore, the flow shear suppression of the turbulence is the plausible mechanism of the transport barrier generation.

References
[2.1-1] Ida, K., et al., Phys. Fluids., **B4**, 2552 (1992).
[2.1-2] Hoshino, K., et al., Phys. Rev. Lett., **63** (7), 770 (1989).
[2.1-3] Ido, T., et al., Plasma Phys, Control. Fusion, **37**, 175 (1997).
[2.1-4] Hoshino, K., et al., Proc. 8th IAEA TCM of H-mode Physics and Transport Barriers Physics, Toki, Japan, 13 (2001).

2.2 Reduction of Turbulence-Induced Particle Loss in H-Mode

By the HIBP measurement [2.2-1], we could observe the rapid change of the plasma potential at the L-H transition[2.2-2] for the first time. The cross-field particle flux by the plasma turbulence can be obtained by the simultaneous measurement of density fluctuation and potential fluctuation. By utilizing the advantage of the fast response of the HIBP measurement for density fluctuation and potential fluctuation, we could obtain this particle flux during the L-mode and the H-mode at the plasma edge in the initial study (Fig.II.2.2-1). It was revealed that the contribution of the high frequency turbulence of ~ a few 10 kHz to the fluctuation-induced particle loss was large during the L-mode and the fluctuation-induced particle loss decreased to less than ~1/20 of the L-mode level after the H-mode transition. Now, it is important to study dependence of this flux on various plasma parameters such as electron density, plasma current, additional heating power and so on. Contribution of the flux to the global plasma particle/energy confinement is also an important issue to study.

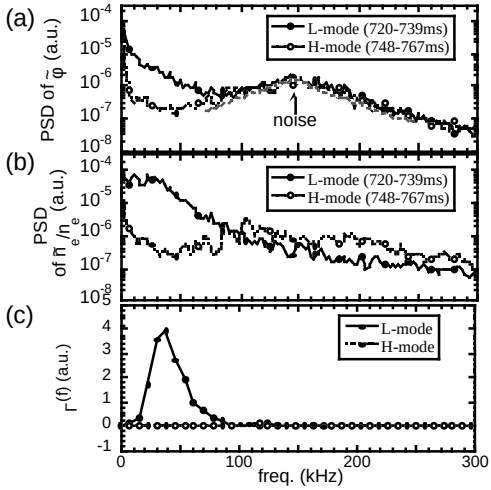

Fig.II.2.2-1 Frequency spectrum of plasma potential (a),density fluctuation(b) and fluctuation induced particle flux (c) at ~2 cm inside of the separatrix of the single null divertor plasma with NBH.

References
[2.2-1] Hamada, Y., et al., Plasma Phys. Control. Fusion, **36**, 1743 (1994).
[2.2-2] Ido, T., et al., Phys. Rev. Lett., **88**(5), 055006 (2002).

2.3 Studies on Scrape-Off Plasma

2.3.1 Radial Electric Field and Transport in the Scrape-Off Plasma

Spatial profiles of the saturation current and floating potential in the scrape-off layer of the single null divertor plasma were obtained by using a fast reciprocating probe (1 mm/1 ms). A radial electric field was observed at the outside of the separatrix at the H-mode transition. The

fluctuation of the ion saturation current decreased to ~1/10, and an improvement of the particle transport was observed. We have also found that the correlation of the floating potential fluctuations between the two electrodes with ~4 mm separation disappears twice for short time period of 2~3 ms when the reciprocating probe is supposed to cross the separatrix, move into and out of the core plasma. When the probe crosses the separatrix, it happens that one electrode is inside the separatrix and the other electrode is outside the separatrix. The phenomenon is considered to relate to the relative position between the two electrodes and the separatrix and may be possible to use to measure the location of the separatrix. These studies are in progress under collaboration with the University of Tokyo.

2.3.2 Transport Coefficients in the Scrape-Off Plasma

Under the collaboration program with Physical and Chemical Research (RIKEN) and the Yokohama National University, the transport model of scrape-off layer (SOL) plasma in a tokamak was developed. Using particle and energy conservation laws, particle and thermal diffusivities for both ions and electrons perpendicular to the flux surface at the SOL were evaluated just outside the magnetic separatrix. The source terms due to ionization, charge exchange loss and the effect of the temperature gradient were exactly included. We have found that the diffusivities can be expressed in terms of e-folding length of the density, temperatures and Mach number. Those absolute values were evaluated from the data obtained by using the electrostatic probe in a SOL plasma in the JFT-2M tokamak. As a result, it was found for the first time that $\chi_{\perp}^{e} > D_{\perp}^{Bohm} > \chi_{\perp}^{i} > D_{\perp}^{e} > D_{\perp}^{i} > \chi_{\perp}^{i\ Neo}$ for the SOL plasma in JFT-2M, where $D_{\perp}^{Bohm}$ is the Bohm diffusion coefficient and $\chi_{\perp}^{i\ Neo}$ is the neo-classical ion thermal diffusivitiy [2.3-1].

Reference

[2.3-1] Uehara, K. et al., “Transport Model of Boundary Plasma and Evaluation of Transport Coefficients”, submitted to J. Phys. Soc. Japan.

2.4 Compact Toroid Injection

Compact toriod (CT) injection has been considered as a possible candidate for a core fueling of a fusion reactor. In JFT-2M, CT injection experiments have been performed under the collaboration with Himeji Institute of Technology and Hokkaido University.

In order to increase a CT plasma volume and to avoid the rapid deceleration by a focus-cone-type drift tube, we made a new outer electrode for the CT formation and a new straight drift tube. Furthermore, we have developed a curved drift tube to change the CT injection direction from a horizontal direction to a vertical direction. It has been observed that a CT can be transported smoothly through curved drift tubes without an appreciable change in the CT parameters such as magnetic field, electron density and CT speed.

A large magnetic fluctuation observed in the CT injection experiment was analyzed by a

time-frequency analysis method. From this analysis, the magnetic fluctuation lasted for a time scale of magnetic reconnection time and was accompanied with characteristic frequency chirping. This frequency chirping can be explained by a frequency change of Alfvén waves excited by the CT injection and the particle fueling by it. This result is expected to lead to an elucidation of the dynamics of particles fuelled by the CT injection.

3. Maintenance and Machine Improvements

3.1 Tokamak Machine

In the JFT-2M tokamak, the vacuum vessel were modified during February 2001 to February 2002 for the 3rd-stage experiment of the Advanced Material Tokamak Experiment (AMTEX) [3.1-1].

The interior wall of the vacuum vessel was fully covered with ferritic steel plates; this wall is referred to as “Ferritic Inside Wall (FIW)”. The closed divertor structure was removed and new graphite tiles were installed for divertor plates. Inner and outer guard limiters of graphite were also replaced with new graphite tiles. All electromagnetic sensors were also renewed. The inside view of the JFT-2M vacuum vessel after the installation of the FIWs is shown in Fig.II.3.1-1.

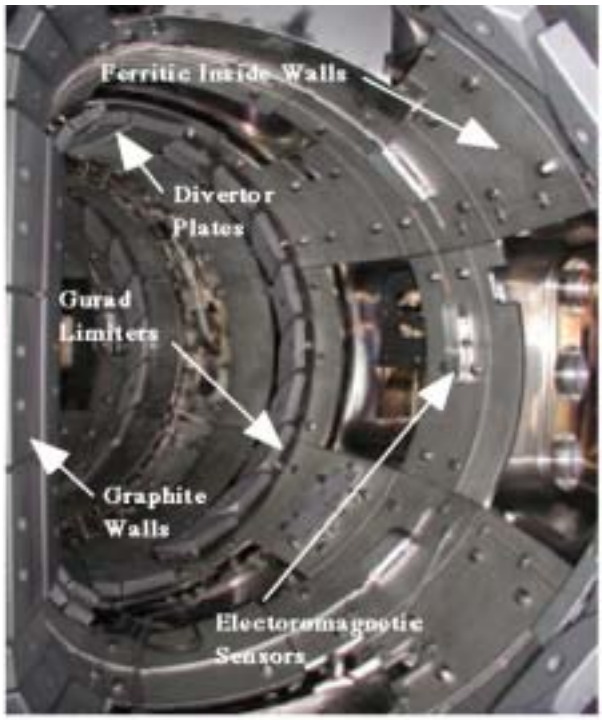

Fig. II 3.1-1 Inside view of the JFT-2M vacuum vessel after the installation of Ferritic Inside Wall (FIW)

The deformation of the vacuum vessel was measured at twenty poloidal sections before installing the FIWs. All FIW were fixed with bolts by considering the deformation of the vacuum vessel at each poloidal section. The structural checks of the FIWs were carried out under the toroidal field. Before and after installing the FIWs, three dimensional magnetic field distribution inside the vacuum vessel was measured with the magnetic field measurement device developed in FY2000 [3.1-2].

All plasma diagnostics were reinstalled after the installation of the FIWs. All the modification work mentioned above was finished in March 2002.

So as to start plasma experiments in April 2002, evacuation of the vacuum vessel was started in March 2002. The vacuum vessel was baked at 120°C for 21days. No air leakage was

detected and the vacuum pressure of 10^{-6} Pa and the outgas rate of 10^{-6} Pa/m^3/s were obtained at the room temperature. These values are comparable to those before installation of the FIWs.

No tokamak operation in FY2001 was carried out because of the modification inside the vacuum vessel. However, magnetic fields were applied for 1243 times for measuring the magnetic fields inside the vacuum vessel before and after the installation of the FIWs and for checking the mechanical condition of newly installed in vessel structures. The Taylor-type discharge cleaning for 20 hours was done by applying the steady toroidal magnetic field.

The control system was modified for the auxiliary facilities consisting of vacuum pumping system, boronization system, gas injection system, leak detection system, glow discharge cleaning system, cooling water facility. The operation status of these auxiliary facilities can be monitored by one personal computer. The modification improved capability and reliability in the information collection and operation significantly.

In previous X-rays monitor system [3.1-3], X-rays measurement was performed by four fixed sensors. A new X-rays monitor system based on a fiber optic x-rays monitor was developed. This system can measure continuously the X-ray distribution along the sensor cable made of scintillation fiber, that is installed around the JFT-2M tokamak.

3.2 Heating and Power Supply System

The electrolytic capacitor of the electron cyclotron heating (ECH) system was renewed. The beam dump of the neutral beam injection system (NBI) was replaced because the armor tiles made of tungsten were broken by irradiation of 200,000 beam shots after the installation.

The emergency diesel generator was renewed. The direct current generator (DCG) with a flywheel was operated monthly for maintenance.

References

[3.1-1] Kimura, H., Sato, M. and JFT-2M group, Fusion Eng. Design, **56-57**, 837 (2001).

[3.1-2] Yamamoto, M., Tsuzuki, K., Okano, F., et al., “Development of the Device for 3D-measurement of the Magnetic Field Profile in the Toroidal Device”, Proc. Symp. on Technol. in Laboratories 2001, 65 (2002) (in Japanese).

[3.1-3] Okano, F., Umino, K., ”Development of a Multi-channel X-ray Monitor System for the JFT-2M Tokamak”, JAERI-Tech 99-070 (in Japanese).

III. THEORY AND ANALYSIS

The principal objective of theoretical and analytical studies is to understand physics of tokamak plasmas. The dynamics of internal transport barrier formation and the relation between the core confinement and the L-mode base were investigated. Progress was also made on the study of MHD instabilities. Also, investigations on universality of VDE event, the effect of polarization current on neoclassical tearing mode (NTM), feasibility of suppressing NTM by electron cyclotron current drive (ECCD), and divertor characteristics in JT-60SC were carried out. Progress has been made with the NEXT (Numerical EXperiment of Tokamak) project in order to research complex physical processes both in core and in divertor plasmas by using massively parallel computers. Substantial progress was made in the studies of turbulence and MHD reconnection and codes were developed to analyze divertor transport in a realistic geometry.

1. Confinement and Transport

Abrupt in time (correlated within a few ms with L-H and H-L transitions) and wide in space (from the edge up to ~0.3 of minor radius in the extreme case) variations of electron heat diffusivity $\delta\chi_e$ were found in reversed shear (RS) JT-60U tokamak plasmas with internal transport barrier (ITB) for various profiles of safety factor q [1-1, 1-2]. The $\delta\chi_e$ profile follows the position of q minimum (q_{min}) and penetrates deeper into the RS region for the weak ITB than the strong one, suggesting the presence of "global" edge-core connection throughout q_{min} at L-H and H-L confinement bifurcations. The $\delta\chi_e$ value at the position of q_{min} is small for the strong ITB (~0.05 m^2/s) and increases by an order of magnitude for the weak ITB. The ITB event is another non-local transport bifurcations (improvement and degradation) inside and around ITB [1-1]. The strong ITB formation in H-mode via a series of ITB events in ELM-induced L-mode is found. It was found that the L-H transition caused the ITB degradation in the positive shear zone.

An energy confinement scaling for RS plasmas with box-type ITB and L-mode edge is developed based on the JT-60U data [1-3]. The stored energy is divided into two parts: L-mode base part and the core part surrounded by the ITB. The core stored energy W_{core} does not simply increase with the net heating power P_{net}. A scaling of the core stored energy is given as $W_{scale} = C\ \varepsilon_f^{-1} B_{p,f}^{2} V_{core}$, where ε_f is the inverse aspect ratio at the ITB foot, $B_{p,f}$ is the poloidal magnetic field at the outer midplane ITB foot, and V_{core} is the core volume inside the ITB foot. This scaling is equivalent to the condition for the core poloidal beta $\varepsilon_f \beta_{p,core} = C_1$ with $C_1 \sim 1/4$. Though W_{core} has little dependence on P_{net}, the estimated heat diffusivity in the ITB region moderately correlates with the neo-classical diffusivity, and the neo-classical transport is not inconsistent with the data.

References
[1-1] Neudatchin, S.V., Takizuka, T., Shirai, H., et al., Plasma Phys. Control. Fusion, **44**, A383 (2002).
[1-2] Neudatchin, S.V., Takizuka, T., Shirai, H., et al., JAERI-Research 2001-056 (2001).
[1-3] Takizuka, T., Sakamoto, Y., Fukuda, T., et al., Plasma Phys. Control. Fusion, **44**, A423 (2002).

2. Stability

Ferromagnetic wall effects on free boundary MHD modes have been analyzed. It was found that the critical poloidal beta values can be reduced to 90% at $\mu/\mu_0=2$, 78% at $\mu/\mu_0=4$ in comparison with the value at $\mu/\mu_0=1$ (μ: permeability of the wall). These results should be considered in reactor design [2-1].

It was found that toroidal shear flows damp the energy of perturbation perpendicular to the equilibrium fields in the good curvature region for high-n (n: toroidal mode number) ballooning modes. This damping effect plays a crucial role in determining the stability. The damping effect is strong with the D-shaped plasma. In addition, the growth rate in the exponentially growing phase becomes smaller by the D-shaping. Thus the ballooning modes are effectively stabilized by the simultaneous effects of the toroidal shear flow and the D-shaping [2-2].

To avoid the VDE, validation studies of “neutral point” of vertical plasma position have been carried out under trilateral large tokamak collaborations [2-3-2-4]. It was clarified that the neutral point does exist in the Alcator C-Mod and ASDEX-Upgrade tokamaks as well as in the JT-60U. A new driving mechanism that governs the VDE dynamics has been revealed by axisymmetric MHD simulations. A rapid flattening of the plasma current profile during the disruption plays a substantial role in dragging a single null-diverted plasma vertically towards the divertor. As a consequence, downward-going VDEs predominates over the upward-going ones in the lower single null discharges. The dragging effect explains many details of the VDE dynamics during the entire period of disruptive termination in ASDEX-Upgrade [2-6].

The neoclassical tearing mode (NTM) is considered to limit increase of the β-value in low collisional plasmas and to cause confinement degradation in tokamaks. It is important to prevent the NTM and clarify the excitation mechanisms of the NTM. A model of the polarization current term that includes the effects of the toroidal rotation and the pressure gradient was evaluated using JT-60U experimental data. Destabilization or stabilization by the polarization current term with the observed toroidal rotation was analyzed to be consistent with the excitation or suppression of the NTM. When the toroidal rotation has a destabilizing effect on the NTM, the NTM will grow rapidly without a seed island by both effects of the bootstrap current term and the polarization current term [2-7].

Simulation on the stabilization of the NTM by electron cyclotron current drive (ECCD) in JT-60SC superconducting tokamak has been performed by using a time-dependent model based on the modified Rutherford equation, the plasma transport equations, the current diffusion

equation and the EC code. Local EC current on the center of the island can fully stabilize NTM. Off-center EC current can decrease the island width, but it does not fully stabilize NTM. EC current moves the rational surface through the background current profile modification and decreases the stabilizing efficiency of EC. The conditions of full stabilization are investigated for various EC powers, current locations and profiles. Low power and peaked current profiles are effective in the full stabilization. When detection the island center is difficult, high power and broad current profile are required [2-8].

References

[2-1] Kurita, G., Tuda, T., Takeji, S., et al., "Analysis of RWM in JT-60 Super-Conducting Modification", 43rd Annual Meeting of DPP, Long Beech, CA (2001).
[2-2] Furukawa, M., Tokuda, S., Wakatani, M., Joint session of US/Japan MHD workshop and ITPA on MHD (2002).
[2-3] Lister, J.B., Khayrutdinov, R., Limebeer, D.J.N., et al., Fusion Engineering and Design, **56-57**, 755 (2001).
[2-4] Nakamura, Y., J. Plasma and Fusion Research, **77**, 843 (2001) (in Japanese).
[2-5] Nakamura, Y., Yoshino, R., Granetz, R.S., et al., J. Plasma and Fusion Research, **78**, 347 (2002) (in Japanese).
[2-6] Nakamura, Y., Pautasso, G., Gruber, O., et al., "Axisymmetric Disruption Dynamics including Current Profile Changes in the ASDEX-Upgrade Tokamak", Plasma Phys. Control. Fusion (in press).
[2-7] Takei, N., Ozeki, T., Smolyakov, A., et al., "Analysis of Toroidal Rotation Effects of the Ion Polarization Current on the Neoclassical Tearing Mode", to be published in J. Plasma Fusion Res.
[2-8] Hayashi, N., Ozeki, T., Hamamatsu, K., et al., "Simulation on Neoclassical Tearing Mode Stabilization by ECCD for JT-60 Superconducting Tokamak", to be published in J. Plasma Fusion Res.

3. Divertor

The divertor characteristics in JT-60SC are investigated with the SOLDOR/NEUT2D code with a simple radiation model. A fraction of carbon impurity is assumed to be 1.0% of the deuterium density and the radiation loss coefficient is enhanced by impurity transport effect of $n_e \cdot \tau_{recycle} = 10^{16}$ s/m^3 ($\tau_{recycle}$ is the mean recycling time of impurities). Capability of detachment control in JT-60SC divertor was demonstrated [3-1]. For standard operation (the edge density $n_{edge} = 3.2\times10^{19}$ m^{-3}, the power flow from the core plasma $Q_{electron} = Q_{ion} = 6$ MW, and the conductance of inner and outer cryopanels $C_{in} = C_{out} = 50$ m^3/s), the inner divertor plasma is partially detached while the outer divertor plasma is attached. The inner divertor is controlled from partially detached to attached plasma by increasing the inner pumping to $C_{in} = 150$ m^3/s. The outer divertor can be changed from attached to partially detached by the gas puffing of 8×10^{21} s^{-1}, which corresponds to 80% of the particle outflux from the main plasma.

Reference

[3-1] Sakurai, S., Shimizu, K., Masaki, K., et al., "Particle Control Design for Modification of JT-60 with Superconducting Coils", to be published in Plasma Phys. Control. Fusion.

4. Numerical Experiment of Tokamak (NEXT)

4.1 Transport and MHD Simulation

Zonal flow dynamics in the electron temperature gradient (ETG) turbulence was investigated by performing a gyro-fluid simulation. Modulational instability analysis based on a five-wave interaction model shows that ETG-generated zonal flows are weaker compared with the ITG counterpart, and that they hardly work for suppression of the turbulent electron transport [4.1-1]. The spectral analysis of 3-D nonlinear simulations show generation, evolution and saturation of ETG-generated zonal flows may be subjected to the same modulation process found in weak turbulence.

A Gyrokinetic Toroidal particle code has been developed for 3-Dimensional nonlinear simulation (GT3D) based on a finite element PIC method. An efficient field representation, where a ballooning phase factor is extracted analytically, is used to enable an analysis of reactor relevant large tokamak parameters with a/ρ_{ti}~500. The code has been optimized for parallel processing on JAERI Origin 3800 system. The code is applied for a linear global analysis of the ion temperature gradient driven (ITG) mode in normal and reversed shear tokamaks with a/ρ_{ti}=320~460 [4.1-2]. From comprehensive global analyses over a wide range of an unstable toroidal mode number spectrum (n=0~100), the ITG mode is found to change its property drastically around the q_{min} surface region of the reversed shear tokamaks, where a steep temperature gradient due to the internal transport barrier (ITB) is often observed. When the ion temperature is sufficiently high, most unstable high-n modes are excited in the outside of the q_{min} surface region, through global profile effects arising from the pressure profile and the magnetic configuration. Residual low-n global modes in the q_{min} region show slab like feature. The growth rate of this slab like mode is reduced by a peaked density profile, which can be formed by a pellet injection.

From the reduced MHD simulations, it is shown that there are three types of nonlinear behavior of the double tearing mode (DTM) [4.1-3]: the magnetic reconnection obeying the Kadomtsev's model, saturation of magnetic islands and the nonlinear destabilization of DTM. When the coupling between two rational surfaces is weak enough, the inner and outer islands saturate without interacting with each other. On the other hand, when the coupling between two rational surfaces is strong enough, the islands interact with each other keeping the linear growth rate almost up to the end of this process. When the coupling between two rational surfaces is intermediate, DTM is nonlinearly destabilized after long time scale evolution in the Rutherford type regime. During the Rutherford regime, higher harmonics are excited and the inner islands deform triangularly. The deformation forms the current point and the x-type reconnection region around the x-point of the outer island. The dependence of the spontaneous growth rate on the resistivity, η, is very weak, $\gamma \sim \eta^{\alpha}$, $\alpha \sim 0$, in the nonlinear destabilization phase. On the other hand, the Sweet-Parker type current sheet is formed and the x-type reconnection region changes to the

double y-type in the nonlinear phase of the strongly coupled DTM. Since the resistivity is very small in high temperature plasma, the DTM shows explosive growth after long time evolution in the Rutherford type regime. This feature may explain the fast time scale, low beta plasma collapse observed in JT-60U reversed shear discharges. It is the first time that the current point formation was found within the resistive MHD from the simulation.

References
[4.1-1] Jiquan Li and Kishimoto, Y., Phys. Plasmas, **9**, 1241(2002).
[4.1-2] Idomura, Y., Tokuda, S. and Kishimoto, Y., "Gyrokinetic Global Analysis of Ion Temperature Gradient Mode in Reversed Shear Tokamaks", IAEA Technical Meeting on Theory of Plasma Instabilities, 9-12 April 2002, Kloster Seeon, Germany.
[4.1-3] Ishii, Y., Azumi, M. and Kishimoto, Y., "Nonlinear Destabilization of Double Tearing Modes", The 4th China-Japan Workshop on Advanced Technologies and Physics in Toroidal Devices, Kumming, P.R.China (2001).

4.2 Divertor Simulation

Simulation codes have been developed to understand divertor physics. The divertor characteristics strongly depend on the divertor geometry and non-linear interactions among plasma, neutral and impurity. To analyze their transport in a realistic geometry, three codes, i.e., a 2D plasma fluid code (SOLDOR), a 2D Monte-Carlo neutral code (NEUT2D) and a 2D impurity Monte-Carlo code (IMPMC) have been developed. A new model for the thermal force including kinetic effect was incorporate into IMPMC [4.2-1]. Simulations were carried out for carbon impurity in detached plasmas. The kinetic effect is found to be small because the friction force dominates the thermal force for carbons sputtered from target plates. Recently, we incorporated a model of elastic collisions between neutral particles and plasma ions into NEUT2D, and analyzed the divertor characteristics in JT-60SC [4.2-2]. It was found that the elastic collision in a dense and cold divertor plasma ($n_e > 5\times10^{20}$ m^{-3}, $T_e < 5$ eV) plays an important role on detachment. A particle simulation code PARASOL has also been developed to understanding the basic physics of scrape-off layer and divertor plasmas. The PARASOL was extended to 2D double-null magnetic configuration to study drift effects in detail, and was used for the simulation of flow control with divertor biasing and gas puffing [4.2-3].

References
[4.2-1] Shimizu, K., Takizuka, T., "Impurity Behavior in MARFE Plasma", Proc. 27th EPS Conf. on Controlled Fusion and Plasma Physics, Budapest (2000).
[4.2-2] Shimizu, K., Takizuka, T., Sakurai, S., et al., "Simulation Analysis of Divertor Characteristics in JT-60 with Superconducting Coils", to be published in J. Nucl. Mater..
[4.2-3] Takizuka, T., Hosokawa, M., Shimizu, K., "Two-dimensional Particle Simulation of the Flow Control in SOL and Divertor Plasmas", to be published in J. Nucl. Mater..

IV. FUSION POWER PLANT DESIGN, SAFETY AND SOCIO-ECONOMIC STUDY

Research on fusion reactor design and safety was mainly devoted to; conceptual design of a tight aspect ratio tokamak reactor, physics design of a fusion power reactor A-SSTR2, high heat flux first walls, uses of fusion energy and a reduction of radioactive wastes from the DEMO plant. Marked progress was made in the study of the cost reduction, the fueling, the first wall engineering, the socio-economic potential and the waste management of fusion plants.

1. Fusion Reactor Design

1.1 Design of Tight Aspect Ratio Tokamak Reactor

In accordance with an intense requirement for the cost reduction in constructing fusion power reactors, a tight aspect ratio tokamak reactor VECTOR (Very Compact Tokamak Reactor) was newly proposed. The ST-like concept of the VECTOR with an aspect ratio of ~ 2 and a plasma major radius of ~3 m was found to be possible by adopting a net shield thickness of ~ 70 cm and a superconducting toroidal field (SCTF) coil system. We newly considered 1) removal of the center solenoid (CS) coil and 2) compromise of the tritium breeding in the inboard blanket. The key factor of this reactor concept depends on the feasibility of the high field and compact SCTF coil. The TF coil inner legs naturally become a solid-like integrated center post (CP) structure, leading to the maximum field of 20 ~ 23 T with the CP radius of 60 ~ 70 cm. Fusion power of 3.7 GW can be achievable. The reactor size comparison between ITER, A-SSTR2 which is our former design concept and VECTOR is shown in Fig. IV.1.1-1.

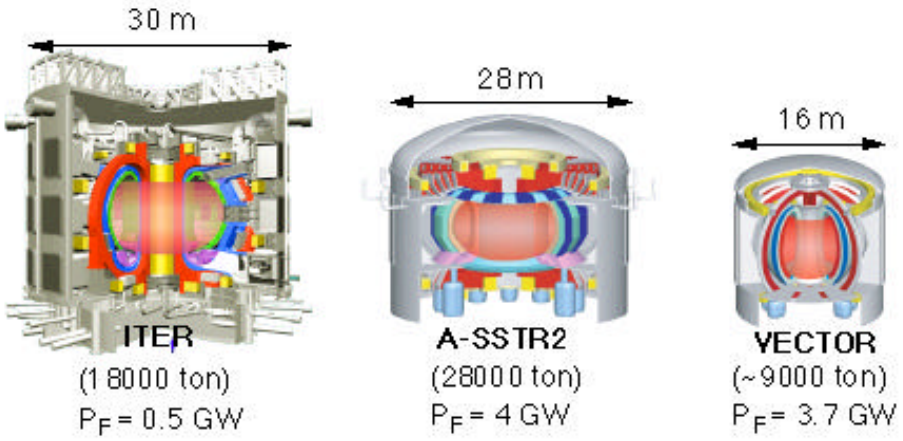

Fig.IV.1.1-1 Reactor size comparison between ITER, A-SSTR2 and VECTOR.

1.2 Assessment of Physical Issues in Fusion Reactors

Fuel supply in the fusion reactor A-SSTR2 was investigated with a transport code incorporated with a recently developed Parks model (E×B drift model). The initial result indicates that the rating of the reactor is maintained when pellets with a diameter of about 10 mm are injected at an initial speed of about 2 km/s from the high field side. The analysis also

indicates that the pellet injection is accompanied by about 10% fluctuations of output power, which is caused by a transient plasma cooling just after the injection.

Plasma wall interactions are understood as a critical matter in the first wall design. Analysis with the B2/EIRENE code suggests that the erosion rate of the first wall by charge exchange (CX) neutrals in a Demo reactor can be as low as 10 μm/y for tungsten. This is a consequence of dense scrape-off layer (SOL) where CX neutrals produced at lower energies in the outer SOL. Furthermore, we have assessed the interactions of lost alpha particles with wall materials, and uncovered the such important effect that the erosion rate by the alpha particles is comparable (about 20 μm/y for tungsten) with that by CX neutrals. Blistering due to alpha particle loss is also a matter of concern, in that the alpha particle fluence may exceed a critical fluence for blistering during the operation period of blanket modules (2-3 y).

1.3 Liquid Wall Divertor and Structural Integrity of First Wall

Using the finite element analysis code, thermal transfer characteristics of the free surface liquid flow with the secondary flow was evaluated to evaluate the possibility in the use for high heat flux components. The secondary flow was found to improve the apparent heat conductivity by three or four times and expected to remove the surface heat flux of 100 MW/m^2.

Concerning the structural integrity of first wall, a nonlinear thermal-plastic analysis with the finite element analysis code was carried out to study the behavior of cracks in the first wall. Assuming a crack depth of 1.0 mm on the plasma side of a SiC-based first wall of thickness 4.0 mm, it was shown that the bending stress around the crack is mostly compressing in the steady state, however the tensile stress concentration beyond the allowable stress can appear in a limited region around the crack tip [1.3-1, 1.3-2].

References

[1.3-1] Kurihara, R., "Thermofluid Analysis of Free Surface Liquid Divertor in Tokamak Fusion Reactor", to be published in Fusion Eng. Design.
[1.3-2] Kurihara, R., Nishio, S., Konishi, S., "Thermal Stress Analyses in First Wall Subjected to High Heat Flux from Fusion Plasma", Proc. of THERMAL STRESSES 2001, 81, Osaka, June (2001).

1.4 Use of Fusion Heat for Fuel Production

As an application of fusion energy, material recycling process, $C_lH_mO_n + H_2O \rightarrow xCO_2 + yH_2$, was identified to have advantages, and a plant for material recycle purpose was designed based on the previously reported A-SSTR2 reactor. If the entire energy of the 4 GW reactor is used for the material recycle, the expected electricity by using hydrogen fuel cells is estimated to be equivalent to 10 GW or more. Such a use of fusion energy for production of fuels for transportation is expected to expand the potential share of the fusion in energy market [1.4-1].

References

[1.4-1] Konishi, S., Fusion Eng. Design, **58-59**, 1103 (2001).

2. Fusion Safety

2.1 Tritium Safety Issue for Power Plants

Tritium safety issues are investigated considering the concept of DEMO plant following ITER as the next target. Water detritiation system, particularly for power blanket coolant was identified to dominate the safety feature of the entire plant by its technical difficulty and importance. Under off-normal conditions, this coolant tritium process can remove possible spill within the confinement, and thus fusion plant will not have any major process dedicated for accidents [2.1-1].

References

[2.1-1] Konishi, S., Tobita, K., Nishio, S., et al., Fusion Sci. Technol., **41**, 817 (2002).

2.2 Tritium Fuel Supply and Fusion Market Issue

Tritium balance in fusion reactor was studied [2.2-1]. The impact of tritium supply on the possible market share of fusion energy in the future was investigated with world energy and environment model. After introduction to the market, share of the fusion energy will be strongly restricted by the initial tritium supply, and capability to produce initial loading of tritium removes this limitation, and future fusion share could be doubled [2.2-2].

References

[2.2-1] Aoki, I., Konishi, S., et al., Fusion Sci. Technol., **41**, 835 (2002).
[2.2-2] Tokimatsu, K., Asaoka, Y., Okano, K., et al., Fusion Sci. Technol., **41**, 831 (2002).

2.3 Waste Management

Based on our previously proposed concept to reduce the radioactive wastes from a SiC/SiC-based fusion reactor A-SSTR2 by reinforcing the neutron shielding, we have confirmed that the same method is applicable to a ferritic steel-based DEMO, reducing the radioactive wastes to 6,600 tons after 50 years cooling time. The remaining portion of 19,500 tons can be treated as clearance wastes equivalent to industrial wastes. After additional 30 years cooling, the contact dose of all metal radioactive wastes will be 10 mSv/h or less so that the wastes will be recyclable by remote and hands-on accesses. This means that fusion energy has potential to establish a low emission system of materials.

Appendix A.1 Publication List (April 2001 – March 2002)

A.1.1 List of JAERI Report

1) Abe, T., Hiroki, S., Tanzawa, S., "Preliminary Joining Experiment of Alumina Pipes by Using Ceramics Sleeve", JAERI-Research 2001-029 (2001) (in Japanese).

2) Akasaka, H., Sueoka, M., Takano, S., et al., "Development of a New Discharge Control System Utilizing UNIX Workstations and VME-bus Systems for JT-60", JAERI-Tech 2001-087 (2001) (in Japanese).

3) Chiba, S., Kawano, Y., Tsuchiya, K., et al., "Development of Control and Data Processing System for CO_2 Laser Interferometer", JAERI Research 2001-50 (2001) (in Japanese).

4) Enoeda, M., Ohara, Y., Akiba, M., et al., "Conceptual Design of Solid Breeder Blanket System Cooled by Supercritical Water", JAERI-Tech 2001-078 (2001) (in Japanese).

5) Hosokawa, M., Takizuka, T., "Massively Parallel Computation of PARASOL Code on the Origin 3800 System", JAERI-Data/Code 2001-026 (2001) (in Japanese).

6) IFMIF International Team (Edited by Nakamura, H., et al.), "IFMIF International Fusion Materials Irradiation Facility Key Element Technology Phase Interim Report", JAERI-Tech 2002-022 (2002).

7) Iga, T., Okumura, Y., Kashiwagi, M., "Development of a High Brightness Ion Source for IFMIF and Preliminary Test Results", JAERI-Tech 2001-028 (2001) (in Japanese).

8) Kasai, S., Nakayama, T., Ishitsuka, E., "Development of Magnetic J x B Sensor", JAERI-Tech 2001-082 (2001).

9) Kashiwagi, M., Okumura, Y., Hanada, M., et al., "Development of Plasma Neutralizer Using DC Arc Discharge", JAERI-Tech 2001-046 (2001) (in Japanese).

10) Kawai, M., Akino, N., Ebisawa, N., et al., "Construction of Negative-ion Based NBI for JT-60U", JAERI-Tech 2002-073 (2001) (in Japanese).

11) Kuroda, T., Sato, K., Akiba, M., "Development of Fabrication Technologies for ITER In-vessel Components", JAERI-Tech 2002-044 (2002) (in Japanese).

12) Nakahira, M., Shibanuma, K., Kajiura, S., "Development of Fabrication Technology for ITER Vacuum Vessel", JAERI-Tech 2002-029 (2002) (in Japanese).

13) Nakamichi, M., Akutsu, H., Yamaguchi, K., et al., "Irradiation Data Analysis Program on Fusion Blanket," JAERI-Data/Code 2002-10 (2002) (in Japanese).

14) Nakamura, H., Hayashi, T., O'hira, S., et al., "Permeation Behavior of Deuterium Implanted into Beryllium", JAERI-Research 2001-042 (2001).

15) Neudatchin, S.V., Takizuka, T., Shirai, H., et al., "Dynamic Behavior of Transport in Normal and Reversed Shear Plasmas with Internal Transport Barriers in JT-60U", JAERI-Research 2001-056 (2001).

16) Nishitani, T., Ebisawa, K., Walker, C., et al., "Design of In-vessel Neutron Monitor Using Micro Fission Chambers", JAERI-Tech 2001-066 (2001).

17) Nishitani, T., Ebisawa, K., Walker, C., et al., "Design of Neutron Monitor Using Flowing Water Activation for ITER", JAERI-Tech 2002-033 (2002).

18) Nishitani, T., Shikama, T., Sugie, T., et al., "Irradiation Effects on Plasma Diagnostic Components (II)", JAERI- Research 2002-007 (2002).

19) Ohshima, T., "Data Processing System of GA and PPPL", JAERI-Review 2001-034 (2001) (in Japanese).

20) Sato, S., Kawasaki, N., Kume, E., "Development of Monte Carlo Gamma-ray Transport Calculation System", JAERI-Data/Code 2001-017 (2001) (in Japanese).

21) Sugimoto, M., Isono, T., Matsui, K., et al., "TF Insert Experiment Log Book-2nd Experiment of CS Model Coil- ", JAERI Tech 2001-085 (2001).

22) Takahashi, H., Nakahira, M., Yabana, S., "Characteristic Evaluation of High Compression Seismic Isolator for International Thermonuclear Experimental Reactor (ITER)", JAERI-Tech 2001-064 (2001) (in Japanese).

23) Terakado, T., Okano, J., Shimada, K., et al., "Pulse Operation Test of the ITER Central Solenoid Model Coil Using the JT-60 Power Supply", JAERI-Tech 2001-056 (2001) (in Japanese).

24) Yamauchi, M., Nishitani, T., Ochiai, K., et al., “Performance Test of Micro-fission Chambers for In-vessel Neutron Monitoring of ITER”, JAERI-Tech 2002-032 (2002).

A.1.2 List of papers published in journals

1) Ando, T., Isono, T., Nishijima, G., et al., “Design of a 60kA HTS Current Lead for Fusion Magnets and its R&D”, IEEE Trans. ASC, **11**, 2535 (2001).

2) Asakura, N., Sakurai, S., Tamai, H., et al., “Pumping Effects on the Plasma Flow and Detachment in JT-60U W-shaped Divertor”, J. Nucl. Mater., **290-293**, 825 (2001).

3) Bak, P. E., Asakura, N., Miura, Y., et al., “Multifractality in Edge Localized Modes in Japan Atomic Energy Research Institute Tokamak-60 Upgrade”, Physics of Plasmas, **8**, 1248 (2001).

4) Bakhtiari, M., Yoshino, R., Nishida, Y. “Fast Thermal Shutdown of Tokamak Discharges without Runaway Electron Avalanching”, Fusion Sci. Technol., **41**, 77 (2002).

5) Bruskin, L. G., Mase, A., Yamamoto, A., et al., “Analytical Study of Ultra-short Pulse Reflectometry1”, Plasma Phys. Control. Fusion, **43**, 1333 (2001).

6) Bruskin, L., G. Mase, A., “Analytical Simulation of Microwave Reflectometry of a Plasma Cylinder”, Rev. Sci. Instrum., **72**, 4139 (2001).

7) Cardella, A., Elio, F., Enoeda, M., et al., “Improvements in the Design and Manufacture of the ITER FEAT First Wall Towards Cost Minimization”, Fusion Eng. Des., **56-57**, 211 (2001).

8) Costley, A., Campbell, D., Kasai, S., et al., “ITER R&D: Auxiliary Systems: Plasma Diagnostics”, Fusion Eng. Des., **55**, 331 (2001).

9) Daenner, W., Carcella, A., Enoeda, M., et al., “ITER R&D: Vacuum Vessel and In-vessel Components: Shield Blanket Module”, Fusion Eng. Des., **55**, 205 (2001).

10) Enoeda, M., Moriyama, K., Kuroda, T., et al., “Safety Analysis of Test Module for Water Cooled Pebble Bed Blanket in ITER”, J. Nucl. Sci. Technol., **38**, 921 (2001).

11) Ezato, K., Suzuki, S., Sato, K., et al., “Critical Heat Flux Test on Saw-toothed Fin Duct under One-sided Heating Conditions”, Fusion Eng. Des., **56-57**, 291 (2001).

12) Ezato, K., Taniguchi, M., Sato, K., et al., “Ultrasonic Non-destructive Testing on CFC Monoblock Divertor Mock-up”, Physica Scripta, **T91**, 110 (2001).

13) Fujii, T., Moriyama, S., “High-voltage Test of Feedthroughs for a High-power ICRF Antenna”, IEEE Trans. Plasma Sci., **29**, 318 (2001).

14) Fujita, T., Ide, S., Kamada, Y., et al., “Quasisteady High-confinement Reversed Shear Plasma with Large Bootstrap Current Fraction under Full Noninductive Current Drive Condition in JT-60U”, Phys. Rev. Lett., **87**, 085001, (2001).

15) Fujita, T., Kamada, Y., Ide, S., et al., “Sustainment of High Confinement in JT-60U Reversed Shear Plasmas”, Nucl. Fusion, **42**, 180 (2002).

16) Fujita, T., Oikawa, T., Suzuki, T., et al., “Plasma Equilibrium and Confinement in a Tokamak with Nearly Zero Central Current Density in JT-60U”, Phys. Rev. Lett., **87**, 245001 (2001).

17) Fujiwara, Y., Hanada, M., Okumura, Y., et al., “Thermo-mechanical Analysis of an Acceleration Grid for the International Thermonuclear Experimental Reactor Neutral Beam Injection System”, Fusion Eng. Des., **55**, 35 (2001).

18) Fujiwara, Y., Inoue, T., Miyamoto, K., et al., “Influence of Radiation on Insulation Gas at the ITER-NBI System”, Fusion Eng. Des., **55**, 1 (2001).

19) Fukuda, T., Tsuchiya, K., Hatae, T., et al., “H-mode Edge Structure in JT-60U High Density Improved Confinement Plasmas”, J. Plasma Fusion Res., **4**, 243 (2001).

20) Furukawa, M., Nakamura, Y., Hamaguchi, S., et al., “High-n Ballooning Instabilities in Toroidally Rotating Tokamaks”, Phys. Plasmas, **11**, 4889 (2001).

21) Gao, X., Isayama, A., Kamada, Y., et al., “A New Regime for Studying the High Bootstrap Current Fraction”, Plasma Chinese Physics Letters, **18**, 931 (2001).

22) Gung, C.Y., Michael, P.C., Martovetsky, N.N., et al., “Instrumentation of the Central Solenoid Model Coil and the CS Insert”, IEEE Trans. ASC., **11**, 1881 (2001).

23) Hamada, K., Kato, T., Kawano, K., et al., “Experimental Results of Pressure Drop Measurement in ITER CS Model Coil Tests”, Advances in Cryogenic Engineering, **47**, 407 (2001).

24) Hanada, M., Kashiwagi, M., Morishita, T., et al., “Development of Negative Ion Source for the ITER

Neutral Beam Injector", Fusion Eng. Des., **55-57**, 505 (2001).

25) Hatae, T., Sugihara, M., Hubbard, A. E., et al., "Understanding of the H-mode Pedestal Characteristics Using the Multimachine Pedestal Database", Nucl. Fusion, **41**, 285 (2001).

26) Higashijima, S., Kubo, H., Sugie, T., et al., "Impurity Behavior Before and During the X-point MARFE in JT-60U", J. Nucl. Mater., **623**, 290 (2001).

27) Hirose, T., Tanigawa, H., Ando, M., et al., "Small Specimen Test Technology for Evaluation of Fatigue Properties of Fusion Structural Materials", Mater. Trans., **42**, 389 (2001).

28) Horton, W., Porcelli, F., Kishimoto, Y., et al., "Ignitor Physics Assessment and Confinement Projections", Nucl. Fusion, **42**, 169 (2002).

29) Hosogane, N. and JT-60 team, "Progress of JT-60U Facilities and Experimental Research Toward Steady High Performance Plasmas", Fusion Eng. Des., **56-57**, 813 (2001).

30) Ide, S., and JT-60 team, "Formation of Internal Transport Barriers and its Impact on the JT-60U Plasmas", J. Plasma Fusion Res., **4**, 99, (2001).

31) Ido, T., Kamiya, K., Miura, Y., et al., "Observation of the Fast Potential Change at L-H Transition by a Heavy-ion-beam Probe on JFT-2M", Phys. Rev. Lett., **88**, 055006 (2002).

32) Idomura, Y., Tokuda, S., Kishimoto, Y., et al., "Gyrokinetic Theory of Drift Waves in Negative Shear Tokamaks", Nucl. Fusion, **41**, 437 (2001).

33) Imai, T., Kobayashi, N., Temkin, R., et al., "ITER R&D; Electron Cyclotron Heating and Current Drive System", Fusion Eng. Des., **55**, 281 (2001).

34) Inoue, T., Hemsworth, R., Kulygin, V., et al., "ITER R&D: Auxiliary Systems: Neutral Beam Heating and Current Drive System", Fusion Eng. Des., **55**, 291 (2001).

35) Inoue, T., Pietro, Di., Hanada, M., et al., "Design of Neutral Beam System for ITER-FEAT", Fusion Eng. Des., **56-57**, 517 (2001).

36) Isayama, A., Isei, N., Ishida, S., et al., "A 20-channel Electron Cyclotron Emission Detection System for a Grating Polychromator in JT-60U", Rev. Sci. Instrum., **73**, 1165 (2001).

37) Isayama, A., Kamada, Y., Ozeki, T., et al., "Long Sustainment of Quasi-steady-state High β_p H-mode Discharges in JT-60U", Nucl. Fusion, **41**, 761 (2001).

38) Ishitsuka, E., Kan, S., Kawamura H., et al., "In Situ Characterization of a Small Sized Motor Under Neutron Irradiation", Fusion Eng. Des., **58-59**, 517 (2001).

39) Ishitsuka, E., Uchida, M., Sato, K., et al., "High Heat Load Tests of Neutron Irradiated Divertor Mockups", Fusion Eng. Des., **56-57**, 421 (2001).

40) Ishizawa, A., Tokuda, S., Wakatani, M., "Improved Theory of Forced Magnetic Reconnection due to an Error Field and its Application to Seed Island Formation for the NTM", Nucl. Fusion, **41**, 1857 (2001).

41) Isono, T., Matsui, K., Kato, T., et al., "Quench Characteristics of the ITER CS Insert Coil", Cryogenic Eng., **36**, 373 (2001).

42) Itami, K., Coad, P., Fundameski, W., et al., "Observation of Detachment in the JET MkIIGB Divertor Using CCD Camera Tomography", J. Nucl. Mater., **290-293**, 633 (2001).

43) Itami, K., Tamai, H., Sakurai, S., et al., "Impurity Injection to Plasmas with Improved Plasma Confinement", J. Plasma Fusion Res., **77**, 1027 (2001).

44) Kamada, Y., and JT-60 team, "Extended JT-60U Plasma Regimes for High Integrated Performance", Nucl. Fusion, **41**, 1311 (2001).

45) Kamiya, K., Kimura, H., Hoshino, K., et al., "The Multichannel Motional Stark Effect Diagnostic Discriminating Radial Electric Field in the JFT-2M Tokamak", Rev. Sci. Instrum., **72**, 2931 (2001).

46) Kanari, M., Abe, T., Kosaku, Y., et al., "Repeated Impact Test on Plasma Sprayed Alumina Insulation Film for Fusion Reactor", J. At. Energy Soc. Japan, **43**, 12 (2001) (in Japanese).

47) Kashiwagi, M., Morishita, T., Okumura, Y., et al., "Optimization of Plasma Grid Material in Cesium-seeded Volume Negative-ion Sources", Rev. Sci. Instrum., **73**, 664 (2002).

48) Kasugai, Y., Maekawa, F., Ikeda, Y., et al., "Measurement of Activation Cross Section for Mercury Isotopes in the Neutron Energy Range between 13.4 and 14.9 MeV", J. Nucl. Sci. Technol., **38**, 1048 (2001).

49) Kato, T., Nakajima, H., Isono, T., et al., “CS Model Coil Test Facility”, Cryogenic Eng., **36**, 315 (2001).

50) Kawamura, Y., Konishi, S., Nishi, M., “Development of a Micro Gas Chromatograph for the Analysis of Hydrogen Isotope Gas Mixtures in the Fusion Fuel Cycle”, Fusion Eng. Des., **58-59**, 389 (2001).

51) Kikuchi, M. and JT-60 team, “Advanced Scenarios in JT-60U: Integration towards a Reactor Relevant Regime”, Plasma Phys. Control. Fusion, **43**, 217 (2001).

52) Kimura, H., Sato, M., Kawashima, H., et al., “Progress of Advanced Material Tokamak Experiment (AMTEX) Program on JFT-2M”, Fusion Eng. Des., **56-57**, 831 (2001).

53) Kishimoto, Y., Masaki, T., Tajima, T., “High Energy Ions and Nuclear Fusion in Laser-plasma Interaction”, Phys. Plasmas, **11**, 589 (2001).

54) Kobayashi, K., Hayashi, T., Iwai, Y., et al., “Results of Experimental Study on Detritiation of Atmosphere in Large Space”, Fusion Eng. Des., **58-59**, 1059 (2001).

55) Koizumi, N., Ando, T., Takahashi, Y., et al., “Analysis of Current after Normal Transition in Cable-in-conduit Conductor”, IEEE Trans. ASC, **11**, 2575 (2001).

56) Koizumi, N., Takahashi, Y., Nakajima, H., et al., “Evaluation of Critical Current Performance of an Nb_3Al Conductor with Stainless Steel Conduit”, Cryogenic Eng., **36**, 478 (2001).

57) Konishi S., “Use of Fusion Energy as a Heat for Various Applications”, Fusion Eng. Des., **58-59**, 1103 (2001).

58) Konishi S., Tobita, K., Nishio S., et al., “Tritium Issues toward Fusion Plants”, Fusion Sci. Technol., **41**, 817 (2002).

59) Konno, C., Maekawa, F., Wada, M., et al., “DORT Analyses of Decay Heat Experiment on Tungsten for ITER”, Fusion Eng. Des., **58-59**, 961 (2001).

60) Konoshima, S., Leonard, A. W., Ishijima, T., et al., “Tomographic Reconstruction of Bolometry for JT-60U Diverted Tokamak Characterization”, Plasma Phys. Control. Fusion, **43**, 959 (2001).

61) Kramer, G. J., Cheng, C. Z., Kusama, Y., et al., “Magnetic Safety Factor Profile before and after Sawtooth Crashes Investigated with Toroidicity and Ellipticity Induced Alfven Eigenmodes”, Nucl. Fusion, **41**, 1135 (2001).

62) Lee, S., Kondo, T., Miura, Y., “Development of Advanced Collective Thomson Scattering for Impurity, Helium Ash Density, and D/T Ratio Measurements”, J. Plasma Fusion Res., **77**, 919 (2001).

63) Lister, J.B., Khayrutdinov, R., Limebeer, D.J.N., et al., “Linear and Non-linear Plasma Equilibrium Responses on the JT-60U and TCV Tokamaks”, Fusion Eng. Des., **56-57**, 755 (2001).

64) Maekawa, F., Ochiai, K., Shibata, K., et al., “Benchmark Experiment on Silicon Carbide with D-T Neutrons and Validation of Nuclear Data Libraries”, Fusion Eng. Des., **58-59**, 595 (2001).

65) Martovetsky, N., Michael, P., Minervini, A., et al., “ITER CS Model Coil and CS Insert Test Results”, IEEE Trans. ASC, **11**, 2030 (2001).

66) Matsui, K., Nunoya, Y., Kawano, K., et al., “AC Loss Performance of CS Insert Coil”, Cryogenic Eng., **36**, 361 (2001).

67) Matsukawa, M., Ishida, S., Sakasai, A., et al., “A Design Study of the Power Supply System for Superconducting JT-60”, Fusion Technol., **39**, 1106 (2001).

68) Matsumoto, H., “Simulation of 3He Minority ICRF Heating in ITER”, J. Appl. Phys., **40**, 1187 (2001).

69) Matsumoto, T., Tokuda, S., Kishimoto, Y., et al., “Generation of Radial Electric Field in the Process of Full Reconnection by Kinetic Kink Mode”, Earth Planets Space, **53**, 565 (2002).

70) Michael, P.C., Vieira, R., Jayakumar, R.V., et al., “Mechanical Preloading of the Central Solenoid Model Coil”, IEEE Trans. ASC, **11**, 1877 (2001).

71) Mitarai, O., Honda, T., Nishitani, T., et al., “Comparative Studies of the dW/dt Effect in the Net Heating Power for Ignition Analysis ”, Fusion Eng. Des., **55**, 477 (2001).

72) Miura, I., Nishio, T., Kondo, T., et al., “Neutron-nuclear Data Benchmark for Copper and Tungsten by Slab Assembly Transmission Experiments with DT Neutrons”, Fusion Eng. Des., **58-59**, 617 (2001).

73) Miura, Y.M., Matsukawa, M., Nakano, H., “A Deadbeat Control Method for a PWM Converter Applied to a Superconducting Magnet”, Fusion Eng. Des., **58-59**, 57 (2001).

74) Miura, Y., Ido, T., Kamiya, K., et al., “Relations among Potential Change, Fluctuation Change and Transport Barrier in the JFT-2M Tokamak”, Nucl. Fusion, **41**, 973 (2001).

75) Morishita, T., Kashiwagi, M., Hanada, M., et al., “Mechanism of Negative Ion Production in a Cesium Seeded Ion Source”, Jpn. J. Appl. Phys., **40**, 4709 (2001).

76) Morishita, T., Miyamoto, K., Fujiwara, Y., et al., “Spatial Uniformity of Negative Ion Production in Volume Negative Ion Source”, Rev. Sci. Instrum., **73**, 1064 (2002).

77) Murata, I., Nishio, T., Kondo, T., et al., “Neutron-nuclear Data Benchmark for Copper and Tungsten by Slab Assembly Transmission Experiments with DT”, Fusion Eng. Des., **58-59**, 617 (2001).

78) Nagao, Y., Nakamichi, M., Tsuchiya, K. et al., “Neutronic and Thermal Estimation of Blanket In-pile Mockup with Li_2TiO_3 Pebbles”, Fusion Eng. Des., **58-59**, 673 (2001).

79) Nagata, M., Fukumoto, N., Ogawa, H., et al., “Behavior of Compact Toroid Injected into an External Magnetic Field”, Nucl. Fusion, **41**, 1687 (2001).

80) Nakahira, M., Takahashi, H., Koizumi, K., et al., “ Progress and Achievements on the R&D Activities for ITER Vacuum Vessel”, Nucl. Fusion, **41**, 375 (2001).

81) Nakamichi, M., Kawamura, H., “Out-of-pile Characterization of Al_2O_3 Coating as Electrical Insulator,” Fusion Eng. Des., **58-59**, 719 (2001) .

82) Nakamichi, M., Kawamura, H., Teratani, T., “Characterization of Chemical Densified Coating as Tritium Permeation Barrier,” J. Nucl. Sci. Tech., **38,** 1007 (2001).

83) Nakamura, H., Hayashi, T., Nishi, M., et al., “Implantation Driven Permeation Behavior of Deuterium through Pure Tungsten”, Fusion Eng. Des., **55**, 513 (2001).

84) Nakamura, H., Ida, M., Sugimoto, M., et al., “Status of Lithium Target System for International Fusion Materials Irradiation Facility (IFMIF)”, Fusion Eng. Des., **58-59**, 919 (2001).

85) Nakamura, H., Tadokoro, T., Shu, W.M., et al., “Tritium Permeation Behavior implanted into Pure Tungsten and its Isotope Effect”, J. Nucl. Mater., **297**, 285 (2001).

86) Nakamura, Y., Pautasso, G., Gruber, O., et al., “Axisymmetric Disruption Dynamics Including Current Profile Changes in the ASDEX-upgrade Tokamak”, Plasma Phys. Control. Fusion, **44**, 1471 (2002).

87) Nakayama, T., Abe, M., Takeuchi, K., et al., “Development of a Decision Method for Optimum Ferromagnetic Board Arrangements to Reduced Toroidal Magnetic Ripple”, Jpn. J. Appl. Phys., **40**, 3409 (2001).

88) Neudatchin, S.V., Takizuka, T., Shirai, H., et al., “Analysis of Internal Transport Barrier Heat Diffusivity from Heat Pulse Propagation Induced by an ITB Event in JT-60U Reverse Shear Plasmas”, Plasma Phys. Control. Fusion, **43**, 661 (2001).

89) Neudatchin, S.V., Takizuka, T., Shirai, H., et al., “Dynamics and Interplay of L-H-L Transitions and ITB Events in Reversed Shear Plasmas with Internal Barriers in JT-60U”, Plasma Phys. Control. Fusion, **44**, A383 (2002).

90) Ninomiya, A., Arai, K., Takano, K., et al., “Acoustic Emission in ITER CS Model Coil and CS Insert Coil”, Cryogenic Eng., **36**, 344 (2001).

91) Nishitani, T., Shikama, T., Fukao, M., et al., “Neutron Irradiation Tests on Diagnostic Components at JAERI”, Fusion Eng. Des., **56-57**, 905 (2001).

92) Nunoya, Y., Isono, T., Sugimoto, M., et al., “Critical Current and Sharing Temperature of the ITER-CS Insert Coil”, Cryogenic Eng., **36**, 354 (2001).

93) Oikawa, T., Kamada, Y., Isayama, A., et al., “Reactor Relevant Current Drive and Heating by N-NBI on JT-60U”, Nucl. Fusion, **41**, 1575 (2001).

94) Ogawa, T., Hoshino, K., Kanazawa, S., et al., “Radio Frequency Experiments in JFT-2M: Demonstration of Innovative Applications of a Travelling Wave Antenna”, Nucl. Fusion, **41**, 1767 (2001).

95) Oguri, H., Okumura, Y., Hasegawa, K., et al., “Development of an H-ion Source for the High Intensity Proton Linac”, Rev. Sci. Instrum., **73**, 1021 (2002).

96) Ohga, T., Umeda, N., Akino, N., et al., “Present Status of the Negative Ion Based Neutral Beam Injector for JT-60U”, Rev. Sci. Instrum., **73**, 1058 (2002).

97) O'hira, S., Tada, E., Hada, K., et al., “Safety Activities in JAERI Related to ITER”, Fusion Eng. Des., **54**, 515 (2001).

98) O'hira, S., Tada, E., Hada, K., et al., “Safety Design Concepts for ITER-Tritium Facility”, Fusion Sci. Technol., **41**, 642 (2002).

99) Ohshima, T., Matsuda, T., Tsugita, T., et al., “Mass Data Acquisition Systems in JT-60 Data Processing System”, Rev. Sci. Instrum., **72**, 517 (2001).

100) Oikawa, A., Miya, N., Kodama, K., et al, “Tritium Experience in JT-60 DD Plasma Operation”, Fusion Sci. Technol., **41**, 303 (2002).

101) Okuno, K., Bessette, D., Ferrari, M., et al., “Key Features of the ITER-FEAT Magnet System”, Fusion Eng. Des., **58**-**59**, 157 (2001).

102) Ongena, J., Budny, R., Dumortier, P., et al., “Recent Progress toward High Performance above the Greenwald Density Limit in Impurity Seeded Discharges in Limiter and Divertor Tokamaks”, Physics of Plasmas, **8**, 2188 (2001).

103) Onozuka, M., Alfile, J.-P., Aubert, Ph., et al., “Manufacturing and Maintenance Technologies Developed for a Thick Wall Structure of the ITER Vacuum Vessel”, Fusion Eng. Des., **54**, 397 (2001).

104) Oyama, N., Shinohara, K., “Heterodyne O-mode Reflectometer on the JT-60U Tokamak”, Rev. Sci. Instrum., **73**, 1169 (2002).

105) Oya, Y., Kobayashi, K., Shu, W., et al., “Tritium Contamination and Decontamination Study on Materials for ITER Remote Handling Equipment”, Fusion Eng. Des., **55**, 449 (2001).

106) Oya, Y., Tadokoro, T., Shu, W.M., et al., “Tritium Decontamination from Co-deposited Layer on Tungsten Substrate by Ultra Violet Lamp and Laser”, J. Nucl. Sci. Technol., **38**, 967 (2001).

107) Oyama, N., Shinohara, K., Kamada, Y., et al., “Collapse of Density Pedestal by Giant ELM on JT-60U Plasma”, Phys. Control. Fusion, **43**, 717 (2001).

108) Sakamoto, Y., Kamada, Y., Ide, S., et al., “Characteristics of International Transport Barriers in JT-60U Reversed Shear Plasmas”, Nucl. Fusion, **41**, 865 (2001).

109) Sakamoto, Y., Takizuka, T., Shirai, H., et al., “Active Control of Internal Transport Barrier and Confinement Database in JT-60U Reversed Shear Plasma”, J. Plasma Fusion Res., **4**, 249 (2001).

110) Piazza, G., Enoeda, M., Ying, A., “Measurements of Effective Thermal Conductivity of Ceramic Breeder Pebble Beds”, Fusion Eng. Des., **58**-**59**, 661 (2001) .

111) Sakasai, A., Takenaga, H., Kubo, H., et al., “Helium Exhaust in Divertor-closure Configuration with W-shaped Divertor of JT-60U”, J. Nucl. Mater., **290**-**293**, 957 (2001).

112) Sakurai, S. and JT-60 Team, “Impurity Behavior in High Performance Radiative Discharges of JT-60U”, J. Nucl. Mater., **290**-**293**, 1002 (2001).

113) Sato, K., Ishitsuka, E., Uchida, M., et al., “Thermal Cycle Experiments of the Neutron-irradiated CFC/Cu Mock-ups”, Physica Scripta, **T91**, 113, (2001).

114) Sato, S., Enoeda, M., Kuroda, T., et al, “Characteristic Evaluation of HIP Bonded SS/DSCu Joints for Surface Roughness”, Fusion Eng. Des., **58**-**59**, 749 (2001).

115) Seki, M., Maebara, S., Fujii, T., “R&D of the Heat-Resistant LH Antenna”, Fusion Eng. Des., **56**-**57**, 581 (2001).

116) Shibanuma, K., Honda, T., “Blanket Remote Handling Systems”, Fusion Eng. Des., **55**, 247 (2001).

117) Shimomura, Y., “ITER Opportunity of Fusion Burning Plasma Studies”, Plasma Phys. Control. Fusion, **43**, A385 (2001).

118) Shinohara, K., Kusama, Y., Takechi, M., et al., “Alfvén Eigenmodes Driven by Alfvénic Beam Ions in JT-60U”, Nucl. Fusion, **41**, 603 (2001).

119) Smolyakov, A. I., Lazzaro, E., Azumi, M., et al., “Stabilization of Magnetic Islands due to the Sheared Plasma Flow and Viscosity”, Plasma Phys. Control. Fusion, **43**, 1661 (2001).

120) Suzuki, T., Ide, S., Oikawa, T., et al., “Measurement of Current Driven by Electron Cyclotron Waves in JT-60U”, Plasma Phys. Control. Fusion, **44**, 1 (2002).

121) Suzuki, Y., Hayashi, T., Kishimoto, Y., “Theory and MHD Simulation of Fuelling by Compact Toroid Injection”, Nucl. Fusion, **41**, 873 (2001).

122) Takahashi, K., Imai, T., Sakamoto, K., et al., “Development and Design of an ECRF Launching System for ITER”, Fusion Eng. Des., **56**, 587 (2001).

123) Takahashi, Y., Matsui, K., Nishii, K., et al., “AC Loss Measurement of 46 kA-13T Nb_3Sn Conductor for ITER”, IEEE Trans. ASC, **11**, 1546 (2001).

124) Takayanagi, T., Ikehata, T., Okumura, Y., et al., “Optimization of Negative Ion Extractor in a JAERI 400 keV H-ion Source”, Rev. Sci. Instrum., **73**, 1061 (2002).

125) Takayanagi, T., Ikehata, T., Okumura, Y., et al., “Measurement of Grid Heat Loading in a Negative Ion Source for Producing Intense H-ion Beam by Aperture Displacement Focusing Technique”, Rev. Sci. Instrum., **72**, 3829 (2001).

126) Takeji, S., Tokuda, S., Fujita, T., et al., “Resistive Instabilities in Reversed Shear Discharges and Wall Stabilization on JT-60”, Nucl. Fusion, **42**, 5 (2002).

127) Takenaga, H., and JT-60 Team, “Improved Particle Control for High Integrated Plasma Performance in Japan Atomic Energy Research Institute Tokamk-60 Upgrade”, Physics of Plasmas, **8**, 2217 (2001).

128) Takenaga, H., Mahdavi, M. A., Baker, D. R., “Comparison of Particle Confinement in the High Confinement Mode Plasmas with the Edge Localized Mode of the Japan Atomic Energy Research Institute Tokamak-60 Upgrade and DIII-D Tokamak”, Physics of Plasmas, **8**, 1607 (2001).

129) Takenaga, H., Sakasai, A., Kubo, H., et al., “Study of Particle Pumping Characteristics for Different Pumping Geometries in JT-60U and DIII-D Divertors”, Nucl. Fusion, **41**, 1777 (2001).

130) Takizuka, T., Hosokawa, M., Shimizu, K., “Particle Simulation of Detached Plasma in the Presence of Diffusive Particle Loss and Radiative Energy Loss”, J. Nucl. Mater., **290-293**, 753 (2001).

131) Takizuka, T., Sakamoto, Y., Fukuda, T., et al., “Energy Confinement Scaling for Reversed-shear Plasmas with Internal Transport Barrier in JT-60U”, Plasma Phys. Control. Fusion, **44**, A423 (2002).

132) Tanigawa, H., Ando, M., Katoh, Y., et al., “Response of Reduced Activation Ferritic Steels to High-fluence Ion-irradiation”, J. Nucl. Mater., **297**, 279 (2001).

133) Tanzawa, S., Hiroki, S., Abe, T., et al., “Preliminary Experiments on Continuous Separation of H_2/He Mixture Gas”, J. Vac. Soc. Jpn., **44**, 667 (2001) (in Japanese).

134) Tivey, R., Akiba, M., Driemeyer, D., et al., “ITER R&D: Vacuum Vessel and In-vessel Components: Divertor Cassette”, Fusion Eng. Des., **55**, 219, (2001).

135) Tokimatsu K., Asaoka Y., Okano K., et al., “Potential of Fusion Energy in the Context of Tritium Supply”, Fusion Sci. Technol., **41**, 831 (2002).

136) Tokuda, S., “An Innovative Method for Ideal and Resistive MHD Stability Analysis of Tokamaks”, Nucl. Fusion, **41**, 1037 (2001).

137) Totsuka, T., Akasaka, H., Sueoka, M., et al., “Development of a New Discharge Control System for JT-60 with UNIX Workstation and VME-bus System”, Fusion Eng. Des., **60**, 409 (2001).

138) Tsuchiya, K., Nakamichi, M., Nagao, Y. et al., “In-situ Tritium Recovery Experiments of Blanket In-pile Mockup with Li_2TiO_3 Pebble Bed in Japan”, J. Nucl. Sci. Tech., **38**, 996 (2001).

139) Tsuchiya, K., Kabutomori, T., Kawamura, H., “Study of the High Efficiency of ZrNi Alloys for Tritium Gettering Properties”, Fusion Eng. Des., **58-59**, 401 (2001).

140) Tsuchiya, K., Kikukawa, A., Enoeda, M., et al., “In-situ Tritium Release Behavior from Li_2TiO_3 Pebble-bed”, Fusion Eng. Des., **58-59**, 679 (2001).

141) Tsuchiya, Y., Kikuchi, K., Minakawa, N., et al., “Neutron Diffraction Experience at RESA for Engineering-aided Application”, J. Phys. Soc. Jpn., **70**, 520 (2001).

142) Tsuji, H., Ando, T., Takahashi, Y., et al., “Progress of the ITER Central Solenoid Model Coil Program”, Nucl. Fusion, **41**, 645 (2001).

143) Tsuji, H., Egorov, S., Minervini, J., et al., “ITER R&D: Magnets: Central Solenoid Model Coil”, Fusion Eng. Des., **55**, 153 (2001).

144) Tsuji, H., Egorov, S., Minervini, J., et al., “ITER R&D: Magnets: Conductor and Joint Development”, Fusion Eng. Des., **55**, 141 (2001).

145) Uehara, K., Maeda, M., Tsushima, A., et al., “Particle and Thermal Diffusivities in the Scrape-off Layer Plasma in JFT-2M Tokamak”, Contrib. Plasma Phys., **42**, 384 (2002).

146) Uno, Y., Kaneko, J., Nishitani, T., et al., “Absolute Measurement of D-T Neutron Flux with a Monitor Using Activation of Flowing Water ”, Fusion Eng. Des., **56-57**, 895 (2001).

147) Urano, H., Kamada, Y., Kubo, H., et al., “Pedestal Structure and Thermal Energy Confinement of ELMy H-mode in JT-60U”, J. Plasma Fusion Res., **4**, 239 (2001).

148) Urata, K., Suzuki, Y., Kudough, F., et al., “Dynamic Analyses of Electromagnetic Force on Ferritic Board for AMTEX on JFT-2M”, Fusion Eng. Des., **56**-**57**, 849 (2001).

149) Wang, S., Ozeki, T., Tobita, K., “Effects of Circulating Energetic Ions on Sawtooth Oscillations”, Phys. Rev. Lett., **88**, 105004 (2002).

150) Watanabe, K., Amemiya, T., Hanada, M., et al., “Development of a Large Volume Negative-ion Source for ITER Neutral Beam Injector ”, Rev. Sci. Instrum., **73**, 1090 (2002).

151) Yanagi, Y., Sato, S., Enoeda, M., et al., “Nuclear and Thermal Analyses of Supercritical-water-cooled Solid Breeder Blanket for Fusion DEMO Reactor”, J. Nucl. Sci. Technol., **38**, 1014 (2001).

A.1.3. List of papers published in conference proceedings

1) Ando, M., Tanigawa, H., Jitsukawa, S., et al., “Evaluation of Plastic-deformation Behavior on Dual Ion Irradiated Reduced Activation Ferritic/Martensitic Steels by Ultra-micro-identification Technique”, Proc. 10th Int. Conf. on Fusion Reactor Mater. (ICFRM-10) (2001), to be published in J. Nucl. Mater..

2) Aoki, I., Konishi, S., Kurihara, R., et al., “Time Dependent Tritium Inventories of a Fusion Reactor”, Proc. 6th Int. Conf. on Tritium Sci. Technol.. (2001), to be published in Fusion Sci. Technol..

3) Arita, T., Yamanishi, T., Iwai, Y., et al., “Experimental Study for Parameters affecting Separation Factor of Cryogenic Wall Thermal Diffusion Column”, Proc. 6th Int. Conf. on Tritium Sci. Technol. (2001), to be published in Fusion Sci. Technol..

4) Baba, M., Aoki, T., Hasegawa, M., et al., “Experimental Studies on the Neutron Emission Spectrum and Induced Radioactivity of the 7Li(D,N) Reaction in 20-40 MeV Region”, Proc. 10th Int. Conf. on Fusion Reactor Mater. (ICFRM-10), (2001), to be published in J. Nucl. Mater..

5) Costley, A.B., Donne, A.J.H., Ebisawa, K., et al., “ The Challenge of ITER Diagnostics”, Proc. 28th EPS Conf. on Control. Fusion and Plasma Phys., OR.27 (2001).

6) Furuya, K., Wakai, E., Ando, M., et al., “Microstructure and Hardness of HIP-bonded Regions in F82H Blanket Structures” , Proc. 10th Int. Conf. on Fusion Reactor Mater. (ICFRM-10) (2001), to be published in J. Nucl. Mater..

7) Futatsuki, T., Tajima, Y., Abe, T., et al., “Low Cost and Compact Solution for Recycling PFCs by the Continuous Gas Chromatography”, 2001 IEEE Int. Symp. on Semiconductor Manufacturing (ISSM2001), 465 (2001).

8) Hatae, T., Naito, M., “Very High Electron Temperature Diagnostics Using Combined Ruby and YAG Laser Thomson Scattering Systems in JT-60U”, Proc. 10th Int. Symp. on Laser-aided Plasma Diagnostics, 160 (2001).

9) Hayashi, N., Ozeki, T., Hamamatsu, et al., “Stabilization of Neoclassical Tearing Mode by ECCD for JT-60 Super-conducting Tokamak”, Proc. Joint Conf. 12th Int. Toki Conf. on Plasma Phys. Control. Nucl. Fusion and 3rd General Scientific Assembly of Asia Plasma Fusion Assoc. (2001), to be published in J. Plasma and Fusion Res. (JPFR series Vol. 5).

10) Hayashi, T., Kobayashi, K., Iwai, Y., et al., “Tritium Confinement Demonstration using Caisson Assembly for Tritium Safety Study at TPL/JAERI”, Proc. 6th Int. Conf. on Tritium Sci. Technol. (2001), to be published in Fusion Sci. Technol..

11) Hayashi, T., Suzuki, T., Konishi, S., et al., “Development of ZrCo Beds for ITER Tritium Storage and Delivery”, Proc. 6th Int. Conf. on Tritium Sci. Technol. (2001), to be published in Fusion Sci. Technol..

12) Hirata, S., Kakuta, T., Hayashi, T., et al., “Design of Atmosphere Detritiation System for ITER”, Proc. 6th Int. Conf. on Tritium Sci. Technol.. (2001), to be published in Fusion Sci. Technol..

13) Hirose, T., Tanigawa, H., Ando, M., et al., “Radiation Effects on Low Cycle Fatigue Properties of Reduced Activation Ferritic/Martensitic Steels”, Proc. 10th Int. Conf. on Fusion Reactor Mater. (ICFRM-10) (2001), to be published in J. Nucl. Mater..

14) Ida, M., Horiike, H., Akiba, M., et al., “Water Jet Flow Simulation and Lithium Free Surface Flow Experiments for the IFMIF Target”, Proc. 10th Int. Conf. on Fusion Reactor Mater. (ICFRM-10) (2001), to be published in J. Nucl. Mater..

15) Igitkhanov, Yu., Sugihara, M., Pogutse, O.P., et al., “A Physics of Type I ELMs”, Proc. 28th EPS Conf. on Control. Fusion and Plasma Phys., P4.101 (2001).

16) Isayama, A. and JT-60 team, “ECRF Experiments on JT-60U”, Proc. 14th Topical. Conf. on Radio Frequency Power in Plasmas”, 267 (2001).

17) Isobe, K., Imaizumi, H., Hayashi, T., et al., “Demonstration of Fuel Cleanup System consisting of Electrolytic Reactor and Tubular Reservoir Tank for Fusion Reactors”, Proc. 6th Int. Conf. on Tritium Sci. Technol. (2001), to be published in Fusion Sci. Technol..

18) Iwai, Y., Nakamura, H., Konishi, S., et al., “Study on Sudden Loss of Cryogenic Coolant Accident happened in the Hydrogen Isotope Separation System for Fusion Reactor”, Proc. 6th Int. Conf. on Tritium Sci. Technol. (2001), to be published in Fusion Sci. Technol..

19) Iwai, Y., Misaki, Y., Hayashi, T., et al., “The Water Detritiation System of the ITER Tritium Plant”, Proc. 6th Int. Conf. on Tritium Sci. Technol. (2001), to be published in Fusion Sci. Technol..

20) Janeschitz, G., Igitkhanov, Yu., Sugihara, M., et al., “A Self-consistent Model of the H-mode Plasma Implemented in 1-D Simulations”, Proc. 28th EPS Conf. on Control. Fusion and Plasma Phys., P2.036

(2001).

21) Kakuta, T., Shikama, T., Nishitani, T., et al., “Round Robin Irradiation Test of Radiation Resistance Optical Fibers for ITER Diagnostic Application”, Proc. 10th Int. Conf. on Fusion Reactor Mater. (ICFRM-10) (2001), to be published in J. Nucl. Mater..

22) Kashiwagi, M., Amemiya, T., Iga, T., et al., “Long Pulse Production of High Density Negative (H-/D-) Ion Beams in Negative Ion Source Development for NBI”, Proc. of the 12th Symp. on Beam Eng. of Advanced Mater. Syntheses (BEAMS2001), 37 (2001) (in Japanese).

23) Kato, M., Sugai, H., Hayashi, T., et al., “Development of Compact Tritium Gas Recycling System”, Proc. Int. RIKEN Conf. on Muon Catalyzed Fusion and Related Exotic Atoms, (2001).

24) Kato, M., Itoh, T., Sugai, H., et al., “Development of Electrochemical Hydrogen Pump under Vacuum Condition for a Compact Tritium Gas Recycling System”, Proc. 6th Int. Conf. on Tritium Sci. Technol. (2001), to be published in Fusion Sci. Technol..

25) Kawamura, Y., Konishi, S., Nishi, M., et al., “Transport Properties of Hydrogen Isotope Gas Mixture through Ceramic Protonic Conductor”, Proc. 6th Int. Conf. on Tritium Sci. Technol. (2001), to be published in Fusion Sci. Technol..

26) Kawashima, H., Tsuzuki, K., Isei, N., et al., “Study of Ripple Loss of Fast Ions with Ferritic Insertion on JFT-2M”, Proc. 28th EPS Conf. on Control. Plasma Physics, **25A**, 4.001 (CD-ROM) (2001).

27) Kikuchi, M., Inoue, N., “Role of Fusion Energy for the 21 Century Energy Market and Development Strategy with International Thermonuclear Experimental Reactor”, Proc. 18th World Energy Congress, Energy Markets: The Challenges of the New Millennium, (CD-ROM) (2001).

28) Kobayashi, K., Hayashi, T., Iwai, Y., et al., “Tritium Behavior Study for Detritiation of Atmosphere in a Room”, Proc. 6th Int. Conf. on Tritium Sci. Technol. (2001), to be published in Fusion Sci. Technol..

29) Kubo, H., Sakura, S., Asakura, N., et al., “Radiation Enhancement and Impurity Behavior in JT-60U Reversed Shear Discharges”, Proc. 28th EPS Conf. on Control. Fusion and Plasma Phys., **25A**, 1353 (2001).

30) Kurihara, R., Nishio, S., Konishi, S., “Thermal Stress Analyses in First Wall Subjected to High Heat Flux from Fusion Plasma”, Proc. Thermal Stresses 2001, 81 (2001).

31) Kutsukake, C., Tanaka, S., Abe, Y., et al., “Tritium Distribution Measurement of FNS Tritium Target by Imaging Plate”, Proc. 6th Int. Conf. on Tritium Sci. Technol. (2001), to be published in Fusion Sci. Technol..

32) Laesser, R., Glugla, M., (Hayashi, T.), et al., “The Analytical System of the ITER Tritium Fuel Processing Plant”, Proc. 6th Int. Conf. on Tritium Sci. Technol. (2001), to be published in Fusion Sci. Technol..

33) Laesser, R., Doerr, L., (Hayashi, T.), et al., “The Storage and Delivery System of the ITER Tritium Fuel Processing Plant”, Proc. 6th Int. Conf. on Tritium Sci. Technol. (2001), to be published in Fusion Sci. Technol..

34) Li, J., Kishimoto, Y., Tuda, T., et al., “Dependence of Radial Structure of Trapped Ion Mode on Pressure and Q Profile”, J. Plasma Fusion Res. SERIES, **4**, 276 (2001).

35) Matsui, H., Chernov, V., (Takeuchi, H.,) et al., “IFMIF Status and Perspectives”, Proc. 10th Int. Conf. on Fusion Reactor Mater. (ICFRM-10) (2001), to be published in J. Nucl. Mater..

36) Morimoto, Y., Ochiai, K., Maekawa, F., et al., “Decay Heat Measurements of Fusion Related Materials in an ITER-like Neutron Field”, Proc. 10th Int. Conf. on Fusion Reactor Mater. (ICFRM-10) (2001), to be published in J. Nucl. Mater..

37) Morishita, T., Kashiwagi, M., Okumura, Y. et al., “High Current Negative Ion Production in a Low-pressure Discharge”, Proc. 12th Symp. on Beam Eng. of Advanced Mater. Syntheses (BEAMS2001), 33 (2001) (in Japanese).

38) Morita, K., Suzuki, H., (Nakamura, H.), et al, “Exchange of Tritium Implanted into Oxide Ceramics for Protium by Exposure to Air Vapors at Room Temperature”, Proc. 10th Int. Conf. on Fusion Reactor Mater. (ICFRM-10) (2001), to be published in J. Nucl. Mater..

39) Moriyama, S. and JT-60 team, “Upgrade of ECH System in JT-60U Featuring an Antenna for Toroidal/Poloidal Beam”, Proc. 14th Topical Conf. on Radio Frequency Power in Plasmas, 322 (2001).

40) Murata, I., Kokooo, (Terada, Y.), et al., “Fusion Neutronics Benchmark Experiment on Structural and Advanced Blanket Materials-Leakage Neutron Spectrum Measurement-”, Proc. Int. Conf. on Nucl. Data for Sci. Technol., **6**-P-19 (2001).

41) Murata, I., Nishio, T., Terada, Y., et al., “(n,2n)Reaction Cross Section Measurement with a Beam DT Neutron Source”, Proc. Int. Conf. on Nucl. Data for Sci. Technol., **1.3**-P-50 (2001).

42) Nakamura, H., Burgazzi, L., Cevolani, S., et al., “Status of Activities on the Lithium Target in the Key Element Technology Phase of IFMIF”, Proc. 10th Int. Conf. on Fusion Reactor Mater. (ICFRM-10) (2001), to be published in J. Nucl. Mater..

43) Nakamura, H., Ida, M., Sugimoto, M., et al., “Removal and Control of Tritium in Lithium Target for International Fusion Materials Irradiation Facility”, Proc. 6th Int. Conf. on Tritium Sci. Technol. (2001), to be published in Fusion Sci. Technol..

44) Nakamura, H., Shu, W., Hayashi, T., et al., “Study on Deuterium Permeation through Copper and F82H Low Activation Steel by Ion Implantation”, Proc. 6th Int. Conf. on Tritium Sci. Technol. (2001), to be published in Fusion Sci. Technol..

45) Narui, M., Yamasaki, M., Shikama, T., et al., “Dimensional Stability of Mica Film Under Fission Reactor Irradiation”, Proc. 10th Int. Conf. on Fusion Reactor Mater. (ICFRM-10) (2001), to be published in J. Nucl. Mater..

46) Nishi, M., Hayashi, T., Shu, W., et al, “Tritium Engineering Research and Development for Fusion Reactor at the Tritium Process Laboratory of JAERI”, Proc. Int. Workshop on Interaction of Hydrogen Isotopes with Structural Mater., (2001).

47) Nishio, T., Terada, Y., Murata, I., et al., “Fusion Neutronics Benchmark Experiment on Structural and Advanced Blanket Materials Leakage Gamma-ray Spectrum Measurement-”, Proc. Int. Conf. on Nucl. Data for Sci. Technol., **6**-P-27 (2001).

48) Nishitani, T., Uno, Y., Kaneko, J., et al., “Fusion Power Measurement Based on 16O(n,p)16N Reaction in Flowing Water”, Proc. Int. Conf. on Nucl. Data for Sci. Technol., **8**-P-6 (2001).

49) Ochiai, K., Klix, A., Terada, Y., et al., “Tritium Measurements for the 6Li-enriched Li_2TiO_3 Breeding Blanket Experiments with D-T neutrons”, Proc. 6th Int. Conf. on Tritium Sci. Technol. (2001), to be published in Fusion Sci. Technol..

50) Ochiai, K., Markovskij, D.V., Morimoto, Y., et al., “Measurement of Tritium Produced from 6Li-enriched Breeding Blanket Assembly Irradiated with D-T Neutron Source”, Proc. Int. Conf. on Nucl. Data for Sci. Technol., **8**-P-8 (2001).

51) Ogiwara, H., Tanigawa, H., Ando, M., et al., “Microstructural Development in Reduced Activation Ferritic/Martensitic Steels under Ion Beam Irradiation to High Fluences”, Proc. 10th Int. Conf. on Fusion Reactor Mater. (ICFRM-10) (2001), to be published in J. Nucl. Mater..

52) Oka, H., Nishikawa, M., (Kobayashi, K.), et al., “Calculation Code of System Effect using Serial Reactor Model”, Proc. 6th Int. Conf. on Tritium Sci. Technol. (2001), to be published in Fusion Sci. Technol..

53) Oya, Y., Shu, W., Suzuki, T., et al., “A Study of Beta-Decay Induced Reaction on T_2O-CO_2 System”, Proc. 6th Int. Conf. on Tritium Sci. Technol. (2001), to be published in Fusion Sci. Technol..

54) Ozeki, T., Smolyakov, A.I., Isayama, A., et al., “Effects of Plasma Rotation on the Neoclassical Tearing Mode in JT-60U”, Proc. 28th EPS Conf. on Control. Plasma Physics, **25A**, P4.003 (2001).

55) Reichle, R., Nishitani, T., Hodgson, E.R., et al., “Radiation Hardness Test of Mica Bolometers for ITER in JMTR ”, Proc. 28th EPS Conf. on Control. Plasma Physics, 1293 (2001).

56) Saigusa, M., Ohkohchi, K., Takei, N., et al., “Cold Test of Deep Groove Polarizer for 170 GHz ECCD System”, Proc. 14th Topical Conference on Radio Frequency Power in Plasmas, 482 (2001).

57) Sakamoto, K., Hayashi, K., Shoyama, H, et al., “Development of 170 GHz Long Pulse Gyrotron for ITER”, Proc. 26th Int. Conf. of Infrared and Millimeter Waves, 74 (2001).

58) Sato, K., Ezato, K., Taniguchi, M., et al., “Thermal Fatigue Experiment of the CuCrZr Divertor Mock-ups”, Proc. 7th Int. Conf. on Creep and Fatigue at Elevated Temperatures (CREEP7), 55 (2001).

59) Shimizu, T., Wada, M., Watanabe, K., et al., “Effect of Electrode Materials on the Production of Negative Ions”, Proc. 12th Symp. on Beam Eng. of Advanced Mater. Syntheses (BEAMS2001), 25 (2001) (in Japanese).

60) Shikama, T., Hodgson, E., Yamamoto, S., et al., “Radiation Induced Electromotive Force Induced in Metal /Ceramics Systems for Burning Plasma Diagnostics”, Proc. 10th Int. Conf. on Fusion Reactor Mater. (ICFRM-10) (2001), to be published in J. Nucl. Mater..

61) Shu, W.M., Kawakubo, Y., O’hira, S., et al., “Tritium Decontamination of TFTR D-T Plasma Facing Components using as Ultra Violet Laser”, Proc. 6th Int. Conf. on Tritium Sci. Technol. (2001), to be published in Fusion Sci. Technol..

62) Skinner, C.H., Gentile, C.A., (Shu, W.), et al., “Tritium Removal by Laser Heating and its Application to Tokamaks”, Proc. 6th Int. Conf. on Tritium Sci. Technol. (2001), to be published in Fusion Sci. Technol..

63) Sugai, H., Yahagi, M., Hamanaka, H., et al., “Tritium and Lithium Diffusion Mechanism in Neutron-Irradiated β-6LiAl”, Proc. 6th Int. Conf. on Tritium Sci. Technol.. (2001), to be published in Fusion Sci. Technol..

64) Sugie, T., Nishitani, T., Kasai, S., et al., “In-situ Transmissivity Measurement of KU-1 Quartz in UV Range under 14 MeV Neutron Irradiation”, Proc. 10th Int. Conf. on Fusion Reactor Mater. (ICFRM-10) (2001), to be published in J. Nucl. Mater..

65) Sugihara, M., Igitkhanov, Yu ., Janeschitz, G., et al., “Simulation Studies on H-mode Pedestal Behavior during Type-I ELMs under Various Plasma Conditions”, Proc. 28th EPS Conf. on Control. Fusion and Plasma Phys., P2.038 (2001).

66) Sugimoto, M., Imai, T., Okumura, Y., et al., “Issues to be Verified by IFMIF Prototype Accelerator for Engineering Validation”, Proc. 10th Int. Conf. on Fusion Reactor Mater. (ICFRM-10) (2001), to be published in J. Nucl. Mater..

67) Sugimoto, M., Nakamura, H., Yutani, T., et al, “Development of Accelerator-driven Fusion Neutron Generation Technology for International Fusion Materials Irradiation Facility”, Proc. Joint Conf. of 12th Int. Toki Conf. on Plasma Phys. and Control. Nucl. Fusion and 3rd General Sci. Assembly of Asia Plasma Fusion Assoc. (2001).

68) Sugio, K., Ohkubo, H., Kuchiwaki, I., et al., “Microstructure Evaluation on D-T Neutron Irradiated FCC Metals”, Proc. 10th Int. Conf. on Fusion Reactor Mater. (ICFRM-10) (2001), to be published in J. Nucl. Mater..

69) Tada, E., Nakahira, M, Takeda, N., et al., “Status on New Design Code Development and Verification of Anti-seismic Techniques for Application to Fusion Experimental Reactor (ITER) in Japan”, Proc. 7th Int. Seminar on Seismic Isolation, Passive Energy Dissipation and Active Control of Vibrations of Structures, 811 (2001).

70) Takei, N., Ozeki, T., Smolyakov, A.I., et al., “Analysis of Effects of the Ion Polarization Current on the Neoclassical Tearing Mode”, Proc. Joint Conf. of 12th Int. Toki Conf. on Plasma Phys. and Control. Nucl. Fusion and 3rd General Sci. Assembly of Asia Plasma Fusion Assoc. (2001), to be published in J. Plasma and Fusion Res. (JPFR series Vol. 5).

71) Tanabe, T., Miyasaka, K., (Kobayashi, K.), et al., “Surface Tritium Detection by Imaging Plate Technique”, Proc. 6th Int. Conf. on Tritium Sci. Technol.. (2001), to be published in Fusion Sci. Technol..

72) Tanaka, S., Nishikawa, M., (Nishi, M.) et al., “Activities of Tritium Studies in Japan”, Proc. 6th Int. Conf. on Tritium Sci. Technol.. (2001), to be published in Fusion Sci. Technol..

73) Tanaka, T., Yonezawa, H., (Nishitani, T.), et al., “Electrical Properties of Mineral Insulated Cables under Irradiation”, Proc. 1st iTRS Int. Symp. on Radiation Safety and Detection Technol., 270 (2001).

74) Tanigawa, H., Hirose, T., Ando, M., et al., “Microstructural Analysis of Mechanical-tested Reduced Activation Ferritic/Martensitic Steels”, Proc. 10th Int. Conf. on Fusion Reactor Mater. (ICFRM-10) (2001), to be published in J. Nucl. Mater..

75) Yamada, Y., Yamanishi, T., Shu, W., et al., “Operation Results on Safety Systems of Tritium Process Laboratory in Japan Atomic Energy Research Institute”, Proc. 6th Int. Conf. on Tritium Sci. Technol., (2001), to be published in Fusion Sci. Technol..

76) Yamamoto, M., Tsuzuki, K., Okano, F., et al., “Development of the Device for 3D-measurement of the Magnetic Field Profile in the Toroidal Device”, Proc. Symp. on Technol. in Laboratories 2001, 65 (2002) (in Japanese).

77) Young, J.S., Sherman, R.H., (Iwai, Y.), et al., “Steady-state Computer Modeling of a Recent H-D-T Cryogenic Distillation Experiment at TSTA”, Proc. 6th Int. Conf. on Tritium Sci. Technol. (2001), to be published in Fusion Sci. Technol..

78) Yutani, T., Nakamura, H., Takeuchi, H., et al., “Tritium Processing and Tritium Laboratory in the International Fusion Materials Irradiation Facility (IFMIF) ”, Proc. 6th Int. Conf. on Tritium Sci. Technol. (2001), to be published in Fusion Sci. Technol..

A.1.4 List of other papers

1) Abe, T., “Increasing Hope for Fusion Energy”, Jpn. Vac. Industry Assoc., **76** (5)**,** 32 **(**2001) (in Japanese).

2) Ando, T., Tsuji, H., et al., “ITER Central Solenoid (CS) Model Coil Project”, Jpn. Cryogenic Eng., **36**, 309 (2001) (in Japanese).

3) Hamada, K., Kawano, K., Hara, E., et al., “Pressure Drop Characteristics and Flow Distribution of ITER CS Model Coil”, Jpn. Cryogenic Eng., **36**, 330 (2001) (in Japanese).

4) Hara, E., Hamada, K., Kawano, K., et al., “Cool-down, Static Heat Load and Warm-up Performance of the Central Solenoid Model Coil and the Central Solenoid Insert Model Coil”, Jpn. Cryogenic Eng., **36**, 324 (2001) (in Japanese).

5) Hayashi, T., Kobayashi, K., Nishi, M., “Room Detritiation Demonstration Test at a Fusion Reactor Scale under US-Japan Collaboration”, Nuclear Viewpoints, **47** (5), 73 (2001) (in Japanese).

6) Ise, H., Izaki, M., (Taguchi, K.,) et al., “Development of Port Plug Handling Tractor for ITER”, FAPIG, **159**, 10 (2001) (in Japanese).

7) Isono, T., “HTS Superconducting Current Lead”, J. IEE Jpn., **122**, 15 (2001) (in Japanese).

8) Isono, T., Matsui, K., Kato, T., et al., “Quench Characteristics of the ITER CS Insert Coil”, Jpn. Cryogenic Eng., **36**, 373 (2001) (in Japanese).

9) Kato, T., Nakajima, H., Isono, T., et al., “CS Mode Coil Test Facility” Jpn. Cryogenic Eng., **36**, 315 (2001) (in Japanese).

10) Kawano, K., Hamada, K., Matsui, K., et al., “Cryogenic System Characteristics for the Transitional Heat Disturbance of the CS Model Coil”, Jpn. Cryogenic Eng., **36**, 381 (2001) (in Japanese).

11) Koizumi, N., Isono, T., Matsui, K., et al., “Pulse Charge Test Results of CS Model Coil and CS Insert Coil”, Jpn. Cryogenic Eng., **36**, 368 (2001) (in Japanese).

12) Kurihara, K., “Final Design Report of ITER on the Net”, J. Institute of Electrical Engineers of Jpn., **121**, 851 (2001) (in Japanese).

13) Kusama, Y., Ozeki, T., “Alfvén Eigenmodes and Fast Ion Loss in Tokamak Plasmas”, BUTSURI, **56**, 262 (2001) (in Japanese).

14) Matsui, K., Nunoya, Y., Kawano, K., et al., “AC Loss Performance of CS Insert Coil”, Jpn. Cryogenic Eng., **36**, 361 (2001) (in Japanese).

15) Mori, M., Shoji, A., Araki, M., et al., “The Summary Report on Engineering Design Activities in the International Thermonuclear Experimental Reactor (ITER) Project”, J. At. Energy Soc. Jpn., **44**, 16 (2002) (in Japanese).

16) Nakamura, Y., “ VDEs: Vertical Displacement Events”, J. Plasma and Fusion Res., **77**, 843 (2001) (in Japanese).

17) Nakamura, Y., Yoshino, R., Granetz, R.S., et al., “Validation of Neutral Point on JT-60U, Alcator C-Mod and ASDEX-upgrade Tokamaks”, J. Plasma and Fusion Res., **78**, 347 (2002) (in Japanese).

18) Ninomiya, A., Arai, K., Takano, K., et al., “Acoustic Emission in ITER CS Model Coil and CS Insert Coil”, Jpn. Cryogenic Eng., **36**, 344 (2001) (in Japanese).

19) Nunoya, Y., Isono, T., Sugimoto, M., et al., “Critical Current and Sharing Temperature of the ITER-CS Insert Coil”, Jpn. Cryogenic Eng., **36**, 354 (2001) (in Japanese).

20) Okada, K., Tsuneoka, M., Murano, Y., et al., ”Experiment of Ground Line for RF Noise Reduction”, J. IEIE. Jpn., **22,** 151 (2002) (in Japanese).

21) Okuno, K., “Fusion-Tokamak”, J. IEE Jpn., **122**, 15 (2001).

22) Ozeki, T., Isayama, A., “Neoclassical Tearing Mode”, J. Plasma and Fusion Res. **77**, 409 (2001) (in Japanese).

23) Shimamoto, S., Murase, A., Nishii, K., et al., “Pulse Field Losses Measurement Result and Coupling Current Circuit of the Large Current Superconducting Conductor”, J. IEE Jpn., **122-B**, 58 (2002) (in Japanese).

24) Shimomura, Y., Tsunematsu, T., Yamamoto, S., et al., “ITER Engineering Design”, J. Plasma Fusion Res., **78** Supplement (2002) (in Japanese).

25) Shimomura, Y., “Present Status and Future Development of ITER from Technical Aspects”, Gensiryoku-eye, **47**, 18 (2001) (in Japanese).

26) Sugimoto, M., Nakajima, H., Tsuchiya, Y., et al., “Experimental Results of CS Model Coil-mechanical Performance-”, Jpn. Cryogenic Eng., **36**, 336 (2001) (in Japanese).

27) Suzuki, Y., Kishimoto, Y., et al., “Scientific Visual Analysis System Required for Large-scale Numerical Simulations”, J. Plasma Fusion Res.,**78**, 59 (2002) (in Japanese).

28) Tokuda, S., Higuchi, T., Suzuki, N., “Relativistic Effects on Chaos-loss Mechanism of Runaway Electrons in a Tokamak -”, J. Plasma and Fusion Res., **77**, 1205 (2001) (in Japanese).

29) Tsunematsu, H., “Final Design Report of ITER on the Net”, J. Plasma and Fusion Res., **77**, 1250 (2001) (in Japanese).

30) Watanabe, K., “Vacuum Physics and Technologies for Future Energy Sources”, J. Inst. Electr. Eng. Jpn., **121**, 384 (2001) (in Japanese).

31) Watanabe, K., Amemiya, T., Hanada, M., et al., “DC Ultra High Voltage Technologies in a 1MeV Class Neutral Beam Injector for Fusion Machines”, Electrical Res., NE-01-12 (2001) (in Japanese).

32) Yonezawa, H., Tanaka, T., (Nishitani, T.), et al., “Electrical Properties of MI Cables under Irradiation”, Radiation, **28**, 159 (2002) (in Japanese).

33) Yoshida, K., Takigami, H., Kubo, H., “Analytical Studies on Hotspot Temperature of Cable-in-conduit Conductor”, Jpn. Cryogenic Eng., **36**, 617 (2001) (in Japanese).

A.2 Scientific Staff in the Naka Fusion Research Establishment (April 2001- March 2002)

Naka Fusion Research Establishment

MATSUDA Shinzaburo	(Director General)
HINO Syuji	(Vice Director General)
MIYAMOTO Kenro	(Invited Researcher)
NISHIKAWA Kyoji	(Invited Researcher)
HORIOKA Kazuhiko	(Invited Researcher)
MATSUI Hideki	(Invited Researcher)
KOHYAMA Akira	(Invited Researcher)
AZUMI Masafumi	(Prime Scientist)
KOIZUMI Koichi	(Staff for Director General)
OGAWA Toshihide	(Staff for Director General)
HASEGAWA Kohichi	(Staff for Director General)

Department of Administrative Services

HINO Syuji	(Director)
KAWAKAMI Hideki	(Deputy Director)

Department of Fusion Plasma Research

KITSUNEZAKI Akio	(Director)
NINOMIYA Hiromasa	(Deputy Director)
WATANABE Tsutomu	(Administrative Manager)

Tokamak Program Division

KIKUCHI Mitsuru	(General Manager)	
ISHIDA Shinichi	KURITA Gen-ichi	KUSAMA Yoshinori
MORI Katsuharu (*16)	MORIOKA Atsuhiko	ODAMAKI Masayoshi (*16)
OGURI Shigeru (*16)	OIKAWA Akira	SAKASAI Akira
SAKURAI Shinji	SHIRAI Hiroshi	SHITOMI Morimasa
TAMAI Hiroshi	TSUCHIYA Katsuhiko	YAMAZAKI Takeshi (*16)

Plasma Analysis Division

OZEKI Takahisa	(General Manager)	
HAMAMATSU Kiyotaka	HAYASHI Nobuhiko	IWASAKI Keita (*30)
MATSUDA Toshiaki	NAITO Osamu	NAKAMURA Yukiharu
OSHIMA Takayuki	SAKATA Shinya	SATO Minoru
SHIMIZU Katsuhiro	SHIRAI Hiroshi	SUZUKI Masaei (*30)
SUZUKI Mitsuhiro (*1)	TAKIZUKA Tomonori	TSUGITA Tomonori
WANG Shaojie (*9)		

Large Tokamak Experiment Division I

USHIGUSA Kenkichi	(General Manager)	
CHIBA Shinichi	FUJITA Takaaki	FUKUDA Takashi
GAO Xiang (*9)	HAMANO Takashi (*26)	INOUE Akira (*26)
ISAYAMA Akihiko	KAMADA Yutaka	KASHIWABARA Tsuneo (*24)
KAWANO Yasunori	KITAMURA Shigeru	KOBAYSHI Shinji (*25)
KOIDE Yoshihiko	KOKUSEN Shigeharu (*24)	LI Wei (*33)
NAGAYA Susumu	OIKAWA Toshihiro	SAKAMOTO Yoshiteru
SAKUMA Takeshi (*26)	SUNAOSHI Hidenori	SUZUKI Takahiro
TAKECHI Manabu (*25)	TAKI Yoshiaki (*24)	TSUKAHARA Yoshimitsu
UEHARA Kazuya		

Large Tokamak Experiment Division II

MIURA Yukitoshi	(General Manager)	
ASAKURA Nobuyuki	BAKHTIARI Mohammad (*37)	BRUSKIN Leonid.G (*15)
CHANKIN Alex V. (*11)	HATAE Takaki	HIGASHIJIMA Satoru
IDE Shunsuke	ISHIKAWA Masao (*36)	ITAMI Kiyoshi
KONDOH Takashi	KONOSHIMA Shigeru	KUBO Hirotaka
NAKANO Tomohide	OYAMA Naoyuki	SUGIE Tatsuo
TAKENAGA Hidenobu		

Plasma Theory Laboratory

KISHIMOTO Yasuaki	(Head)	
IDOMURA Yasuhiro	ISHII Yasutomo	FURUKAWA Masaru (*28)
LI Jiquan (*11)	MATSUMOTO Taro	SUGAHARA Akihiro (*30)
SUZUKI Yoshio (*28)	TOKUDA Shinji	TUDA Takashi

Experimental Plasma Physics Laboratory

KIMURA Haruyuki	(Head)	
HOSHINO Katsumichi	ISEI Nobuaki	KAMIYA Kensaku (*28)
KAWASHIMA Hisato	OASA Kazumi	OGAWA Hiroaki
SASAO Hajime (*28)	SATO Masayasu	SENGOKU Seio
SHIINA Tomio	SHINOHARA Koji	TSUZUKI Kazuhiro

Reactor System Laboratory

KONISHI Satoshi	(Head)	
AOKI Isao	HORIKAWA Toyohiko (*6)	KURIHARA Ryoichi
NISHIO Satoshi	TOBITA Kenji	

Department of Fusion Facilities

SHIMIZU Masatsugu	(Director)
KURIYAMA Masaaki	(Deputy Director)

JT-60 Administration Division

WATANABE Tsutomu	(General Manager)

JT-60 Facilities Division I

HOSOGANE Nobuyuki (General Manager)

AKASAKA Hiromi	FURUKAWA Hiroshi (*26)	HOSOYAMA Hiromi (*12)
KAWAMATA Youichi	MATSUKAWA Makoto	MIURA M Yushi
NODA Masaaki (*16)	OHMORI Shunzo	OHMORI Yoshikazu
OKANO Jun	SEIMIYA Munetaka	SHIMADA Katsuhiro
SUEOKA Michiharu	TAKANO Shoji (*1)	TERAKADO Tsunehisa
TOTSUKA Toshiyuki	UEHARA Toshiaki (*26)	YAMASHITA Yoshiki (*16)
YONEKAWA Izuru		

JT-60 Facilities Division II

MIYA Naoyuki (General Manager)

ARAI Masaru (*16)	ARAI Takashi	GOTOH Yoshitaka (*6)
HIRATSUKA Hajime	HONDA Masao	ICHIGE Hisashi
IWAHASHI Takaaki (*24)	KAMINAGA Atsushi	KIKUCHI Hiroshi (*6)
KIZU Kaname	KODAMA Kozo	KUDO Yusuke
MASAKI Kei	MASUI Hiroshi (*12)	MIYO Yasuhiko
NISHIMIYA Tomokazu	SASAJIMA Tadayuki	URATA Kazuhiro (*22)
YAGYU Jun-ichi		

RF Facilities Division

FUJII Tsuneyuki (General Manager)

ANNO Katsuto	HIRANAI Shinichi	IGARASHI Koichi (*24)
IKEDA Yoshitaka	ISAKA Masayoshi	ISHII Kazuhiro (*26)
MORIYAMA Shinichi	SATO Fumiaki (*24)	SEKI Masami
SHIMONO Mitsugu	SHINOZAKI Shin-ichi	TAKAHASHI Masami (*34)
TERAKADO Masayuki	YOKOKURA Kenji	

NBI Facilities Division

YAMAMOTO Takumi (General Manager)

OHGA Tokumichi (Deputy General Manager)

AKINO Noboru	EBISAWA Noboru	GRISHAM Larry (*29)
HIKITA Shigenori (*24)	HONDA Atsushi	KAWAI Mikito
KAZAWA Minoru	KIKUCHI Katsumi (*26)	KUSANAGI Naoto (*26)
LEI Guangjiu (*9)	MOGAKI Kazuhiko	OOHARA Hiroshi
OSHIMA Katsumi (*24)	TANAI Yutaka (*25)	TOYOKAWA Ryoji (*24)
UMEDA Naotaka	USUI Katsutomi	YAMAZAKI Haruyuki (*6)

JFT-2M Facilities Division

MIYACHI Kengo (General Manager)

YAMAMOTO Masahiro (Deputy General Manager)

AKIYAMA Takashi (*16)	KASHIWA Yoshitoshi	KIKUCHI Kazuo
KIYONO Kimihiro	KOMATA Masao	OKANO Fuminori
SAWAHATA Masayuki	SHIBATA Takatoshi	SUZUKI Sadaaki
TANI Takashi	UMINO Kazumi (*26)	

Department of Fusion Engineering Research

SEKI Masahiro (Director)
TAKATSU Hideyuki (Deputy Director)
SEKI Shogo (Prime Scientist)
KAWATA Kiyoshi (Administrative Manager)
SHIHO Makoto
TSUJI Hiroshi

Blanket Engineering Laboratory

AKIBA Masato (Head)

ABE Tetsuya	ENOEDA Mikio	HATANO Toshihisa
HIROKI Seiji	KASAI Satoshi	KOSAKU Yasuo
KURODA Toshimasa (*19)	MIKI Nobuharu (*35)	TANZAWA Sadamitsu

Superconducting Magnet Laboratory

OKUNO Kiyoshi (Head)

HAMADA Kazuya	HARA Eiji (*10)	HIYAMA Tadao
ISONO Takaaki	KATO Takashi	KAWANO Katsumi
KOIZUMI Norikiyo	KUBO Hiroatsu (*3)	MATSUI Kunihiro
NAKAJIMA Hideo	NUNOYA Yoshihiko	OSHIKIRI Masayuki (*26)
SUGIMOTO Makoto	TAKANO Katsutoshi (*26)	TAKAHASHI Ryukichi (*6)

NBI Heating Laboratory

IMAI Tsuyoshi (Head)

DAIRAKU Masayuki	EZATO Koichiro	HANADA Masaya
IGA Takashi (*6)	INOUE Takashi	KASHIWAGI Mieko
MORISHITA Takatoshi (*28)	SATO Kazuyoshi	SAWAHATA Osamu (*26)
SHIMIZU Takashi (*2)	TAKAYANAGI Tomohiro (*8)	TANIGUCHI Masaki
WATANABE Kazuhiro	YOKOYAMA Kenji	YOSHIDA Hajime (*7)

RF Heating Laboratory

IMAI Tsuyoshi (Head)

IKEDA Yukiharu	MAEBARA Sunao	OHUCHI Hitoshi (*5)
HAYASHI Kenichi (*35)	SAKAMOTO Keishi	TAKAHASHI Koji
TSUNEOKA Masaki	WATANABE Akihiko (*5)	YAMAMOTO Masanori (*6)

Tritium Engineering Laboratory

NISHI Masataka (Head)

ASANUMA Noriko (*28)	IMAIZUMI Hideki (*22)	ISOBE Kanetsugu
IWAI Yasunori	KAWAKUBO Yukio (*6)	KAWAMURA Yoshinori
KOBAYASHI Kazuhiro	MISAKI Yohnosuke (*34)	NAKAMURA Hirofumi
SHU Wataru	SUZUKI Takumi	TERADA Osamu (*19)
YAMADA Masayuki	YAMANISHI Toshihiko	

Reactor Structure Laboratory

SHIBANUMA Kiyoshi (Head)

HIGASHIJIMA Takeshi (*13)	HIYAMA Masayuki (*28)	KAJIURA Soji (*6)

KAKUDATE Satoshi | NAKAHIRA Masataka | OBARA Kenjiro
OKA Kiyoshi | OHSAKI Toshio (*19) | TAGUCHI Kou (*26)
TAKEDA Nobukazu

Office of Fusion Materials Research Promotion

TAKEUCHI Hiroshi (Head)

ANDO Masami (*28) | FURUYA Kazuyuki | HIROSE Takanori (*20)
IDA Mizuho (*10) | NAKAMURA Hiroo | NAKAMURA Kazuyuki
SUGIMOTO Masayoshi | TANIGAWA Hiroyasu | YUTANI Toshiaki (*35)

Fusion Neutron Laboratory

NISHITANAI Takeo (Head)

ABE Yuichi | HORI Jun-ichi (*28) | KLIX Axel (*27)
KUTSUKAKE Chuzo | OCHIAI Kentaro (*28) | OGINUMA Yoshikazu (*26)
MORIMOTO Yuichi (*6) | SATO Satoshi | SEKI Masakazu
TANAKA Shigeru | TERADA Yasuaki (*27) | YAMAUCHI Michinori (*35)

Department of ITER Project

TSUNEMATSU Toshihide (Director)
NAGAMI Masayuki (Deputy Director)
SHIMOMURA Yasuo (Prime Scientist)
ODAJIMA Kazuo

Administration Group

KIMURA Toshiyuki (Leader)

Project Management Group

MORI Masahiro (Leader)
KURIHARA Kenichi

Joint Central Team Group

ANDO Toshiro (Leader)

HONDA Tsutomu (*35) | IIDA Hiromasa | IOKI Kimihiro (*22)
KATAOKA Yoshiyuki (*6) | MARUYAMA So | MIZOGUCHI Tadanori (*6)
OKADA Hidetoshi (*6) | SATO Kouichi (*1) | SHIMADA Michiya
SUGIHARA Masayoshi | TAKAHASHI Yoshikazu | YAMADA Masao (*22)
YAMAGUCHI Kazuhiko(*32) | YOSHIDA Hiroshi | YOSHIDA Kiyoshi

Home Team Design Group

SHOJI Teruaki (Leader)

ARAKI Masanori | KASHIMURA Shinji (*18) | KATAOKA Takahiro (*21)
KITAMURA Kazunori (*35) | MATSUMOTO Hiroshi | MATSUMOTO Kiyoshi
NISHIKAWA Akira (*10) | OHKAWA Yoshinao | OHMORI Junji (*35)
OHNO Isamu (*10) | SAITO Keiji (*6) | SATO Shinichi (*19)
SENDA Ikuo (*35) | SHIMA Hiroaki (*17) | YAGENJI Akira (*4)

YAMAMOTO Shin

Safety Evaluation Group

TADA Eisuke	(Leader)	
ARAKI Takao (*35)	GOTO Yoshinori (*21)	HADA Kazuhiko
HASHIMOTO Masayoshi (*10)	ISHIDA Toshikatsu (*19)	MARUO Takeshi
NEYATANI Yuzuru	NOMOTO Kazuhiro (*21)	OHIRA Shigeru
TSURU Daigo		

Collaborating Laboratories

Oarai Research Establishment
Department of JMTR Project

Blanket Irradiation and Analysis Laboratory

ITO Haruhiko	(Head, since January 2002)	
KAWAMURA Hiroshi	(Head, until December 2001)	
ISHITSUKA Etsuo	TSUCHIYA Kunihiko	NAKAMICHI Masaru
UCHIDA Munenori (*23)	YAMADA Hirokazu (*19)	KIKUKAWA Akihiro (*31)

Tokai Research Establishment
Department of Material Science

Research Group for Radiation Effects

JITSUKAWA Shirou	(Group leader)	
IGAWA Naoki	SAWA Yuji	SHIBA Kiyoyuki
TAGUCHI Tomitsugu	WAKAI Eiichi	YAMADA Reiji

*1 Atomic Energy General Service Corporation
*2 Doshisha University
*3 Fuji Electric Co., Ltd.
*4 Hazama Corporation.
*5 Hitachi High-Technologies Corporation
*6 Hitachi, Ltd.
*7 Hokkaido University
*8 Ibaraki University
*9 Institute of Plasma Physics, Academia Science (China)
*10 Ishikawajima-Harima Heavy Industries Co., Ltd.
*11 JAERI Fellowship
*12 Japan EXpert Clone Corp. (JEX)
*13 JGC Corporation.

*14 JSPS Fellowship
*15 JST Fellowship
*16 Kaihatsu Denki Co., Ltd.
*17 Kajima Corporation
*18 Kandenko Co., Ltd.
*19 Kawasaki Heavy Industries, Ltd.
*20 Kyoto University
*21 Mitsubishi Electric Corporation
*22 Mitsubishi Heavy Industries, Ltd.
*23 NGK Insulators, Ltd.
*24 Nippon Advanced Technology Co., Ltd.
*25 Nissin Electric Co., Ltd.
*26 Nuclear Engineering Co., Ltd.
*27 Osaka University
*28 Post-Doctoral Fellow
*29 Princeton Plasma Physics Laboratory (USA)
*30 Research Organization for Information Science & Technology
*31 Sangyo Kagaku Co., Ltd.
*32 Shimizu Corporation
*33 Southwestern Institute of Science and Technology (China)
*34 Sumitomo Heavy Industries, Ltd.
*35 Toshiba Corporation
*36 Tsukuba University
*37 Utsunomiya University